

AD-A164 493

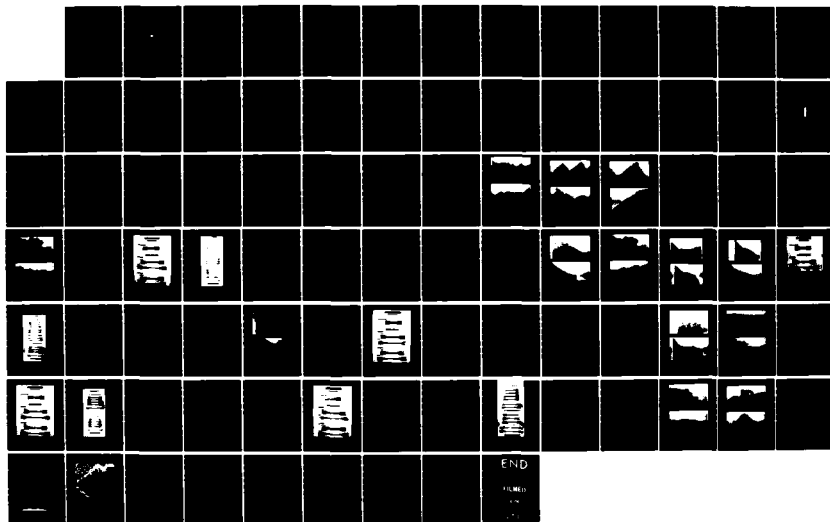
RETAINED AMBIENT TEMPERATURE PROPERTIES OF  
SUPERPLASTICALLY DEFORMED AL-1. (U) NAVAL POSTGRADUATE  
SCHOOL MONTEREY CA K A KLANKOWSKI DEC 85

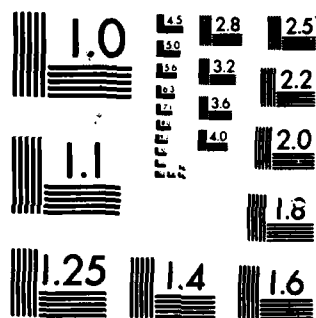
1/1

UNCLASSIFIED

F/G 11/6

NL





MICROCOPY RESOLUTION TEST CHART  
NATIONAL BUREAU OF STANDARDS-1963-A

AD-A164 493

2

# NAVAL POSTGRADUATE SCHOOL

Monterey, California



DTIC  
ELECTE  
FEB 25 1986  
S B D

## THESIS

RETAINED AMBIENT TEMPERATURE PROPERTIES OF  
SUPERPLASTICALLY DEFORMED Al-10%Mg-0.1%Zr,  
Al-10%Mg-0.5%Mn AND Al-10%Mg-0.4%Cu ALLOYS

by

Karl A. Klankowski  
December 1985

Thesis Advisor:

T. R. McNelley

Approved for public release; distribution is unlimited.

DTIC FILE COPY

86 2 25 018

ADA 164 493

## REPORT DOCUMENTATION PAGE

1a. REPORT SECURITY CLASSIFICATION UNCLASSIFIED			1b. RESTRICTIVE MARKINGS		
2a. SECURITY CLASSIFICATION AUTHORITY			3. DISTRIBUTION/AVAILABILITY OF REPORT Approved for public release; distribution is unlimited.		
2b. DECLASSIFICATION/DOWNGRADING SCHEDULE					
4. PERFORMING ORGANIZATION REPORT NUMBER(S)			5. MONITORING ORGANIZATION REPORT NUMBER(S)		
6a. NAME OF PERFORMING ORGANIZATION Naval Postgraduate School		6b. OFFICE SYMBOL (If applicable) Code 69		7a. NAME OF MONITORING ORGANIZATION Naval Postgraduate School	
6c. ADDRESS (City, State, and ZIP Code) Monterey, California 93943-5100			7b. ADDRESS (City, State, and ZIP Code) Monterey, California 93943-5100		
8a. NAME OF FUNDING/SPONSORING ORGANIZATION		8b. OFFICE SYMBOL (If applicable)		9. PROCUREMENT INSTRUMENT IDENTIFICATION NUMBER	
8c. ADDRESS (City, State, and ZIP Code)			10. SOURCE OF FUNDING NUMBERS		
			PROGRAM ELEMENT NO.	PROJECT NO.	TASK NO.
			WORK UNIT ACCESSION NO.		
11. TITLE (Include Security Classification) RETAINED AMBIENT TEMPERATURE PROPERTIES OF SUPERPLASTICALLY DEFORMED Al-10%Mg-0.1%Zr, Al-10%Mg-0.5%Mn and Al-10%Mg-0.4%Cu ALLOYS					
12. PERSONAL AUTHOR(S) Klankowski, Karl A.					
13a. TYPE OF REPORT Master's Thesis		13b. TIME COVERED FROM TO		14. DATE OF REPORT (Year, Month, Day) 1985 December	
15. PAGE COUNT 90					
16. SUPPLEMENTARY NOTATION					
17. COSATI CODES			18. SUBJECT TERMS (Continue on reverse if necessary and identify by block number)		
FIELD	GROUP	SUB-GROUP	Superplasticity, Aluminum, Aluminum Alloys Aluminum-Magnesium Alloys, Tensile Strengths		
19. ABSTRACT (Continue on reverse if necessary and identify by block number) (170) (170) The room temperature mechanical properties of three superplastic, high-Magnesium, Aluminum-Magnesium alloys (Al-10%Mg-0.1%Zr, Al-10%Mg-0.5%Mn, Al-10%Mg-0.4%Cu) were evaluated after simulated superplastic forming at warm temperature. The alloys were initially processed to produce superplastic response. They were then deformed at 300 C to strains of 100 to 200 % at strain rates of $1.7 \times 10^{-3}$ S or $1.7 \times 10^{-2}$ S and samples remachined for ambient temperature testing. Results indicate yield strengths of about 276 MPa (40 KSI) are attainable with ductility varying from about 1 to 14 percent elongation at fracture. Ultimate strengths correspondingly vary up to about 517 MPa (75 KSI). Origin of the variability of the ductility is considered.					
20. DISTRIBUTION/AVAILABILITY OF ABSTRACT <input checked="" type="checkbox"/> UNCLASSIFIED/UNLIMITED <input type="checkbox"/> SAME AS RPT <input type="checkbox"/> DTIC USERS			21. ABSTRACT SECURITY CLASSIFICATION unclassified		
22a. NAME OF RESPONSIBLE INDIVIDUAL McNelly, Terry R.			22b. TELEPHONE (Include Area Code) 408-646-2589		22c. OFFICE SYMBOL 69Mc

Approved for public release; distribution is unlimited.

Retained Ambient Temperature Properties of  
Superplastically Deformed Al-10%Mg-0.1%Zr,  
Al-10%Mg-0.5%Mn and Al-10%Mg-0.4%Cu Alloys

by

Karl A. Klankowski  
Lieutenant, United States Navy  
B.S., University of New Mexico, 1978

Submitted in partial fulfillment of the  
requirements for the degree of

MASTER OF SCIENCE IN MECHANICAL ENGINEERING

from the

NAVAL POSTGRADUATE SCHOOL  
December 1985

Author:

*Karl A. Klankowski*  
Karl A. Klankowski

Approved by:

*T. J. McNeilly*  
T. J. McNeilly, Thesis Advisor

*Stephen J. Hales*  
Stephen J. Hales, Second Reader

*F. J. Marto*  
F. J. Marto, Chairman,  
Department of Mechanical Engineering

*John N. Dyer*  
John N. Dyer,  
Dean of Science and Engineering

## ABSTRACT

The room temperature mechanical properties of three superplastic high-Magnesium, Aluminum-Magnesium alloys (Al-10Mg-0.1Zr, Al-10Mg-0.5Mn, Al-10Mg-0.4Cu) were evaluated after simulated superplastic forming at warm temperature. The alloys were initially processed to produce superplastic response. They were then deformed at 300 C to strains of 100 to 200 % at strain rates of  $1.7 \times 10^{-3} \text{ s}^{-1}$  or  $1.7 \times 10^{-2} \text{ s}^{-1}$  and samples remachined for ambient temperature testing. Results indicate yield strengths of about 276 Mpa (40 KSI) are attainable with ductility varying from about 1 to 14 percent elongation at fracture. Ultimate strengths correspondingly vary up to about 517 MPa (75 KSI). Origin of the variability in ductility is considered.

Accession For  
 NTIS GRA&I ☒  
 DTIC TAB ☐  
 Unannounced ☐  
 Distribution ☐  
 Distribution/Availability Codes  
 and/or  
 Date of Issue

A-1

## TABLE OF CONTENTS

I.	INTRODUCTION . . . . .	9
II.	BACKGROUND . . . . .	11
	A. ALUMINUM-MAGNESIUM ALLOYS . . . . .	11
	B. SUPERPLASTIC BEHAVIOR . . . . .	11
	C. RETAINED AMBIENT TEMPERATURE PROPERTIES . . .	15
	D. ALLOYING ADDITIONS . . . . .	17
	E. PREVIOUS WORK . . . . .	19
III.	EXPERIMENTAL PROCEDURE . . . . .	22
	A. MATERIAL PROCESSING . . . . .	22
	B. SPECIMEN FABRICATION . . . . .	26
	C. SPECIMEN TESTING . . . . .	28
	D. DATA REDUCTION . . . . .	29
	E. METALLOGRAPHY . . . . .	31
IV.	RESULTS AND DISCUSSION . . . . .	32
	A. SOLUTION TREATING TEMPERATURE . . . . .	32
	B. SIMULATED SUPERPLASTIC FORMING . . . . .	41
	C. AL-10MG-0.1ZR SOLUTION TREATED AT 440 C . . .	41
	1. Simulated Superplastic Forming at 300 C . . . . .	41
	2. As-rolled and As-rolled Plus Annealed . .	45
	3. Ambient Temperature Mechanical Properties . . . . .	46
	4. Optical Microscopy . . . . .	47
	D. AL-10MG-0.1ZR SOLUTION TREATED AT 490 C . . .	48
	1. Simulated Superplastic Forming at 300 C . . . . .	48
	2. As-rolled and As-rolled Plus Anneal . . .	48
	3. Ambient Temperature Mechanical Properties . . . . .	56

E.	AL-10MG-0.5MN SOLUTION TREATED AT 440 C . . .	56
1.	Simulated Superplastic Forming at 300 C . . . . .	56
2.	As-rolled and As-rolled Plus Anneal . . .	62
3.	Ambient Temperature Mechanical Properties . . . . .	63
4.	Optical Microscopy . . . . .	64
F.	AL-10MG-0.5MN SOLUTION TREATED AT 490 C . . .	64
1.	Simulated Superplastic Forming at 300 C . . . . .	64
2.	As-rolled and As-rolled Plus Anneal . . .	67
3.	Ambient Temperature Mechanical Properties . . . . .	70
4.	Optical Microscopy . . . . .	72
G.	AL-10MG-0.4CU SOLUTION TREATED AT 425 C . . .	72
1.	Simulated Superplastic Forming at 300 C . . . . .	72
2.	As-rolled and As-rolled Plus Anneal . . .	75
3.	Ambient Temperature Mechanical Properties . . . . .	77
4.	Optical Microscopy . . . . .	78
V.	CONCLUSIONS AND RECOMMENDATIONS . . . . .	84
A.	CONCLUSIONS . . . . .	84
B.	RECOMMENDATIONS . . . . .	85
	LIST OF REFERENCES . . . . .	86
	INITIAL DISTRIBUTION LIST . . . . .	89



# LIST OF TABLES

I	ALLOY COMPOSITION (WEIGHT PERCENT) . . . . .	22
II	SOLUTION TREATMENT TEMPERATURE . . . . .	24
III	REHEAT TIME--THICKNESS REDUCTION SCHEDULE . . . . .	24
IV	AL-10MG-0.5MN BOTH SOLUTION TREATING TEMPERATURES AS-ROLLED, ROOM TEMPERATURE MECHANICAL PROPERTIES . . . . .	33
V	AL-10MG-0.1ZR DATA FOR BOTH SOLUTION TREATMENTS AS-ROLLED AND ROOM TEMPERATURE MECHANICAL PROPERTIES . . . . .	39
VI	DATA FOR AS-ROLLED AL-10MG-0.1ZR SOLUTION TREATED AT 440 C AND TESTED AT ROOM TEMPERATURE . . . . .	46
VII	AMBIENT TEMPERATURE PROPERTIES OF AL-10MG-0.1ZR SOLUTION TREATED AT 440 C, AFTER SIMULATED SUPERPLASTIC FORMING . . . . .	47
VIII	DATA FOR AS-ROLLED AL-10MG-0.1ZR SOLUTION TREATED AT 490 C . . . . .	56
IX	AMBIENT TEMPERATURE TENSILE TEST RESULTS FOR AL-10MG-0.1ZR SOLUTION TREATED AT 490 C . . . . .	60
X	DATA FOR AS-ROLLED AL-10MG-0.5MN TESTED AT AMBIENT TEMPERATURE . . . . .	63
XI	DATA FOR AMBIENT TEMPERATURE MECHANICAL TESTS OF PREVIOUSLY WARM DEFORMED AL-10MG-0.5MN . . . . .	64
XII	AMBIENT TEMPERATURE TEST DATA FOR AL-10MG-0.5MN SOLUTION TREATED AT 490 C . . . . .	71
XIII	AMBIENT TEMPERATURE MECHANICAL TESTS FOR AL-10MG-0.5MN AFTER WARM DEFORMATION AT 300 C . . . . .	72
XIV	AMBIENT TEMPERATURE MECHANICAL TEST DATA FOR AS-ROLLED AL-10MG-0.4CU . . . . .	78
XV	AMBIENT TEMPERATURE MECHANICAL TEST DATA FOR AL-10MG-0.4CU AFTER SIMULATED SUPERPLASTIC FORMING . . . . .	79

## LIST OF FIGURES

2.1	Ashby-Verrall Grain Boundary Sliding Model . . . . .	13
2.2	Phase Diagram for the Aluminum-Magnesium System . . . . .	17
2.3	Phase Diagram for the Al-Mg-Mn System . . . . .	18
2.4	Partial Phase Diagram for the Al-Mg-Cu System . . . . .	19
3.1	Thermomechanical Processing Technique . . . . .	23
3.2	Portion of the Al-Mg Phase Diagram Showing Where Material Processing was Done . . . . .	25
3.3	Superplastic Deformation Specimen Geometry . . . . .	26
3.4	Standard Room Temperature Test Specimen . . . . .	27
3.5	Small Room Temperature Test Specimen . . . . .	27
3.6	Sectioning for Metallographic Examination . . . . .	31
4.1	Al-10Mg-0.5Mn Both Solution Treatments As-rolled, 440 C (a) and 490 C (b), Barkers etch, X100 . . . . .	34
4.2	Al-10Mg-0.5Mn Both Solution Treatments As-rolled, 440 C (a) and 490 C (b), Barkers etch, X800 . . . . .	35
4.3	Al-10Mg-0.1Zr Both Solution Treatments As-rolled, 440 C (a) and 490 C (b) Barkers etch, X800 . . . . .	36
4.4	Al-10Mg-0.1Zr Both Solution Treatments As-rolled, 440 C (a) and 490 C (b), Barkers etch, X100 . . . . .	38
4.5	Al-10Mg-0.1Zr Both Solution Treatments As-rolled, 440 C (a), 490 C (b), Barkers etch, X100 . . . . .	40
4.6	Most Uniform Specimens of Al-10Mg-0.1Zr Solution Treated at 440 C . . . . .	42
4.7	Al-10Mg-0.1Zr Solution Treated at 440 C All Samples Warm Deformed at 300 C . . . . .	43
4.8	True Stress at 0.1 Strain vs. Strain Rate Showing Comparison of Data of this Research to that of Alcamo . . . . .	45
4.9	Al-10Mg-0.1Zr Solution Treated at 440, Warm Deformed at 300 C to 100% Strain . . . . .	50
4.10	Al-10Mg-0.1Zr Solution Treated at 440, Warm Deformed at 300 C to 100% Strain . . . . .	51

4.11	Al-10Mg-0.1Zr Solution Treated at 440, Warm Deformed at 300 C to 100% Strain . . . . .	52
4.12	Al-10Mg-0.1Zr Solution Treated at 440, Warm Deformed at 300 C to 100% Strain . . . . .	53
4.13	Specimens of Al-10Mg-0.1Zr Solution Treated at 490 C. Warm Deformed at 300 C. . . . .	54
4.14	Al-10Mg-0.1Zr Solution Treated at 490 C All Samples Warm Deformed at 300 C . . . . .	55
4.15	Large ZrAl <sub>3</sub> Particles Present in the As-Rolled Al-10Mg-0.1Zr alloy solution treated at 440 C . . . . .	56
4.16	Large ZrAl <sub>3</sub> Particles Present in the As-Rolled Al-10Mg-0.1Zr Alloy Solution Treated at 490 C . . . . .	59
4.17	Al-10Mg-0.5Al Solution Treated at 440 C Warm Rolled at 300 C . . . . .	61
4.18	True Stress at 0.1 Strain vs Strain Rate During Simulated Superplastic Forming at 300 C . . . . .	62
4.19	Al-10Mg-0.5Mn Warm Deformed to 200% Strain Room Temperature Ductility 9.5% (a) and 1.7% (b) Barkers etch X100 . . . . .	66
4.20	Al-10Mg-0.5Mn Warm Deformed to 200% Strain Room Temperature Ductility 9.5% (a) and 3.1% (b) Barkers etch X800 . . . . .	67
4.21	Instron Produced Load vs Elongation Chart for Al-10Mg-0.5Mn Specimen Showing Large Luders Section . . . . .	68
4.22	Al-10Mg-0.5Mn Solution Treated at 490 C Warm Deformed at 300 C . . . . .	69
4.23	Al-10Mg-0.5Mn Solution Treated at 490 C All Specimens Warm Deformed at 300 C . . . . .	70
4.24	Al-10Mg-0.4Cu Solution Treated at 425 C Warm Deformed at 300 C . . . . .	74
4.25	True Stress versus Strain Rate at 0.1 Plastic Strain for Warm Deformation at 300 C . . . . .	75
4.26	Al-10Mg-0.4Cu Solution Treated at 425 C All Specimens Warm Deformed at 300 C . . . . .	77
4.27	Al-10Mg-0.4Cu Warm Deformed to 100 % Strain Room Temp Ductility 6.1 % (A) and 1.9 % (b) . . . . .	80
4.28	Al-10Mg-0.4Cu Warm Deformed to 100 % Strain Ductility 6.1 % (a) and 1.9 % (b) Kellers etch, X800 . . . . .	81
4.29	Second Crack 12 mm Away From Actual Fracture Site. Al-10Mg-0.4Cu, Kellers etch X100 . . . . .	83
4.30	Ends of Second Crack in Al-10Mg-0.4Cu Specimen. Kellers etch, X800 . . . . .	84

## I. INTRODUCTION

In recent years there has been considerable research on superplastic alloys. Superplastic alloys in general exhibit elongations to failure of 200% or more under appropriate conditions of temperature and strain rate. The driving force behind this effort was the many favorable applications for these alloys, such as: (1) application of plastics industry forming methods to metals; (2) ability to form complex shapes in one piece; (3) elimination of fasteners and welds in high strength components with complicated geometries; (4) employment of non heat-treatable alloys by elimination of post forming welds. Research at the Naval Postgraduate School (NPS) has concentrated on high-Magnesium Aluminum-Magnesium alloys. The goal of this research is to determine which of these high-strength, light-weight Al-Mg alloys were suitable for aircraft, missile and spacecraft construction.

Previous research at NPS on high-Mg, Al-Mg alloys has developed a thermomechanical process (TMP) to achieve superplastic response in a number of these alloys [Refs. 1,2]. Others at NPS have investigated the mechanical properties of these same alloys while in the superplastic regime.

The purpose of this research is to investigate the retained ambient temperature properties of three high-Mg, Al-Mg alloys after simulated superplastic forming. The choice of alloys from among those previously investigated at NPS was made on the basis of those showing the best superplastic ductilities at a warm forming temperature of 300 C and strain rates of  $10^{-3} \text{ s}^{-1}$  to  $10^{-2} \text{ s}^{-1}$ . The higher strain rates for superplastic forming were chosen with an eye toward potential application of these alloys; it is generally recognized that the relatively low strain rates for superplastic flow in many alloys restrict their usefulness.

Superplastic deformation to manufacture certain components is currently being used by a number of companies including Pratt and Whitney [Ref. 3] and Rockwell International [Ref. 4]. Since 1981 British Alcan Aluminum has had one subsidiary, Superform Metals Limited, focusing only on superplastic forming of Aluminum alloys.

This thesis presents the data obtained from the microstructural examination conducted using optical microscopy to assist in the evaluation of the test results as well as the results from the mechanical testing of the as rolled and superplastically deformed Aluminum-Magnesium alloys. Review of this work and new questions are posed for subsequent investigation.

## **II. BACKGROUND**

### **A. ALUMINUM-MAGNESIUM ALLOYS**

Aluminum alloys offer several advantages when compared to steels and Ti-alloys, such as low density, good ductility and good fracture toughness. Higher strength aluminum alloys get their increased strength mainly from solid solution and precipitation strengthening. The formation of the second phase precipitate retards dislocation motion and grain growth. The aluminum-magnesium alloy system has been extensively studied at the Naval Postgraduate School. It was selected because of its good strength to weight ratio, lower density, higher ductility and better corrosion resistance than other high strength aluminum alloys. The strength of Al-Mg alloys can be improved through warm working at a temperature below the Mg-solvus but above 200 C. Warm working produces a fine dispersion of the beta phase ( $Mg_5Al_8$ ), and increases the strength through a combination of dislocation substructure, dispersion and solid solution strengthening.

Solid solution strengthening is due to retardation of dislocation motion due to solute interaction with the stress fields of the dislocation. Dislocation substructures present barriers to dislocation motion and hence provide a form of strain hardening. Dispersion strengthening refers to the blockage of dislocation motion by the presence of the dispersed particles.

### **B. SUPERPLASTIC BEHAVIOR**

The phenomenon of superplasticity is considered to be the ability of a material to deform to high tensile elongations (usually in excess of 200%). The generally agreed requirements for achieving superplastic response are: 1) elevated temperatures in the range of 0.5 to 0.7  $T_m$ ; 2) a

second phase with strength comparable to the parent matrix; 3) a fine, equiaxed grain structure with high angle grain boundaries; 4) a thermally stable microstructure; 5) high strain rate sensitivity; and (6) resistance to cavitation.

Typically, grain sizes less than 10  $\mu$  are necessary to achieve superplastic behavior. The grain size effect on superplastic flow has been shown by Sherby and Wadsworth [Ref. 5] to be of the form:

$$\dot{\epsilon} = (D_{eff}/d^p) f(\sigma) \quad (\text{eqn 2.1})$$

where  $\dot{\epsilon}$  is the strain rate,  $p$  is the grain size exponent,  $d$  is the grain size and  $D_{eff}$  is the effective diffusion coefficient. The above equation shows that the  $\sigma$  stress required for deformation will have to increase for a given strain rate if grain growth occurs during superplastic flow. This grain growth during deformation would, in effect, result in "strain hardening". Increased grain size results in larger diffusion distances; this causes the diffusion flux to decrease for a given strength and the result is an apparently stronger, more creep-resistant material.

Two explanations of superplastic behavior frequently presented are: Nabarro-Herring diffusion creep [Ref. 6] and (2) Coble diffusion creep [Ref. 7]. In Nabarro-Herring creep, lattice diffusion is the rate controlling process. In equation 2.1  $D_{eff} = D_L$  and the grain size exponent  $p=2$ . In Coble creep, grain boundary diffusion is the rate controlling process and in 2.1  $D_{eff} = D_g b d^{-1}$  and  $p=3$ . Although neither of these processes fully describe superplastic behavior, experimental observation of  $D_{eff}$  and  $p$  have been made which support these models [Ref. 5].

The above models predict strain rates far below those actually observed. In addition they predict a lengthening of the grains in the direction of major tensile strains which is in conflict with the experimental observation of

superplastically deformed materials. Ashby and Verrall [Ref. 8] have proposed a creep model based on diffusional effects which is more consistent with the strain rates and post-deformation microstructure experimentally observed. Their model is expressed as:

$$\dot{\epsilon} = (98D^3L_V/kTd^2) (\sigma - 0.72\Gamma/d) (1 + (\sigma\delta L_B/dD_V)) \quad (\text{eqn 2.2})$$

where  $\Gamma$  is the grain boundary surface energy,  $\delta$  is the grain boundary thickness,  $D_b$  is the boundary diffusivity,  $D_V$  is the volume diffusivity,  $\sigma$  is the applied stress,  $k$  is Boltzman's constant,  $T$  is the absolute temperature,  $b$  is the Burger's vector,  $c$  is the steady state creep rate and  $d$  is the grain size. Figure 2.1 shows an illustration for the basis of the Ashby-Verrall model. This model shows individual grains moving and changing their relative positions by grain boundary sliding with diffusional accommodation.

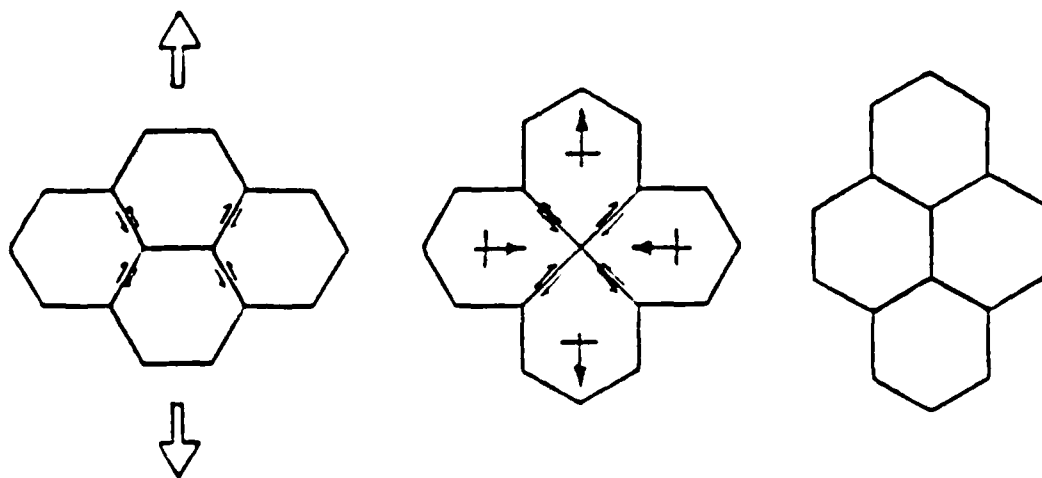


Figure 2.1 Ashby-Verrall Grain Boundary Sliding Model.



Several alternate models which focus on grain boundary sliding with slip accommodation have been proposed. In addition, at high stresses, it is generally accepted that the deformation mode is that of dislocation creep [Ref. 9].

The high temperatures, 0.5 to 0.7  $T_m$  (where  $T_m$  = melting point) used during superplastic forming require a material which has a microstructure which is resistant to grain growth. This requires some form of grain boundary pinning. The Zener-McClean relationship,

$$d = (4r/3f) \quad (\text{eqn 2.3})$$

where  $d$  is the distance between pinning particles of radius  $r$  and volume fraction  $f$ , states that a fine precipitate size will enhance a materials ability to resist grain growth. The particles pinning the grain boundary should be of a strength similar to that of the matrix to allow for their deformation during IMP and subsequent superplastic forming. If they do not deform they will cause cavities to form in the material. Stowell [Ref. 10] notes that cavitation may result from the decohesion of the particle/ matrix interface during plastic deformation.

In the analysis of deformation at high temperature, particularly superplastic behavior, the flow stress is related to the strain rate by a power law equation. Hedworth and Stowell state the relation as: [Ref. 11]

$$\sigma = K\dot{\epsilon}^m \quad (\text{eqn 2.4})$$

where  $\sigma$  is the flow stress,  $K$  is a microstructure and temperature dependent material constant,  $\dot{\epsilon}$  is the strain rate and  $m$  is the strain rate sensitivity coefficient. The coefficient is defined as

$$m = (d(\ln \sigma) / d(\ln \dot{\epsilon})) \quad (\text{eqn 2.5})$$

and is usually experimentally determined from a log-log plot of stress versus strain rate for the material of concern. Superplastic materials typically have  $n$  values of 0.3 to 0.7. The models above (Nabarro-Herring, Coble) predict  $n = 1$ ; Ashby-Verrall also suggest  $n$  tends toward 1. Experimental observation is  $n < 1$ , usually nearer 0.5. Hence, purely diffusional models are not adequate. Also, as McNelley- Lee-Mills [Ref. 12] and Lee-McNelley-Stengel [Ref. 13] report, these alloys are superplastic but have a fine subgrain microstructure rather than a fine grain microstructure. Both Mills and Stengel [Refs. 14, 15: pp. 30, 40] have observed continuous, dynamic recrystallization with grain growth in these alloys during warm (300 C) deformation. With respect to equation 2.1 this grain growth would result in strain hardening of the material. After superplastic forming, these alloys have a fine grain/subgrain structure with a dispersion of precipitate particles.

### C. RETAINED AMBIENT TEMPERATURE PROPERTIES

The high yield strengths, about 300 MPa, of these alloys are attributable to several factors: solid solution strengthening; grain size refinement and precipitation hardening. In aluminum magnesium alloys the major strengthening is due to the magnesium in solid solution. Labusch [Ref. 16: p. 1] gives the yield stress due to solid solution hardening as:

$$\tau_{yb} = (F_{max} c^{1/2} Z \alpha) / T^{1/2} \quad (\text{eqn 2.6})$$

Where  $\tau_y$  is the yield stress,  $b$  is the Burger's vector,  $F_{max}$  is the retarding force on dislocations due to the solute interaction  $c$  is the concentration of the solutes,  $Z$  is the distance from the slip plane to the solute,  $\alpha$  is a numerical factor on the order of unity and  $T$  is the tension in the dislocation line. Meyers and Chawla [Ref. 26: p. 399] also cite the solute atoms as the cause for serrated stress

strain curves. The serrations in stress-strain curves are manifestations of the Portevin-Le Chatelier effect. This arises when the solute atoms are able to diffuse about as fast as the displacement speed of the dislocations (imposed by the applied strain rate) and therefore are able to lock up the dislocations. Eventually, with increasing stress, the dislocations break free causing a drop in the stress-strain curve. This process repeats itself causing the serrations in the stress-strain curve.

The small grain size required for good superplasticity may contribute to the ambient temperature strength. The Hall-Petch relation

$$\sigma = \sigma_0 + K/\sqrt{D} \quad (\text{eqn 2.7})$$

where  $D$  is the grain size,  $\sigma_0$  is the yield strength,  $\sigma_0$  is a frictional stress required to move dislocations and  $K$  is a material constant. The Hall-Petch model is based on the piling up of dislocations against obstacles such as grain boundaries. This concentrates the stresses until they are high enough to cause yielding. Precipitation hardening in these alloys has a lesser effect than the above two effects.

The presence of cavities formed during rolling or superplastic forming would be detrimental to fracture toughness. The effect can be expressed by the relation:

$$K = (a/\sqrt{\sigma}) \quad (\text{eqn 2.8})$$

where  $\sigma$  is the applied stress,  $a$  is the length of a preexisting crack and  $K$  is the fracture toughness expressed in  $M$ . The size of the voids formed may be large enough to serve as crack-like defects of length  $a$ . At high strengths,  $a$  may be sufficient to induce brittle-like fracture.

#### D. ALLOYING ADDITIONS

The opening paragraph of this chapter addressed the effect of the Magnesium addition to the Aluminum. Figure 2.2 shows the binary Al-Mg phase diagram. Of particular note is the eutectic at 451 C. A major precipitate in all three of these alloys is the binary beta phase, ( $Mg_5Al_8$ ).

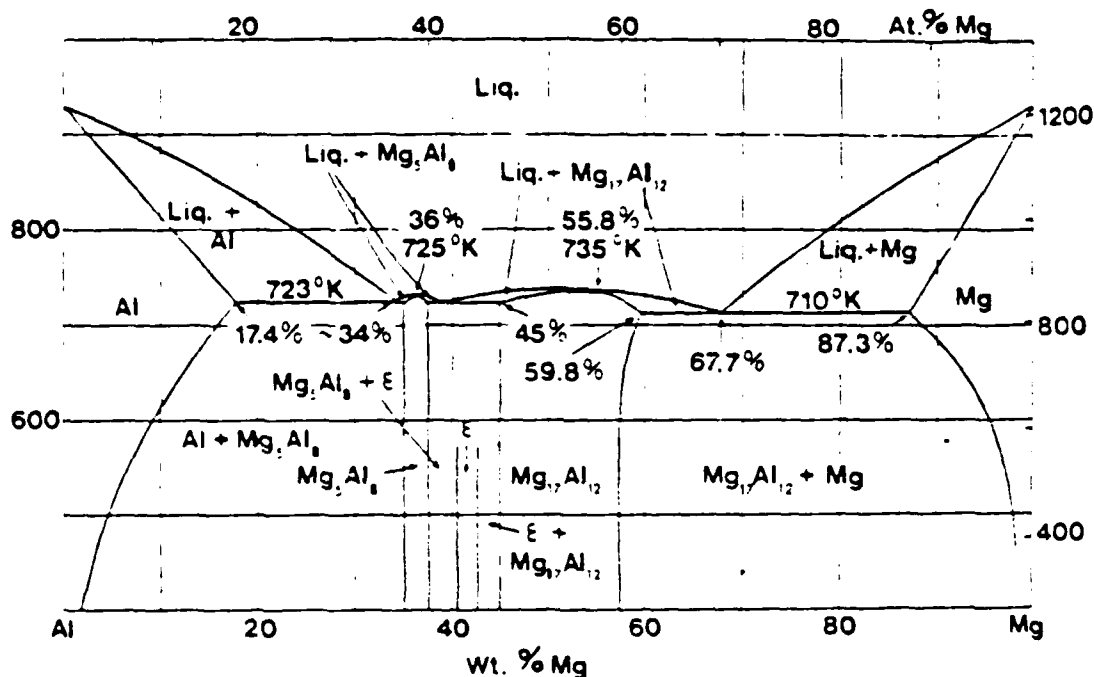


Figure 2.2 Phase Diagram for the Aluminum-Magnesium System.

Figure 2.3 is the partial ternary phase diagram for the Al-Mg-Mn system. At the alloying levels in the alloys considered by this work, the apparent intermetallic phase present would be  $MnAl$ . This has been confirmed by selected area diffraction work conducted by Garg [Ref. 17] on this alloy. The finely dispersed particles of  $MnAl$  facilitate

formation of subgrains and hinder grain growth in Aluminum alloys. Manganese in solution has little or no effect on grain size. Recrystallization and precipitation overlap and interact strongly with the Magnesium addition. At temperatures below 650 K, precipitation precedes recrystallization. [Ref. 18] Manganese and Magnesium have an additive effect on the mechanical properties of this alloy system.

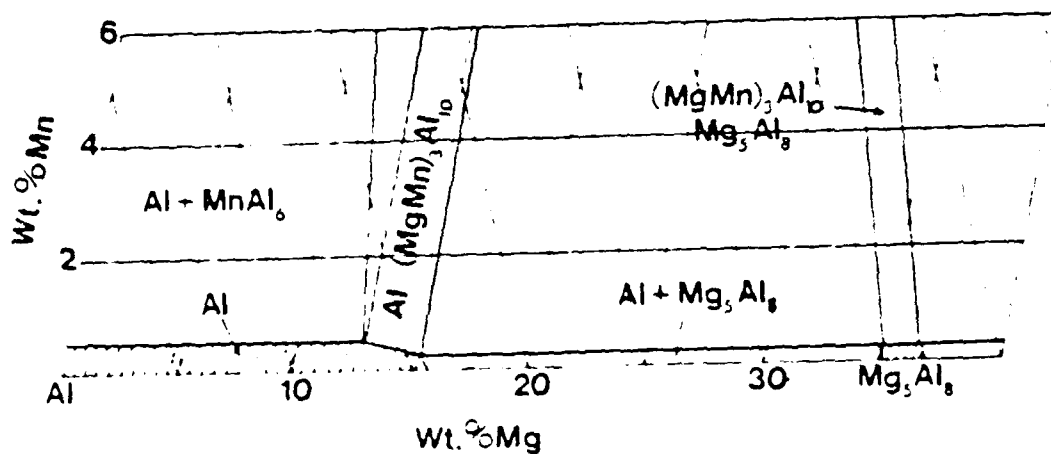


Figure 2.3 Phase Diagram for the Al-Mg-Mn System.

Copper is added to Aluminum alloys to increase the strength of the alloy at low temperatures by heat treatment, and at high temperatures through the formation of compounds with other metals. Copper is a grain refiner in Aluminum alloys. At the temperatures and concentrations considered in this research the composition of the intermetallic would be CuMg<sub>2</sub>Al<sub>3</sub>. Figure 2.4 is a copy of the Al-Mg-Cu phase diagram taken from Mondolfo [Ref. 18: p. 498].

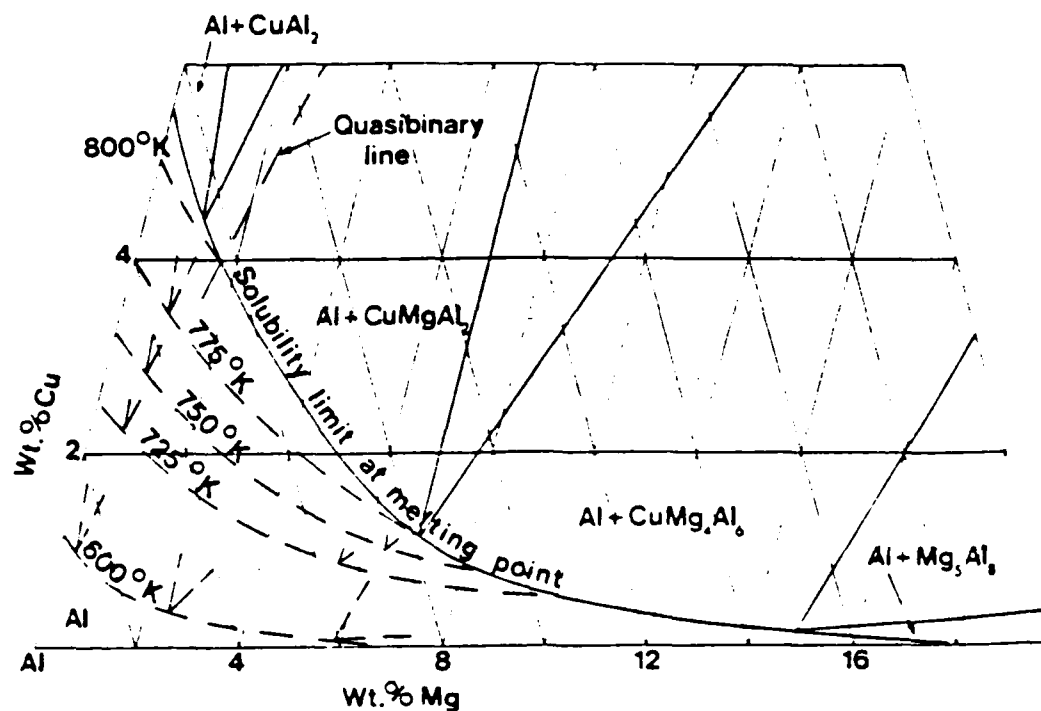


Figure 2.4 Partial Phase Diagram for the Al-Mg-Cu System.

#### E. PREVIOUS WORK

Aluminum-magnesium alloys have been the subject of extensive investigation and study at the Naval Postgraduate School. Following earlier work at NPS, Johnson [Ref. 1], standardized the thermomechanical processing of the 6-10% aluminum magnesium alloys. In these alloys, he reported good ductility and material strength twice that of 5XXX alloys. His procedure was to solution treat the material at 440 C for nine hours, not work, anneal for one hour at 440 C, quench, and then warm roll. Johnson used warm rolling temperatures in the range from 200 C to 340 C. He concluded that the beta phase (Al<sub>18</sub>Mg<sub>5</sub>) contributed by dispersion strengthening to the high strength and good ductility found in these alloys.

Shirah [Ref. 19], improved the microstructural homogeneity by increasing the solution treatment time to 24 hours. This extended treatment minimized precipitate banding while not effecting grain growth.

Becker [Ref. 2], combined previous work, and developed the procedures for isothermal tensile testing at elevated temperatures. His testing centered around temperatures of 250 C and 300 C. His work concentrated on the Al-8Mg-0.4Cu and Al-10Mg-0.5Mn alloys. Becker observed superplastic elongations up to 400%, and concluded that the higher magnesium content in the 10Mg-0.5Mn alloy stabilized grain size and extended the range of superplastic behavior to higher temperatures.

Mills [Ref. 14], extended Becker's work on the Al-10Mg-0.5Mn alloy over a larger temperature range and for additional strain rates. He found activation energies and strain rate sensitivity coefficients consistent with those in the literature. Self [Ref. 20] looked at several aluminum magnesium alloys including: Al-10Mg-0.2Mn, Al-8Mg-0.4Cu, Al-8Mg-0.4Cu-0.5Mn, Al-8Mg, Al-10Mg and Al-10Mg-0.4Cu. He found the use of copper on an equal weight percentage as effective as the use of manganese to promote superplasticity. The primary benefit of manganese is as a grain refiner where as Copper homogenizes the microstructure and has some grain refinement ability. Stengel [Ref. 15] continued the work of Becker and Mills on the Al-10Mg-0.5Mn alloy by using five different annealing treatments following warm rolling. She found that annealing below the rolling temperature, at 200 C, enhanced the superplasticity. She also concluded that recrystallization strengthened the microstructure but resulted in decreased ductility.

Alcorno [Ref. 21] looked at both Al-8Mg-0.12Zr and Al-10Mg-0.12Zr alloys. After initial evaluation of the superplastic response of both alloys, he concentrated his research on the 10% Mg alloy. Alcorno did extensive testing

on the Al-10Mg-0.1Zr alloy at 300 C. He evaluated the variation in the strain rate sensitivity coefficient,  $m$ , with variation in strain and strain rate. He also studied microstructural changes in this alloy using transmission electron microscopy (TEM) for strains varying from 8% to 267% at two different strain rates. The information gained using TEM was used to correlate how  $\sigma$ ,  $\epsilon$ ,  $\dot{\epsilon}$ ,  $d$  and  $m$  vary with deformation. Berthold [Ref. 22] and Hartmann [Ref. 23] concurrently with Alcamo did extensive research on the Al-10Mg-Zr alloy. Berthold concentrated on microstructural aspects, examining the microstructural changes during processing as well as after fracture at various temperatures and strain rates for as rolled, annealed and recrystallized samples. Hartmann did extensive mechanical testing at various temperatures and strain rates for as rolled, annealed and recrystallized samples to determine activation energies and strain rate sensitivity coefficients.



### III. EXPERIMENTAL PROCEDURE

#### A. MATERIAL PROCESSING

The three alloys studied in this research were direct-chill cast at the ALCOA Technical Center, Alcoa Center, PA. Each ingot was produced using 99.99% Aluminum base metal and was alloyed to the desired composition using commercially pure alloying materials and therefore they have low Si and Fe content. 5% Be-Al master alloy and 5% Ti-0.2% B-Al rod were added for oxidation and grain size control respectively during casting. As-received ingots 501300A and 501301A measured 127 mm (5in.) in diameter by 1016 mm (40 in.) in length. As-received ingot S572826 measured 152 mm (6 in.) in diameter by 1016 mm (40 in.) in length. The composition of each alloy is listed in Table I Analysis of Ingot content was provided by ALCOA Technical Center [Ref. 24].

TABLE I  
ALLOY COMPOSITION (WEIGHT PERCENT)

SER. NUM.	Mg	Cu	Mn	Zr	Si	Fe	Ti	Be
501300A	10.2	0.00	0.52	0.00	0.01	0.03	0.01	0.0002
501301A	10.3	0.41	0.00	0.00	0.01	0.03	0.01	0.0002
S572826	9.89	0.00	0.00	0.09	0.01	0.03	0.01	0.0002

The ingots were sectioned to produce billets of dimensions 96 mm (3.75 in), X 32 mm (1.25 in), X 32 mm (1.25 in). These dimensions were selected to facilitate subsequent processing of the billets with available equipment. The procedure for the thermomechanical processing of the billets is similar to that developed by Johnson, [Ref. 1: p. 10] and refined by Becker [Ref. 2]. Figure 3.1 is a schematic diagram showing the steps in the thermomechanical processing (TMP).

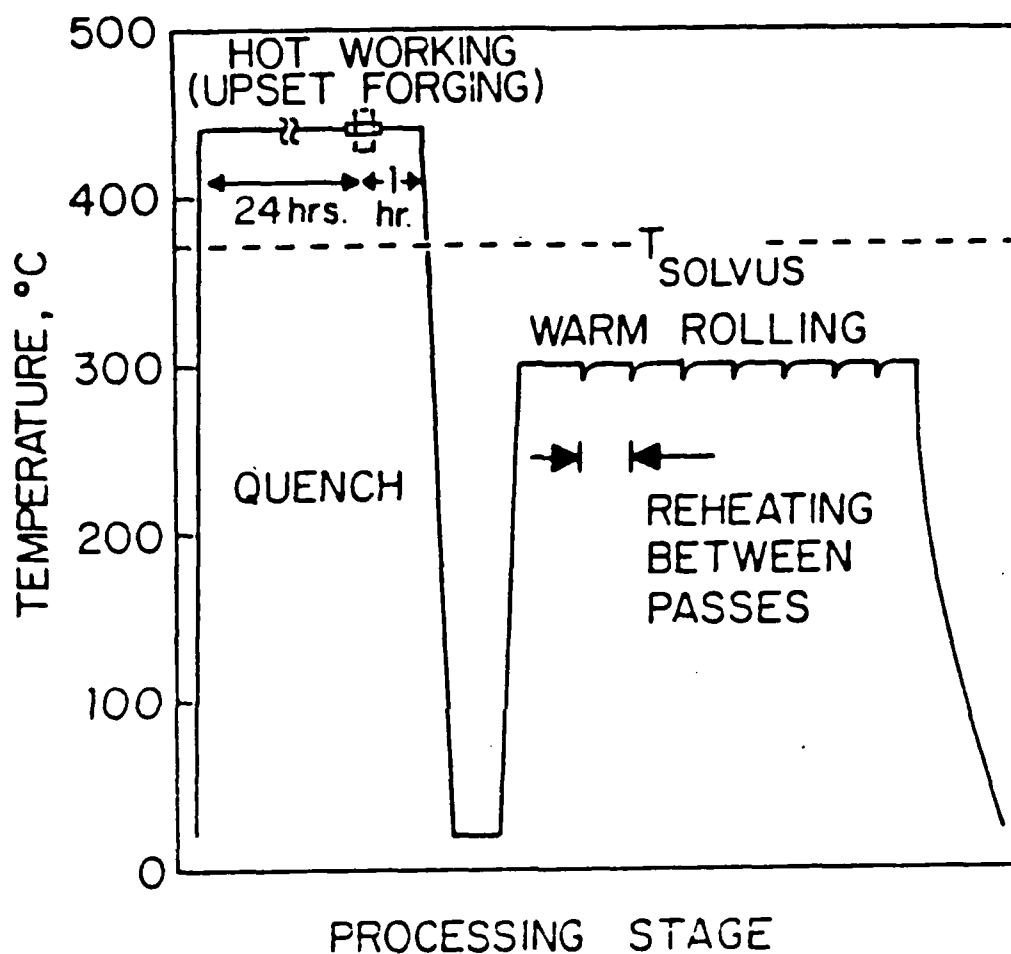


Figure 3.1 Thermomechanical Processing Technique.

The billets were solution treated for 24 hours at the temperatures indicated in Table II .

Two solution treatment temperatures were chosen for both the Al-10Mg-0.12Zr and Al-10Mg-0.5Mn alloys to investigate the effect of solution treatment temperature on retained mechanical properties for both of these alloys. The solution treatment temperature for the Al-10Mg-0.4Cu was lowered from 440 C, as used by Self, [Ref. 20: p. 10] to 425 C to

TABLE II  
SOLUTION TREATMENT TEMPERATURE

<u>ALLOY</u>	<u>TEMPERATURE</u>
Al-10Mg-0.1Zr	440 C
Al-10Mg-0.1Zr	490 C
Al-10Mg-0.5Mn	440 C
Al-10Mg-0.5Mn	490 C
Al-10Mg-0.4Cu	425 C

reduce the possibility of partial melting due to the close proximity of the ternary eutectic temperature in this Al-Mg-Cu alloy. In the rolling of this alloy (as described below) intergranular cracking, was encountered with some billets when prior solution treating was done at 440 c. Reduction of the solution treatment temperature eliminated this problem.

The billets were then upset forged to approximately 29 mm (1.15 in.) on platens heated to the solution treatment temperature, annealed at the solution treating temperature for one hour and then vigorously oil quenched. This hot working reduced the billets by approximately 70%, equivalent to a true strain of about 1.2. Warm rolling was then done at 300 C within 24 hours of upset forging, in the manner described by [Ref. 14: p.10] Isothermal rolling was desired so each billet was placed in the furnace for 30 minutes to heat from room temperature to 300 C before the first rolling pass. Interpass reheating times were controlled according to the schedule below:

TABLE III  
REHEAT TIME--THICKNESS REDUCTION SCHEDULE

<u>Billet thickness</u>	<u>Reheat Time</u>	<u>Thickness Reduction</u>
> 25 mm (> 1.0 in)	10 min	1 mm/pass (.04 in/pass)
12mm to 25mm (.5 to 1. in)	8 min	1 mm/pass (.04 in/pass)
7mm to 12mm (.3 to .5 in)	6 min	1 mm/pass (.04 in/pass)
5mm to 7mm (.2 to .3 in)	6 min	.75mm/pass (.03 in/pass)
< 5 mm (< 0.2 in)	6 min	.50mm/pass (.02 in/pass)

Each billet was rolled to a thickness of about 3.8 mm (.15 in) thickness. This required about 28 passes, resulting in a final warm reduction of approximately 83%, equivalent to a true strain of about 1.8. Figure 3.2 shows on a portion of the Al-Mg phase diagram where the hot and warm working were done.

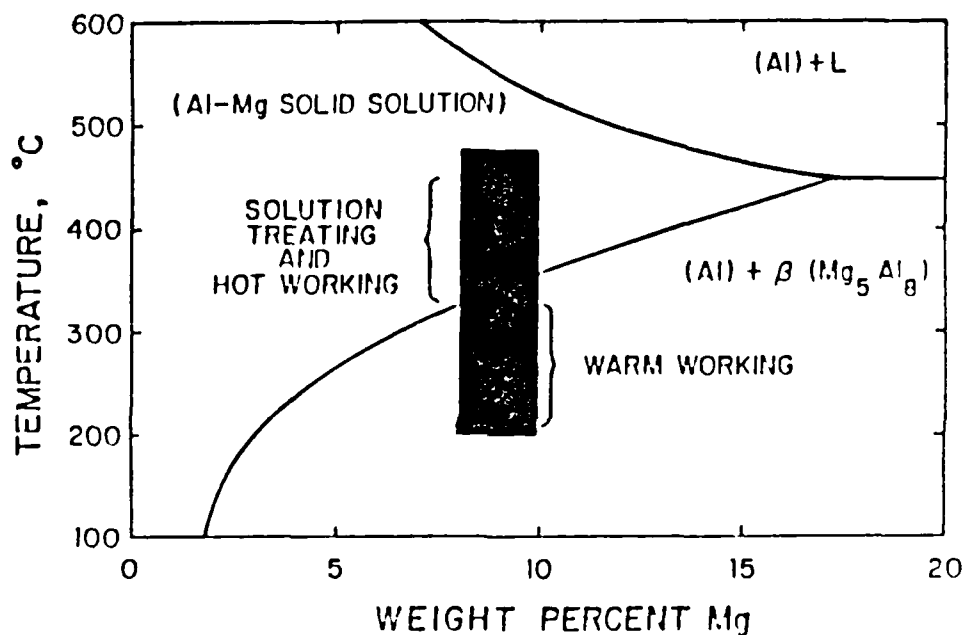


Figure 3.2 Portion of the Al-Mg Phase Diagram Showing Where Material Processing was Done.

## B. SPECIMEN FABRICATION

For the simulated superplastic warm forming, two blanks were cut from each rolled sheet. The blank dimensions were 146 mm (5.75 in) in length by 33 mm (1.3 in) in width. These were machined to give nominal gage dimensions of 20.30 mm (0.800 in) width and 50.80 mm (2.000 in) length. This gave a gage width to length ratio of 1 to 2.5. Shoulder curvature for these specimens was 6.35 mm (0.25 in). Figure 3.3 shows this specimen geometry.

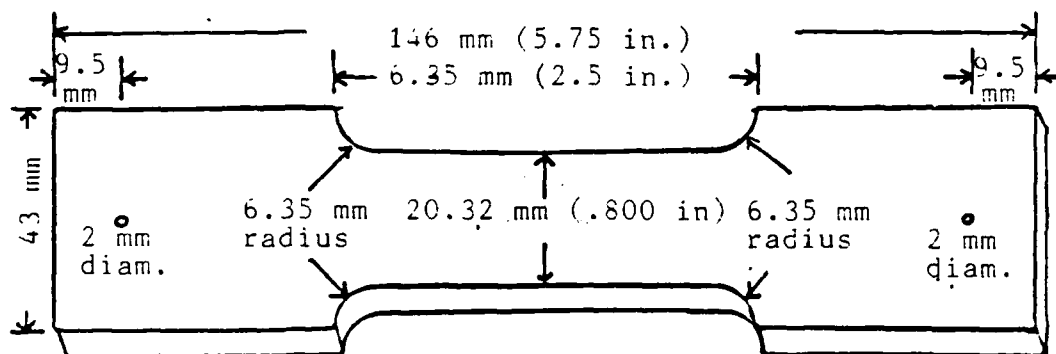


Figure 3.3 Superplastic Deformation Specimen Geometry.

Elongations were based on a 50.8 mm (2.0 in) gage length scribed on the specimens before warm deformation. Additional gage marks were scribed on the specimens at 6.35 mm (.25 in) intervals throughout the gage section to measure local plastic strains within the gage section after nominal deformation of the full specimen. This was necessary due to the inhomogeneous deformation of the gage section encountered when the specimens were superplastically deformed.

Following simulated superplastic forming ambient temperature test blanks 74 mm (2.9 in) long by 12 mm (0.5 in) wide, were cut from the gage sections of the warm deformed specimens. These were machined to give gage dimensions of

6.35 mm (0.250 in) width by 25.4 mm (1.000 in) length. This gave a gage width to length ratio of 1 to 4. The radius of curvature at the ends of the gage section was 0.5 in. as specified in ASTM E-8 for tensile specimens. Figure 3.4 shows this specimen geometry. Due to non-uniform deformation of the gage section in the Zirconium-containing alloy and due to the small gage section width after 200% plastic strain in some specimens, a smaller size ambient temperature test specimen, 66 mm (2.6 in) in length and 10 mm (0.4 in) in width with 5.08 mm (0.200 in) width by 20.32 mm (0.800 in) length gage section was used when necessary. Figure 3.5 shows this specimen geometry.

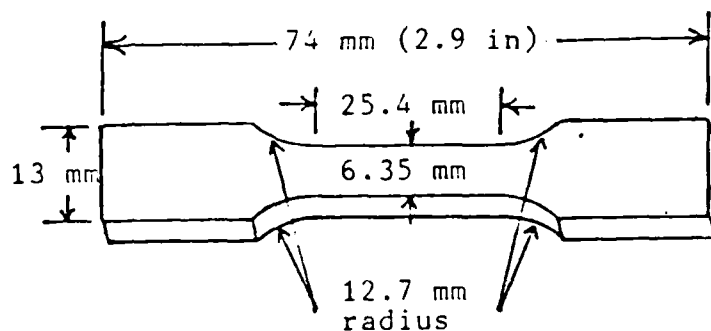


Figure 3.4 Standard Room Temperature Test Specimen.

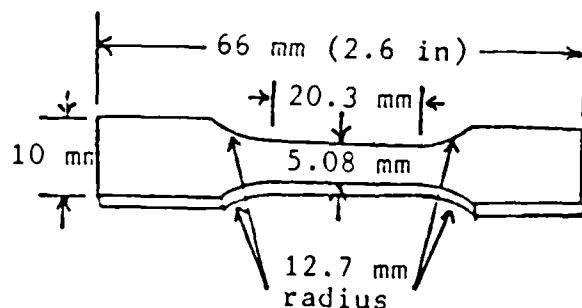


Figure 3.5 Small Room Temperature Test Specimen.

### C. SPECIMEN TESTING

Simulated superplastic forming was done at 300 C at a strain rate of either  $1.7 \times 10^{-3} \text{ S}^{-1}$  or  $1.7 \times 10^{-2} \text{ S}^{-1}$ . An electromechanical Instron machine was used to conduct the warm deformation in a manner similar to that used previously for superplastic testing at NPS, as described by [Ref. 20].

Test specimens were placed in wedge grips and held in place by pins passing through the wedges. The wedges were placed into grip assemblies which were screw mounted on pull rods connected to the Instron machine. The wedges, grips and pull rods were machined from type 304 stainless steel. Heating for the warm temperature superplastic deformation was provided by a Marshall Model 2232 Three-Zone Clamshell Furnace. Furnace temperatures were maintained by three separate controllers, each with its' own thermocouple sensor located midway in its' zone inside the furnace.

Flue effects were reduced by the use of additional insulation on the top and bottom of the furnace. This consisted of insulation mounted inside the top and bottom of the furnace and wrapped around the pull rods. When the furnace was closed, outside top and bottom ceramic plates which fitted around the pull rods were closed and three-one inch thick glass fiber insulation pads were fitted around the pull rods top and bottom and wired to the furnace. Thin strips of fiber insulation were placed between the mating faces of the furnace doors.

Four thermocouples were installed inside the furnace to monitor directly the specimen temperature. Two thermocouples were brought in along each pull rod. These were secured to the pull rod with Nichrome wire. One thermocouple from each end was placed in contact with the end tab of the specimen to directly monitor its temperature. The other thermocouple from each end was placed near, but not touching, the gage section of the specimen. The two thermocouples along the gage section were placed on opposite sides of the gage

section and overlapped by about one inch before deformation to maintain good gage section temperature monitoring during the nominal 2 inches to 4 inches of deformation given to the samples. The furnace controllers were adjusted so that the four thermocouples were all within 1% of 300 C. The furnace, grips and pull rods were heated for 24 hours before a series tests to give the components time to reach thermal equilibrium. After a sample was mounted the furnace was closed and the four thermocouples were monitored until they were back within 1% of 300 C. This would usually take about one hour and then deformation would begin. The crosshead speeds were either 5.08 mm/min (0.2 in/min) or 50.8 mm/min (2.0 in/min). For the specimen geometry this provided strain rates of  $1.7 \times 10^{-3} \text{ s}^{-1}$  or  $1.7 \times 10^{-2} \text{ s}^{-1}$ .

Ambient temperature testing was conducted on the same electromechanical Instron machine. Specimens were mounted in vise action grips. A crosshead speed of 1.27 mm/min (0.05 in/min) was used for all ambient temperature testing. This resulted in a strain rate of  $8.3 \times 10^{-4} \text{ s}^{-1}$  for the 1 inch gage section specimens and a strain rate of  $1.04 \times 10^{-3} \text{ s}^{-1}$  for the 0.8 in gage section specimens.

#### D. DATA REDUCTION

Elongation was determined by measurement of the separation of the scribed gage marks for the warm deformed samples and the outer edges of the gage lines for the ambient temperature specimens. Elongation was calculated using equation 3.1 :

$$\% \text{ Elongation} = (L - L_0) / L_0 \quad (\text{eqn 3.1})$$

Where  $L_0$  was 50.80 mm (2.000 in) for the warm deformation specimens and approximately 25.4 mm (1.0 in) or 20.3 mm (0.8 in) for the ambient temperature test specimens depending on the size specimen tested, and  $L$  was the gage length measured for the deformed (or fractured) test sample. Individually



measured  $L$  values were used for each ambient temperature test specimen. The Instron strip chart recorded the applied load (lbs) vs. chart motion. The magnification ratio between chart speed and crosshead motion was 10 for the warm deformation and 40 for the ambient temperature testing.

From the strip chart, data points of chart displacement and load were taken from the curve. A "floating slope" was used on the strip chart from which measurements were taken. This was used to remove such variables as grip adjustment and elasticity of the samples and Instron components. Using the magnification factor and the specimens initial dimensions a programmable handheld calculator was used to compute engineering stress, engineering strain, true stress and true strain. The following basic formulas were used:

$$S = P/A \quad (\text{eqn 3.2})$$

$$e_p = (L - L_0) / L_0 \quad (\text{eqn 3.3})$$

$$\sigma = S(1+e) \quad (\text{eqn 3.4})$$

$$\epsilon_p = \ln(1+e) \quad (\text{eqn 3.5})$$

where  $e_p$  is the engineering plastic strain,  $\epsilon_p$  is the true plastic strain,  $S$  is the engineering stress and  $\sigma$  is the true stress. Since the relationships for true stress and true strain are only valid up until the onset of necking, true stress vs. true strain plots for the warm deformation show those points past the onset of necking as dashed lines.

There was routinely a discrepancy between the measured elongation and the elongation computed using raw data from the strip chart. This discrepancy was as high as 50 % and averaged about 25% in the warm deformed samples. The discrepancy in the ambient temperature tests was as high as

30% and averaged about 20%. This discrepancy is predominantly caused by the plastic deformation outside of the gage section in the end tab areas in both cases.

#### E. METALLOGRAPHY

After fracture selected ambient temperature test specimens were sectioned as shown in figure 3.6. Specimens for optical microscopy were mounted in standard plastic moulds

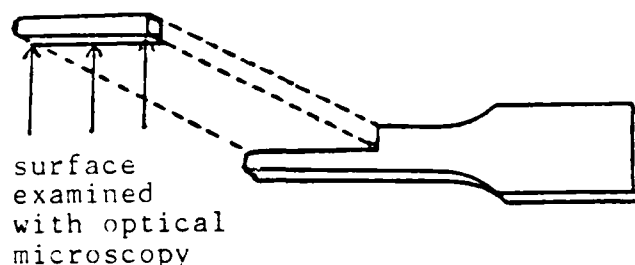


Figure 3.6 Sectioning for Metallographic Examination.

with cold mounting compound. Specimens for scanning electron microscopy were attached to standard stubs with conductive silver paste. All optical microscopy specimens were polished first using 240 to 600 grit paper followed by polishing with Aluminum oxide abrasive and finally polished with Magnesium oxide abrasive. The Al-10Mg-0.1Zr and Al-10Mg-0.5Mn specimens were etched using Barker's reagent (2.5 ml HBF<sub>4</sub> in 100 ml water, electrolytic) at 20 volts d.c. for 40 seconds. The Al-10Mg-0.4Cu specimens were etched using Keller's reagent (2 ml HF, 3 ml HCl, 5 ml HNO<sub>3</sub> and 190 ml water ) for 4 seconds. Zeiss Universal microscope was used for both examination and photographic work. Kodak 35mm Panatomic-X film was used for the optical micrographic recording. All photomicrographs were made on specimens tensile tested to fracture at ambient temperature and usually near the fracture site.

#### IV. RESULTS AND DISCUSSION

##### A. SOLUTION TREATING TEMPERATURE

The thermomechanical process (TMP) shown in Figure 3.1 previously developed at NPS was followed for each of the alloys investigated. Modifications to the solution treating temperatures were made as indicated in the background section. Previous work by Beberdick [Ref. 25] on as-rolled material, had indicated that increasing the solution treating temperature for the Al-10Mg-0.5Mn alloy enhanced its room temperature ductility. The as-rolled room temperature ductilities for both solution treating temperatures shown in Table IV are very similar. The ductility of the 440 C solution treatment varied from 2.8 to 5.8 percent and the ductility for the 490 C solution treatment varied from 2.9 to 5.7 percent. Hence this research does not bear that out.

After a 75 minute anneal at 300 C, the 440 C- solution treatment had a ductility of 14.4% while the 490 C solution treatment gave 12.6% ductility. Optical photomicrographs, Figures 4.1 and 4.2, show no discernible difference in microstructure between the two solution treatment conditions. All photomicrographs are of sections cut from specimens tested in tension to fracture at ambient temperature and are usually from near the fracture site. During simulated superplastic forming it was noted that the 490 C- solution treated material produced more uniform deformation at the higher strain rate,  $1.67 \times 10^{-2} \text{ s}^{-1}$ . This is shown later in this section. Other than noted above, the higher solution treating temperature does not appear to produce any improvement in the mechanical properties of this alloy.

Two solution treating temperatures, 440 C and 490 C, were also applied to the Zirconium containing alloy to determine if increased solution treatment temperature would

**TABLE IV**  
**AL-10MG-0.5MN BOTH SOLUTION TREATING TEMPERATURES**  
**AS-ROLLED, ROOM TEMPERATURE MECHANICAL PROPERTIES**

AL-10MG-0.5MN  
(SOLUTION TREATED AT 440 C)

AS ROLLED:

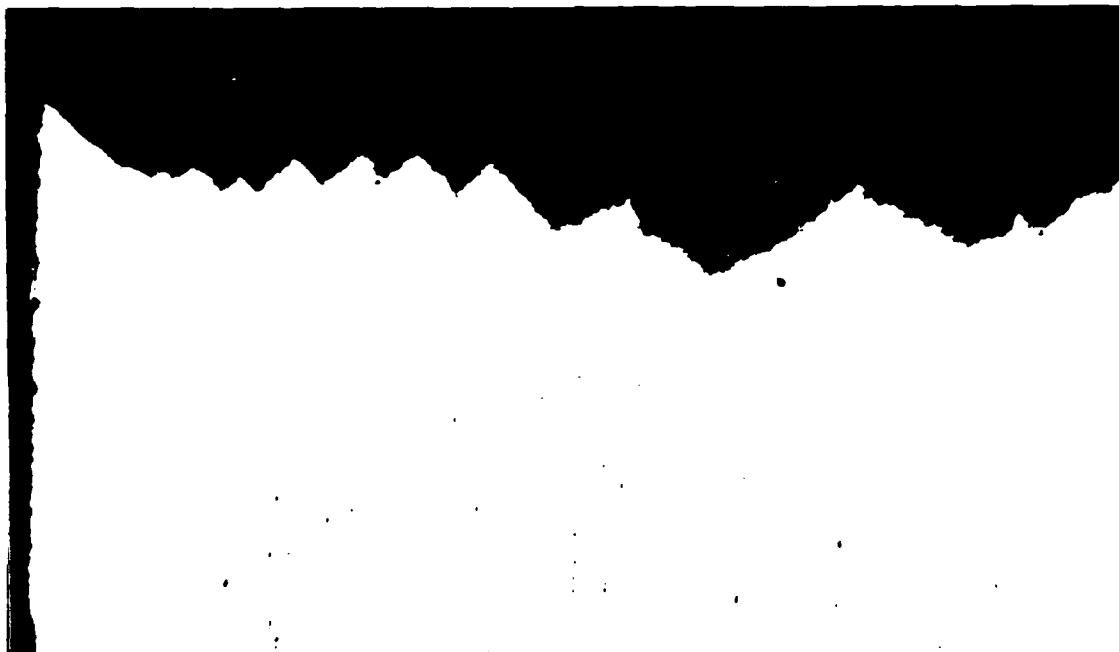
BILLET NUMBER	$S_y$ (MPa)	$S_u$ (MPa)	$\sigma_y$ (MPa)	$\sigma_u$ (MPa)	% STRAIN MEASURED (%)
Mn7-2AR	299.3	470.4	300.0	496.7	2.8
Mn6-3AR	258.8	481.7	259.3	495.9	3.4
Mn2-3AR	309.4	410.7	310.1	514.4	4.0
Mn2-2AR	246.7	482.2	297.3	515.5	4.2
Mn2-1AR	340.6	504.4	341.3	538.2	5.1
Mn7-1AR	375.8	522.0	376.6	552.8	5.8
AS ROLLED--ANNEALED 1 HR AT 300 C					
Mn6-1AR	325.2	446.2	325.8	484.2	7.4
AS ROLLED--ANNEALED 1 HR 15 MIN. AT 300 C					
Mn6-2AR	275.3	462.7	275.9	556.2	14.4

AL-10MG-0.5MN  
(SOLUTION TREATED AT 490 C)

AS ROLLED:

BILLET NUMBER	$S_y$ (MPa)	$S_u$ (MPa)	$\sigma_y$ (MPa)	$\sigma_u$ (MPa)	% STRAIN MEASURED (%)
Mn16-3AR	332.1	485.1	332.8	504.0	2.9
Mn14-1AR	259.7	467.4	260.2	441.8	3.4
Mn16-1AR	338.3	507.3	388.9	541.3	3.5
Mn13-1AR	298.2	492.8	298.8	519.8	4.3
Mn16-2AR	333.4	513.3	334.1	551.9	4.7
Mn11-2AR	271.6	502.5	272.1	546.7	5.7
AS ROLLED--ANNEALED 1 HR 15 MIN. AT 300 C					
Mn11-3AR	291.9	456.8	292.6	531.7	12.6

improve the distribution of the Zr and enhance the room temperature mechanical properties. Optical photomicrographs, Figures 4.3 and 4.4, show a random dispersion of 1-5 micron ZrAl<sub>3</sub> particles with no discernable difference between the two Solution treating temperatures. Table V shows ductilities of 4.9 to 9.2 % for the 440 solution treated material and 4.6 to 10.5 % ductility for the 490 solution treated material tested at room temperature in the as-rolled condition.

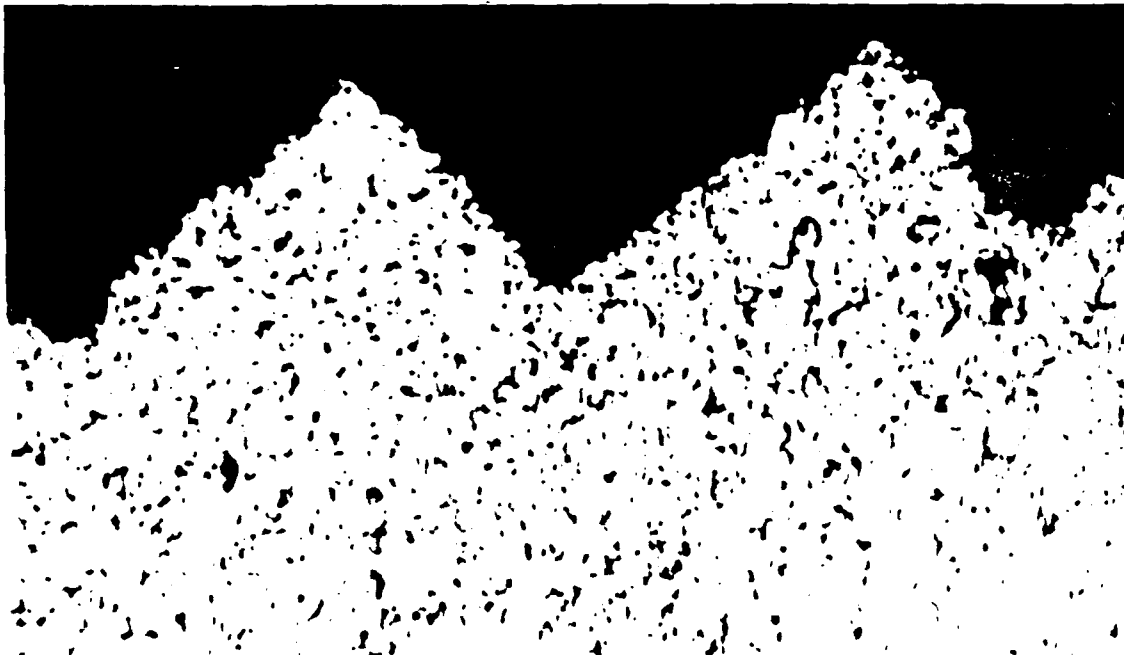


(a)

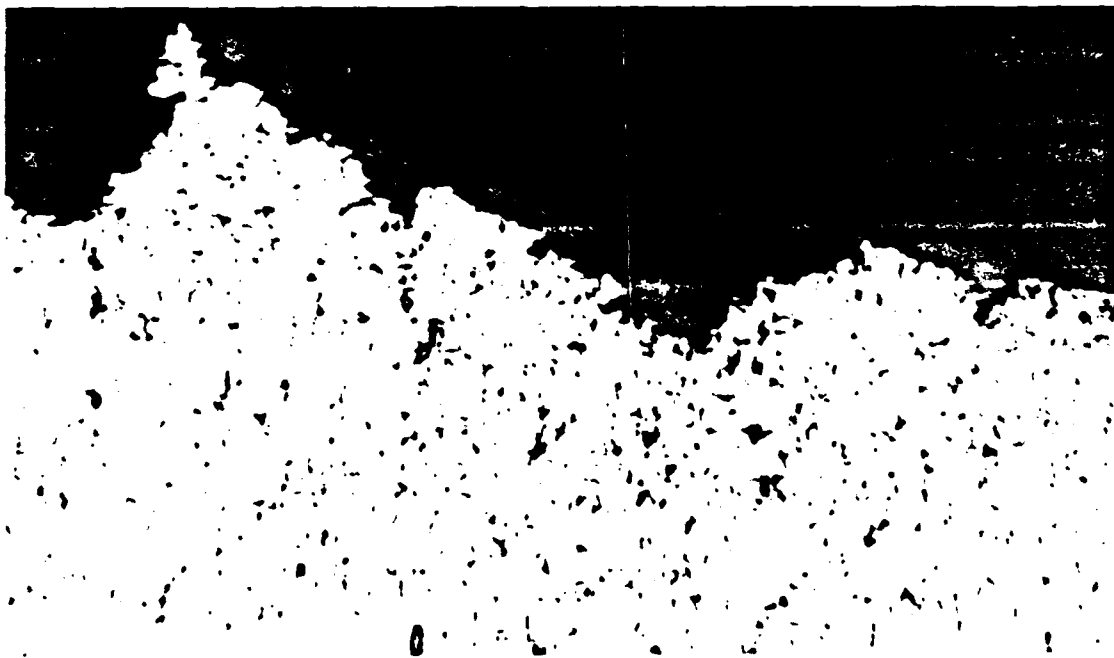


(b)

Figure 4.1 Al-10Mg-0.5Mn Both Solution Treatments  
As-Rolled, 440 C (a) and 490 C (b), Barkers etch, X100.

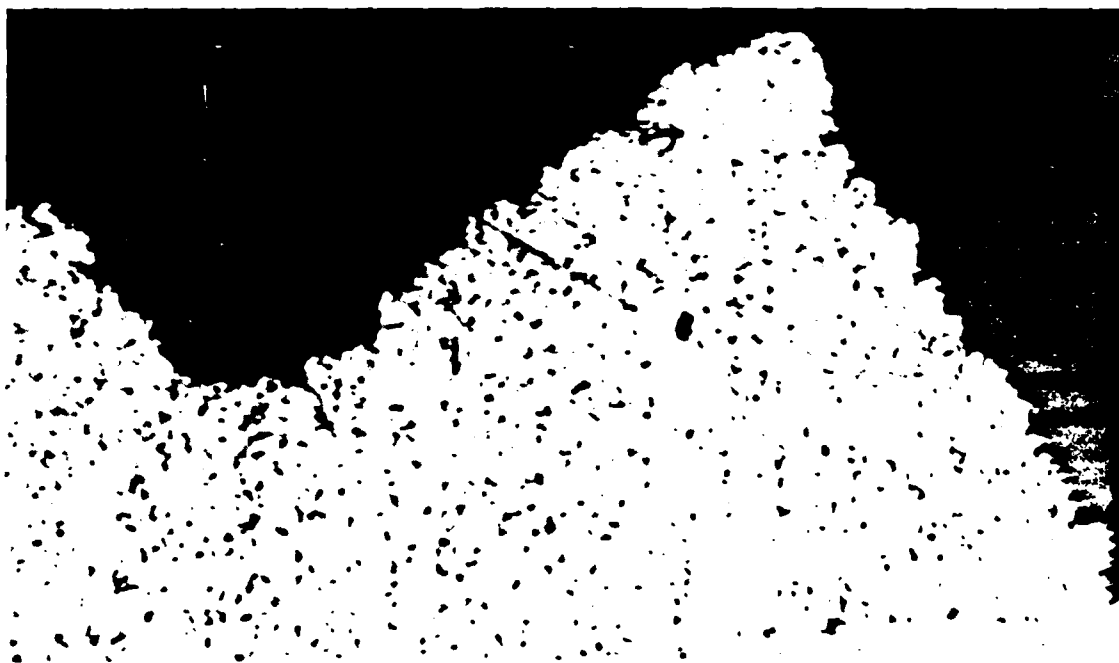


(a)

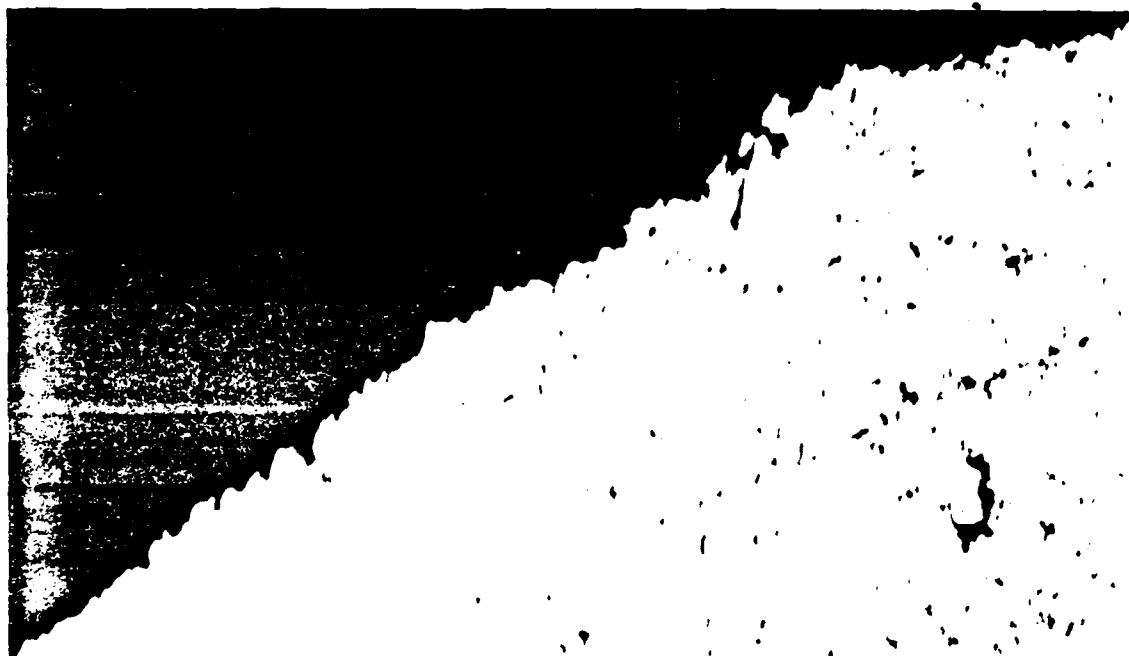


(b)

Figure 4.2 Al-10Mg-0.5Mn Both Solution Treatments  
As-Rolled, 440 C (a) and 490 C (b), Barkers etch, X800.



(a)



(b)

Figure 4.3 Al-10Mg-0.1Zr Both Solution Treatments  
As-Rolled, 440 C (a) and 490 C (b) Barkers etch, X800.

The yield and ultimate strengths are approximately equal for both solution treatments at about 310 MPa (45 KSI) yield and 460 MPa (67 KSI) ultimate strength. Optical photomicrographs 4.5, of material from both solution treatments after 75 minutes of static annealing at 300 C show no apparent effect of the different solution treating temperatures. The mechanical test results in Table V shows better ductility for the lower solution treating temperature. The higher solution treating temperature does not appear to cause dissolution of the  $ZrAl_3$  precipitates.

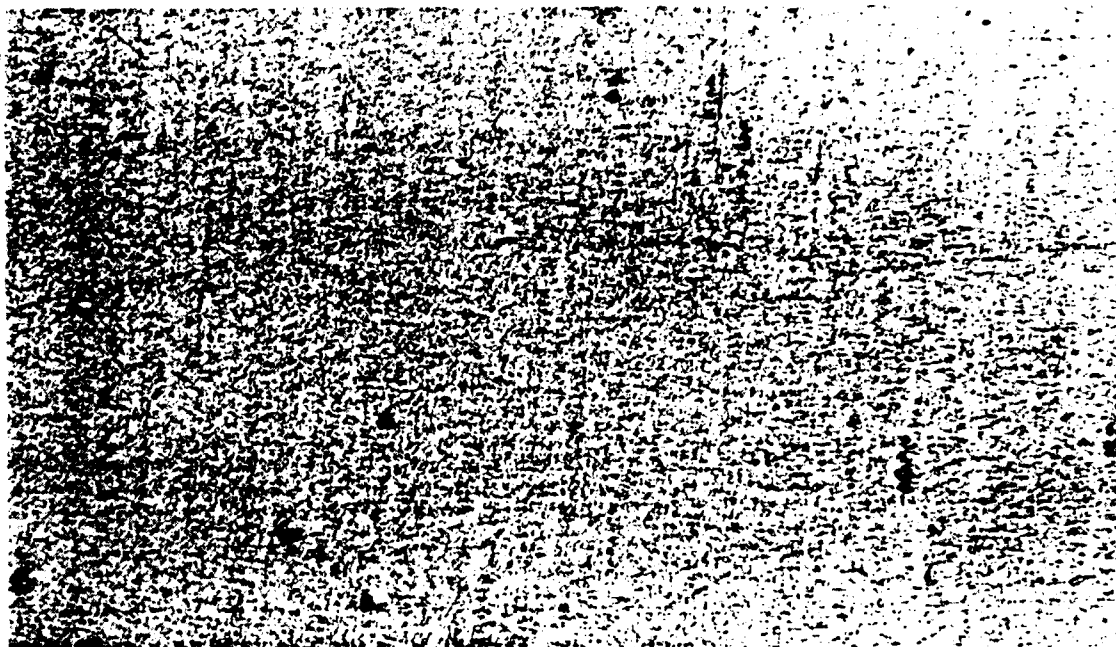
Both the Al-10Mg-0.1Zr and Al-10Mg-0.5Mn alloys solution treated at 490 C were brought directly to that temperature without a hold at 440 C. An initial hold at 440 C is generally recommended to allow the beta Magnesium ( $Mg_5Al_8$ ) to go back into solution to prevent partial melting when going above the 451 C eutectic temperature. Even though this was not done, no cracking problems on rolling, usually associated with partial melting, were observed for either of these alloys. It is felt that this was attributable to several factors; (1) the long (24 hours) solution treating time; (2) the 5%Ti-0.2%B-Al added for grain size control in the casting and (3) the limited segregation during casting due to the direct chill casting process. The long solution treating time appears to have been sufficient for any beta which did melt to go back into the solid solution. Factors two and three limited the size and amount of beta present in the as cast condition. Although this was not the recommended method of heat treating these alloys, no apparent microstructural damage was done to either alloy.

Reducing the solution treating temperature to 425 C for the copper-containing alloy eliminated all cracking problems during warm rolling of this alloy. The need to reduce the solution treating temperature from 440 C was realized from a closer examination of the Al-Mg-Cu ternary phase diagram shown in Figure 2.4 in the background chapter. This





(a) As-rolled plus annealed 75 minutes at 300 C. X100



(b) As-rolled plus annealed 75 minutes at 300 C. X100

Figure 4.4 Al-10Mg-0.1Zr Both Solution Treatments  
As-rolled, 440 C (a) and 490 C (b), Barkers etch, X100.

TABLE V

AL-10MG-0.1ZR DATA FOR BOTH SOLUTION TREATMENTS  
AS-ROLLED AND ROOM TEMPERATURE MECHANICAL PROPERTIESAL-10MG-0.1ZR  
(SOLUTION TREATED AT 440 C)

AS ROLLED

BILLET NUMBER	$S_y$ (MPa)	$S_u$ (MPa)	$\sigma_y$ (MPa)	$\sigma_u$ (MPa)	% STRAIN MEASURED (%)
Zr21-1AR	317.6	484.3	318.2	522.0	4.9
Zr19-1AR	335.3	489.4	336.0	525.8	5.0
Zr19-2AR	308.5	458.9	309.1	496.7	5.1
Zr24-2AR	314.3	445.3	315.0	490.9	8.0
Zr24-1AR	295.6	441.6	296.2	489.3	9.0
Zr34-1AR	281.2	430.9	281.8	487.3	9.1
Zr20-1AR	316.6	496.2	317.2	553.3	9.2

AS ROLLED--ANNEALED 1 HR AT 300 C  
Zr34-2AR 316.3 646 252.9 476.4 12.2

AS ROLLED--ANNEALED 1 HR 15 MIN. AT 300 C  
Zr34-3AR 203.0 407.8 203.3 520.9 12.2

AL-10MG-0.1ZR  
(SOLUTION TREATED AT 490 C)

AS ROLLED:

BILLET NUMBER	$S_y$ (MPa)	$S_u$ (MPa)	$\sigma_y$ (MPa)	$\sigma_u$ (MPa)	% STRAIN MEASURED (%)
Zr26-1AR	331.0	507.3	331.6	552.4	4.6
Zr28-2AR	335.9	475.2	336.5	511.7	5.6
Zr28-1AR	320.7	474.5	321.3	522.6	7.0
Zr28-3AR	341.9	438.6	342.6	462.0	7.4
Zr25-1AR	312.0	448.5	312.6	492.4	9.4
Zr30-2AR	273.5	436.8	274.0	490.1	9.8
Zr30-1AR	286.3	433.3	286.9	488.5	10.5

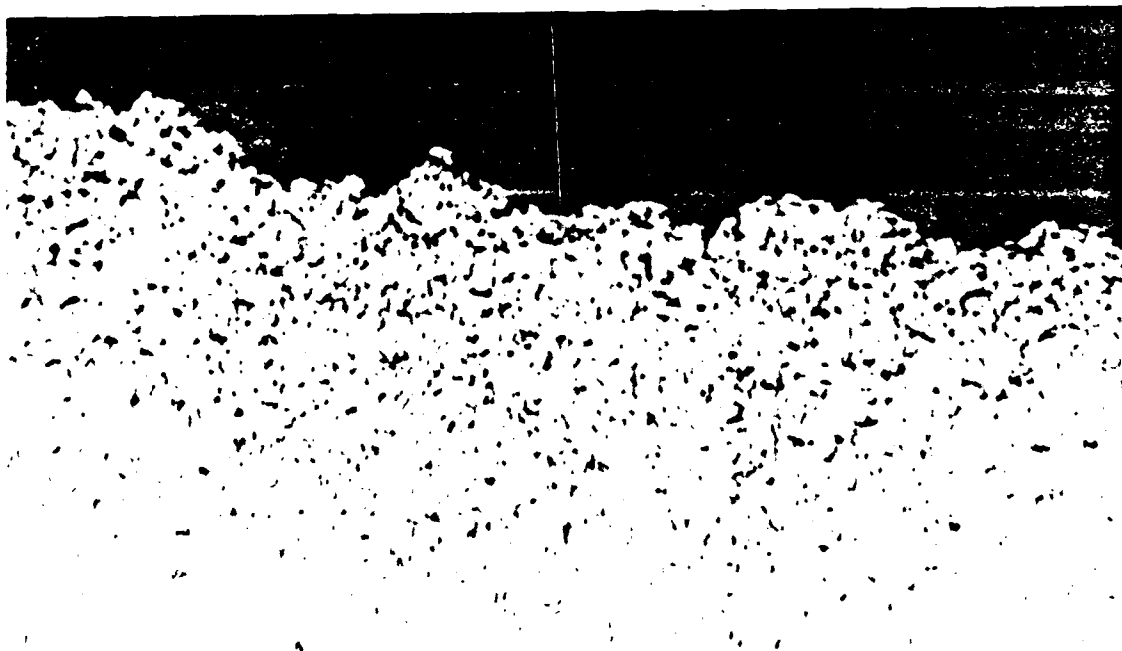
AS ROLLED--ANNEALED 1 HR AT 300 C  
Zr25-2AR 261.4 416.3 261.9 481.1 12.2

AS ROLLED--ANNEALED 1 HR 15 MIN. AT 300 C  
Zr25-3AR 256.5 421.4 257.0 496.2 14.0

was done after cracking problems were experienced when warm rolling the first few billets of the Copper containing alloy solution treated at 440 C as had been done in previous work at NPS. The problem appears to be with the melting point of the ternary intermetallic, CuMg4Al6.



(a) 100 % warm deformation, 1.7 % ambient ductility.



(b) 100 % warm deformation, 1.2 % ambient ductility.

Figure 4.5 Al-10Mg-0.1Zr Both Solution Treatments  
As-Rolled, 440 C (a), 490 C (b), Barkers etch, X100.

## B. SIMULATED SUPERPLASTIC FORMING

The test matrix for this thesis called for simulated superplastic forming of twelve specimens of the as-rolled material for each solution treating temperature of each alloy. The twelve provided for four samples deformed to 100%, four deformed to 200% strain, all at  $1.67 \times 10^{-3}$  strain rate and four deformed to 100% strain at  $1.67 \times 10^{-2}$  S<sup>-1</sup> strain rate. During the simulated superplastic forming phase a thirteenth sample was added for each alloy/solution treating temperature combination. This sample was warm deformed to 200% strain at  $1.67 \times 10^{-2}$  strain rate to check, in a qualitative way, how well each material handled large strains at moderate strain rates. The Al-10Mg-0.1Zr, solution treated at 440 C, was the first to be tested in this category. It was stopped at 160 % nominal to insure that fracture did not occur. The extra specimens for the other four processing conditions were strained to 200 % nominal strain. The specimen with the most uniform deformation of the gage section in this category was the 490 C solution treated Manganese containing alloy shown later.

## C. AL-10MG-0.1ZR SOLUTION TREATED AT 440 C

### 1. Simulated Superplastic Forming at 300 C

Samples of the as rolled material cut to the specimen geometry shown in Figure 3.3 were deformed at 300 C to nominal strains of 100, 140, 160, and 200 % at strain rates of  $1.67 \times 10^{-3}$  or  $1.67 \times 10^{-2}$  S<sup>-1</sup>. Inhomogeneous deformation of the gage section during simulated superplastic forming was a severe problem in this alloy. It was necessary to deform to nominal strains of 140 % to 160 % to obtain the local strains desired (100% or 200%) for subsequent ambient temperature testing. Figure 4.6 shows the most uniform, warm deformation specimen at each condition of strain and strain rate for this alloy.

Figure 4.7 shows all the warm deformation specimens for this combination of alloy and solution treating

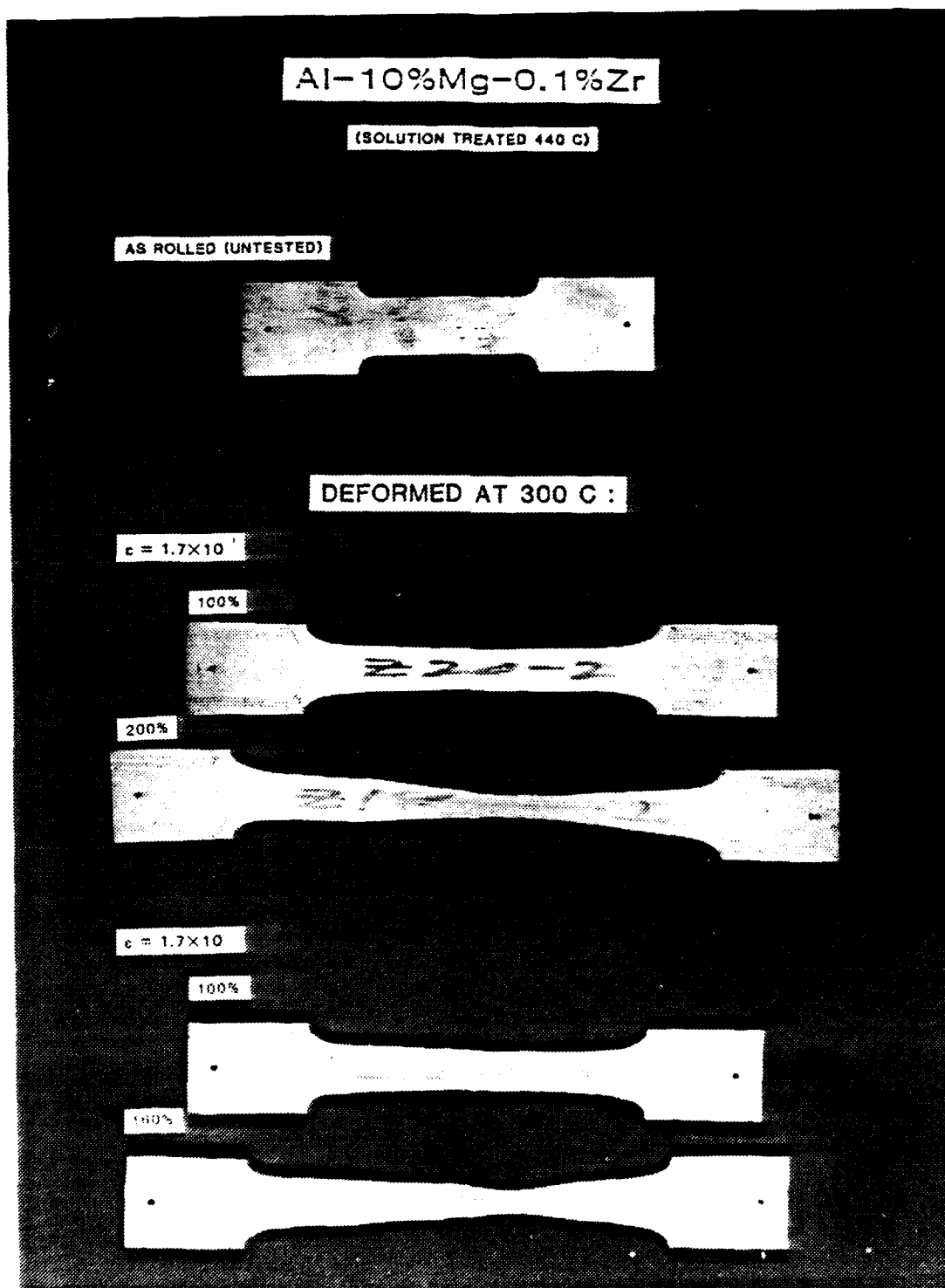


Figure 4.6 Most Uniform Specimens of Al-10Mg-0.1Zr  
Solution Treated at 440 C.

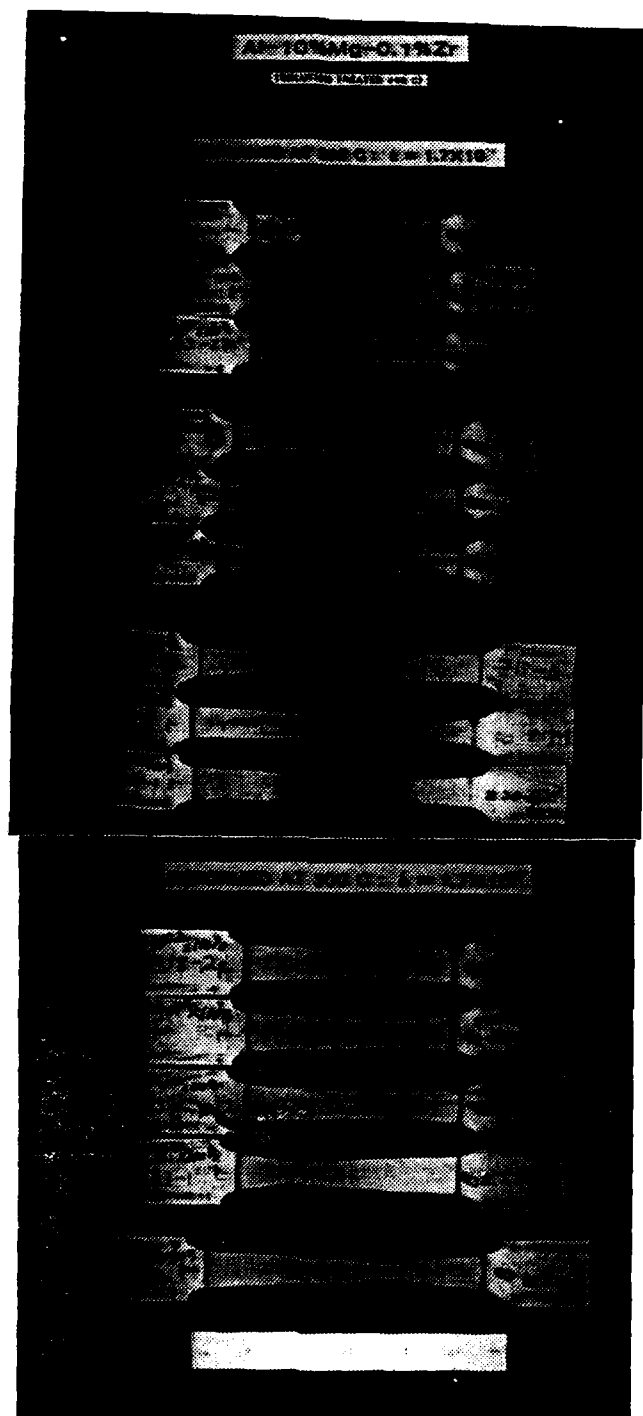


Figure 4.7 Al-10Mg-0.1Zr Solution Treated at 440 C  
All Samples Warm Deformed at 300 C.

temperature. Warm deformation stresses were consistent with those measured by Alcamo [Ref. 21: p. 110] as shown in Figure 4.8.

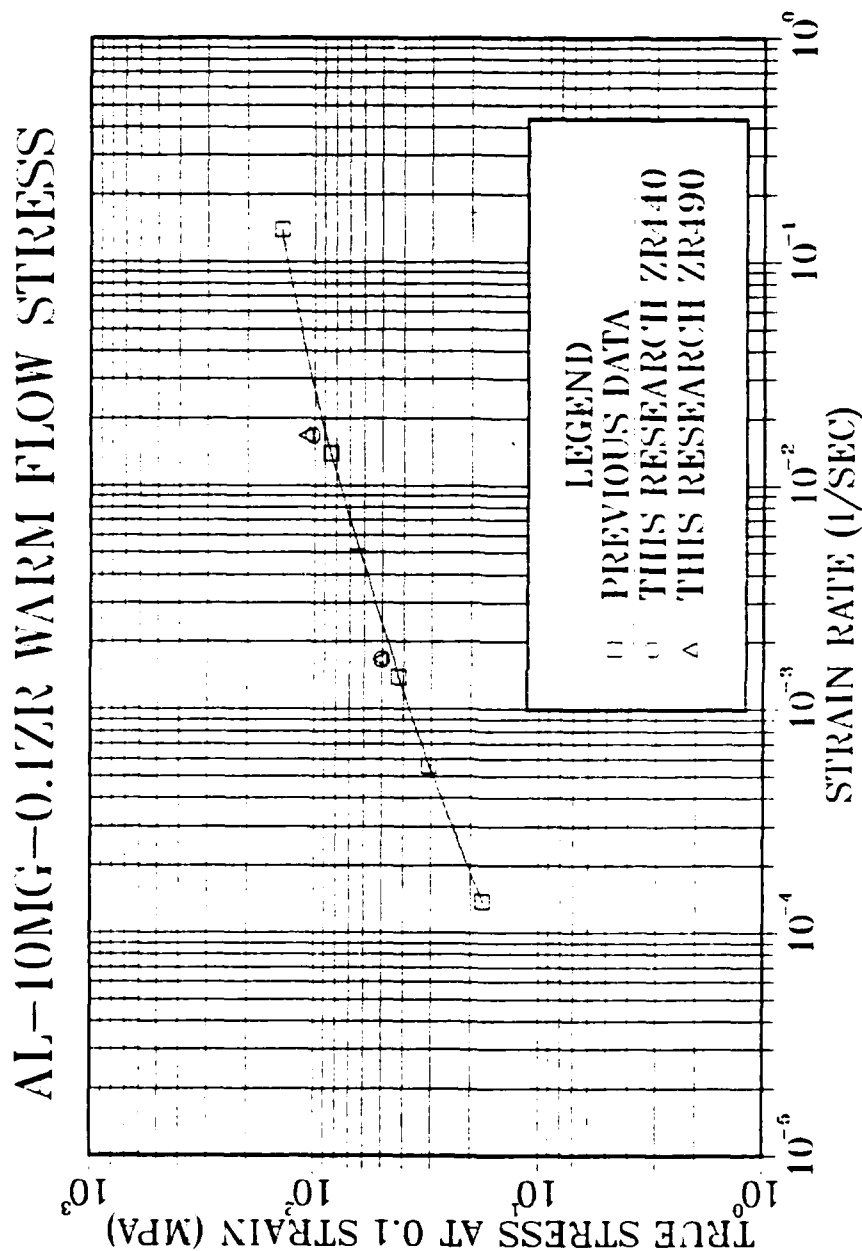


Figure 4.8 True Stress at 0.1 Strain vs. Strain Rate  
Showing Comparison of Data of this Research to that of Alcamo.

## 2. As-rolled and As-rolled Plus Annealed

As-rolled specimens were tested at  $8.3 \times 10^{-4}$  S<sup>-1</sup> strain rate at ambient temperature for comparison with previous work by Alcamo and Hartmann [Refs. 21,23: pp. 47, 50] and to check the consistency of processing through the warm rolling stage. Table VI shows good agreement of mechanical test results when strain rates are approximately equal.

TABLE VI  
DATA FOR AS-ROLLED AL-10MG-0.1ZR SOLUTION  
TREATED AT 440 C AND TESTED AT ROOM TEMPERATURE

AL-10MG-0.1ZR  
(SOLUTION TREATED AT 440 C)

AS ROLLED

BILLET NUMBER		S <sub>y</sub> (MPa)	S <sub>u</sub> (MPa)	σ <sub>y</sub> (MPa)	σ <sub>u</sub> (MPa)	% STRAIN MEASURED (%)
(1)	(a)	**	**	270	456	11.7
(1)	(b)	**	**	310	450	9.5
(2)	(c)	**	**	**	500.8	8.0
(2)	(d)	**	**	**	457.6	13.2
(2)	(e)	**	**	**	445.9	12.2
Zr21-1AR		317.6	484.3	318.2	522.0	4.9
Zr19-1AR		335.3	489.4	336.0	525.8	5.0
Zr19-2AR		308.5	458.9	309.1	496.7	5.1
Zr24-2AR		314.3	445.3	315.0	490.9	8.0
Zr24-1AR		295.6	441.6	296.2	489.3	9.0
Zr34-1AR		281.2	430.9	281.8	487.3	9.1
Zr20-1AR		316.6	496.2	317.2	553.3	9.2

AS ROLLED--ANNEALED 1 HR AT 300 C

Zr34-2AR 310.3 646 252.9 476.4 12.2

AS ROLLED--ANNEALED 1 HR 15 MIN. AT 300 C

Zr34-3AR 203.0 407.8 203.3 520.9 12.2

\* Specimen fractured before 0.1 true strain

\*\* Not available

(1) Alcamo p. 47 Two strain rates (S<sup>-1</sup>)  $1.07 \times 10^{-3}$  (a),  $10^{-2}$  (b)  
(2) Hartmann p. 43 Three strain rates (S<sup>-1</sup>)  $6.67 \times 10^{-4}$  (c),  
 $0.67 \times 10^{-3}$  and  $6.67 \times 10^{-2}$ .

In industrial application of superplastic forming, some portions of a finished part are annealed at the warm forming temperatures while others are deformed. Room temperature tensile test specimens were statically annealed at the warm forming temperature (300 C) to provide data on material



annealed only in addition to the data on samples experiencing superplastic forming. Table VI includes these results. Compared to the as-rolled material, the annealed material shows a sharp increase in ambient temperature ductility with a corresponding decrease in yield and ultimate strengths. This is to be expected for a recovered work hardened material. Berthold [Ref. 22: p. 60] has shown that at 300 C only recovery, not recrystallization, occurs in this material.

### 3. Ambient Temperature Mechanical Properties

The results of ambient temperature tensile testing on specimens cut from the previously warm deformed materials are presented in Table VII.

TABLE VII

AMBIENT TEMPERATURE PROPERTIES OF AL-10MG-0.1ZR SOLUTION  
TREATED AT 440 C, AFTER SIMULATED SUPERPLASTIC FORMING

WARM DEFORMED AT 300 C BILLET NUMBER	STRAIN RATE (S <sup>-1</sup> )	STRAIN (%) NOM	STRAIN (%) LOCAL	S <sub>y</sub> (MPa)	S <sub>u</sub> (MPa)	σ <sub>y</sub> (MPa)	σ <sub>u</sub> (MPa)	%STRAIN MEASURED
Zr21-2	10 <sup>-3</sup>	100	100	244.3	338.1	244.8	347.2	1.7
Zr19-1	10 <sup>-3</sup>	200	100	260.6	382.5	261.1	402.6	4.7
Zr23-2	10 <sup>-3</sup>	100	100	268.0	417.6	268.6	469.8	8.9
Zr22-1B	10 <sup>-3</sup>	140	150	282.7	423.1	283.3	463.9	7.2
Zr22-1A	10 <sup>-3</sup>	140	150	282.3	423.4	282.9	474.4	8.9
Zr34-1	10 <sup>-3</sup>	160	200	263.9	402.2	264.4	439.1	5.8
Zr21-1	10 <sup>-2</sup>	100	75	280.1	407.4	280.6	432.6	4.5
Zr19-2	10 <sup>-2</sup>	100	100	267.5	362.3	268.0	377.9	2.6
Zr18-2	10 <sup>-2</sup>	100	100	285.7	463.3	286.3	531.7	11.2
Zr23-1	10 <sup>-2</sup>	100	200	220.8	438.8	221.2	516.1	12.2

The data shows some very attractive properties for this alloy. It is superplastically deformable at warm temperature to at least 200% strain at strain rates of 1.67X10<sup>-2</sup> S<sup>-1</sup> (i.e. about 2 percent per second). The room temperature yield and ultimate strengths fall only slightly as a result of the warm deformation. The ambient temperature ductilities of this alloy varied from two to twelve percent. The higher

ductilities are excellent in comparison to current commercial superplastic aluminum alloys. The wide variability in the ductilities is of serious concern, however there is no discernible pattern to the scatter in the values obtained. Optical microscopy, up to 800X, provides no clues to the cause of the variability in room temperature ductility of the previously warm deformed material.

The photomicrographs show no cavities and no association of the fracture with 2nd phase particles. When the cause of the variability is discovered and if it can be controlled this will be a very attractive alloy with high strength to weight ratio for superplastic forming.

#### 4. Optical Microscopy

Optical microscopy was performed on this alloy to help determine the cause of the variability in the mechanical test results, particularly the wide scatter in the ambient temperature ductilities after warm deformation. Optical microscopy was also done to see if there was any discernible difference between the two solution treatments applied to this alloy, as was discussed in the previous section of this chapter. Figures 4.9 through 4.11 are of two of the least and most ductile samples at a given strain and strain rate combination. Photomicrographs are of the fracture surface sectioned as shown in Figure 3.6. Magnification is indicated at the bottom of each Figure. The most notable difference between high and low ambient temperature ductility specimens is the size of the flat area perpendicular to the tensile axis. The more ductile the sample the smaller the flat area, example Figure 4.11. This follows the general trend for ductile materials. The angled outer fracture lip is indicative of ductile fracture. The small amount of necking, example Figure 4.12, is typical of high-Magnesium Aluminum-Magnesium alloys, as noted by McNelley-Garg and by McNelley. [Refs. 17,26]. At this level of magnification there are no apparent reasons for the

variability in the ambient temperature ductility between samples with the same prior thermomechanical history. Crack path, as noted previously, does not appear to follow any particular features in the structure.

#### D. AL-10MG-0.1ZR SOLUTION TREATED AT 490 C

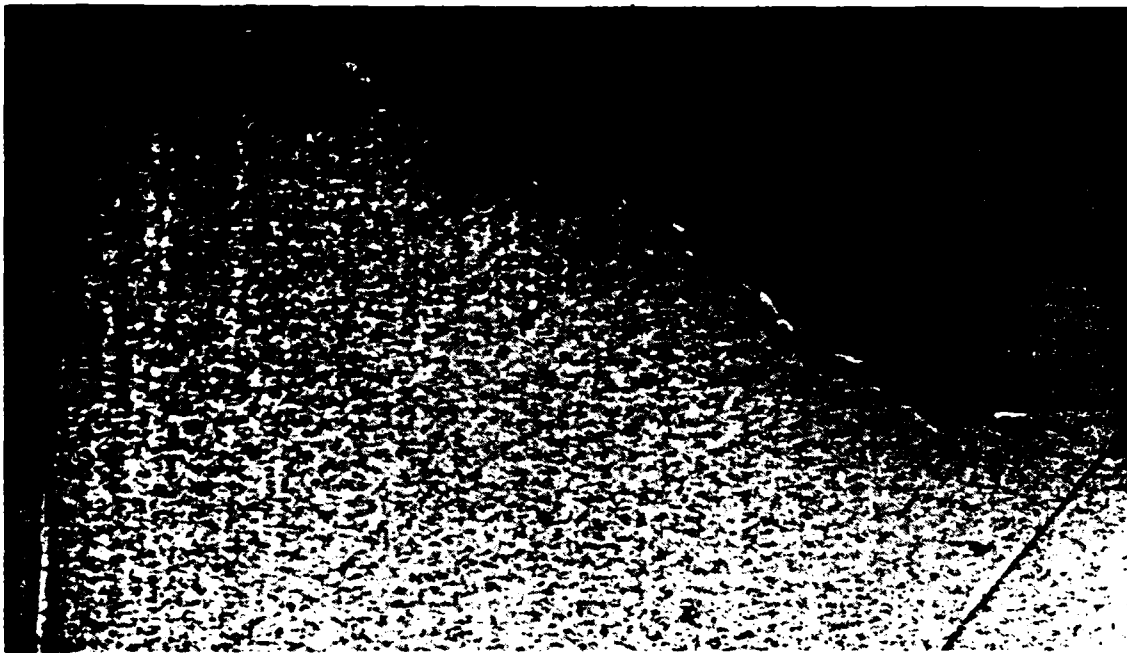
##### 1. Simulated Superplastic Forming at 300 C

Samples of the as-rolled material were warm deformed at 300 C to nominal strains of 100, 150, 170 and 200 percent strain at strain rates of either  $1.67 \times 10^{-3} \text{ S}^{-1}$  or  $1.67 \times 10^{-2} \text{ S}^{-1}$ . As with the 440 solution treated Zirconium alloy, severe inhomogeneities in the deformation of the gage section were experienced. Therefore, the intermediate strains of 150 and 170 percent were used to obtain local deformations of 200 percent in the  $1.67 \times 10^{-3} \text{ S}^{-1}$  strain rate samples. Figure 4.13 shows the most uniform specimens obtained in simulated superplastic forming to 100 and 200 % for both strain rates. All specimens of this test group are shown in Figure 4.14 .

The flow stresses for this alloy are equal to those for the 440 C solution treatment. Previous Figure 4.8 shows this comparison.

##### 2. As-rolled and As-rolled Plus Anneal

Table VIII gives the ambient temperature tensile test results for this processing condition. This solution treatment of this alloy shows ambient temperature ductility in the as-rolled condition ranging from 4.6 to 10.5 percent. Annealing at 300 C produces the expected increase in ductility with corresponding decrease in yield and ultimate strengths for a recovered material. The randomly-distributed, large ZrAl<sub>3</sub> particles shown in Figure 4.15 for the 440 C solution treatment are also present in the 490 C solution treated material, Figure 4.16 The increased solution treating temperature does not appreciably reduce the number or size of the ZrAl<sub>3</sub> particles. As noted

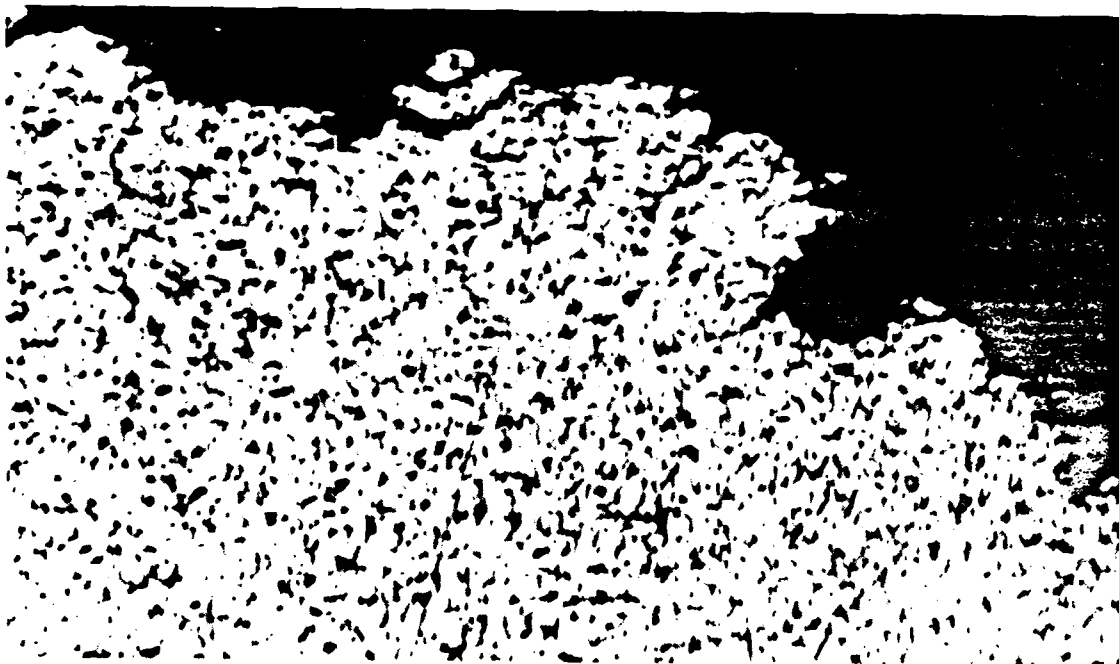


(a) 1.7 % ambient temperature ductility. Barkers etch, X100.

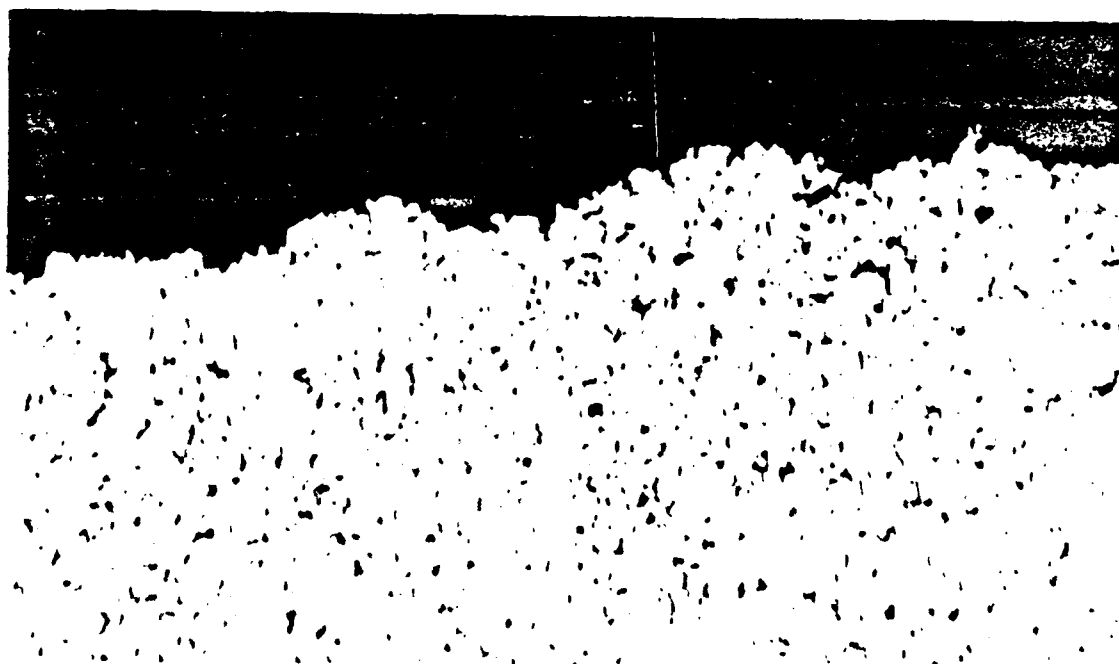


(b) 8.9 % ambient temperature ductility. Barkers etch, X100.

Figure 4.9 Al-10Mg-0.1Zr Solution Treated at 440,  
Warm Deformed at 300 C to 100% Strain.

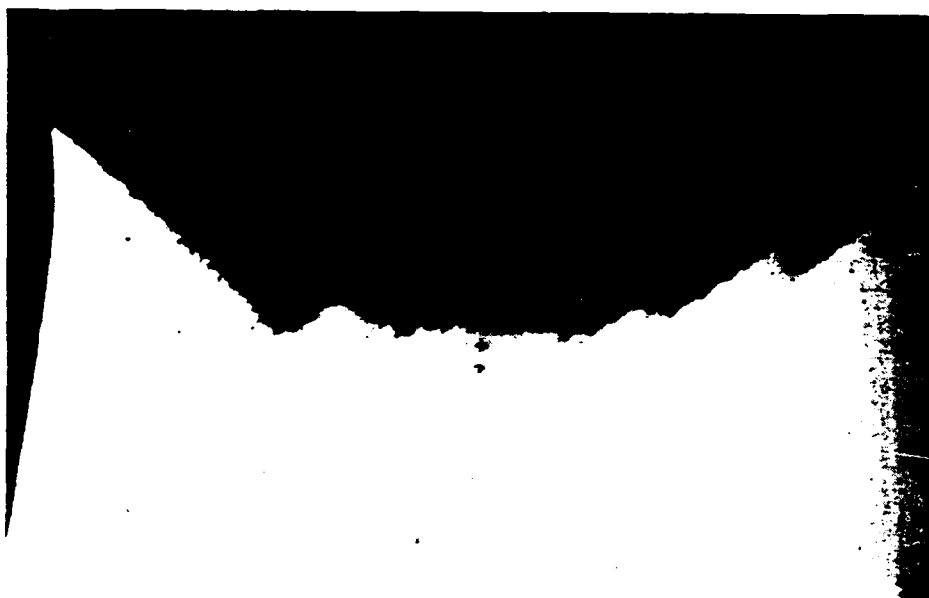


(a) 1.7% ambient temperature ductility. Barkers etch, X800.

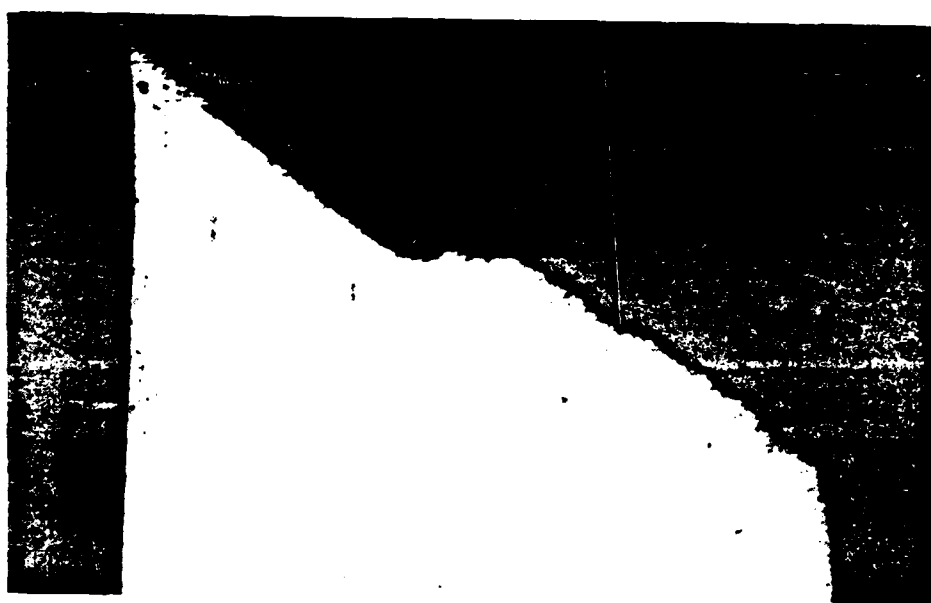


(b) 8.9 % ambient temperature ductility. Barkers etch, X800.

Figure 4.10 Al-10 $\frac{1}{2}$ g-0.12r Solution Treated at 440,  
Warm Deformed at 300 C to 100% Strain.

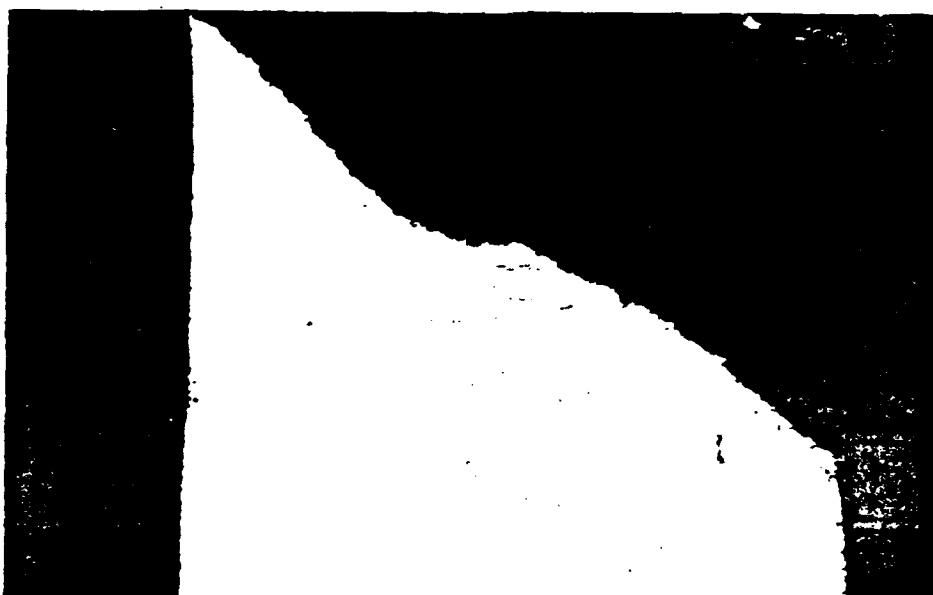


(a) 2.6% ambient temperature ductility. Barkers etch, X80.

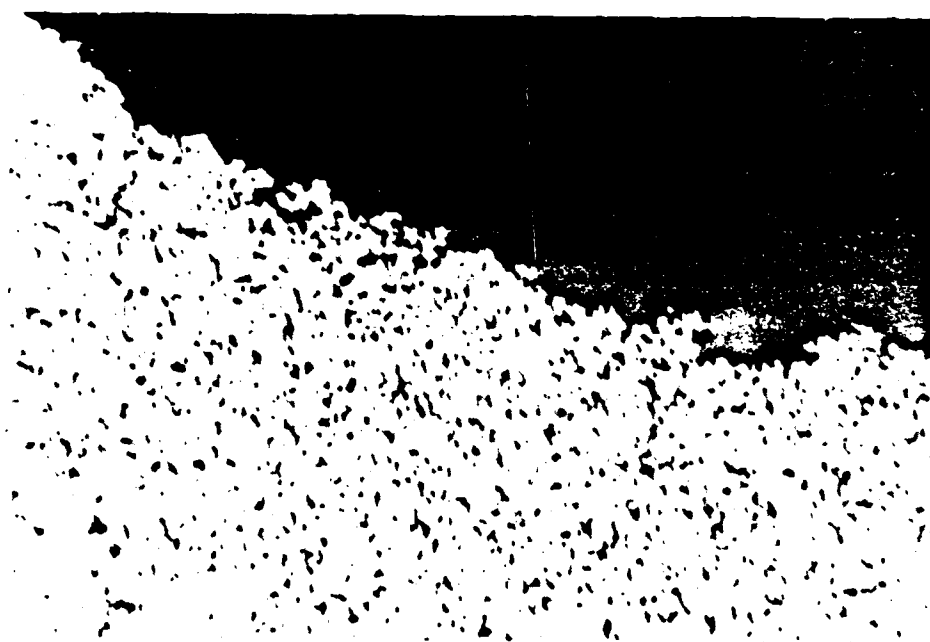


(b) 11.4% ambient temperature ductility. Barkers etch, X80.

Figure 4.11 Al-10Mg-0.1Zr Solution Treated at 440,  
Warm Deformed at 300 C to 100% Strain.



(a) 12.2 % ambient ductility. Barkers etch, X80.



(b) 12.2% ambient ductility . Barkers etch, 640 X

Figure 4.12 Al-10Mg-0.1Zr Solution Treated at 440,  
Warm Deformed at 300 C to 100% Strain.

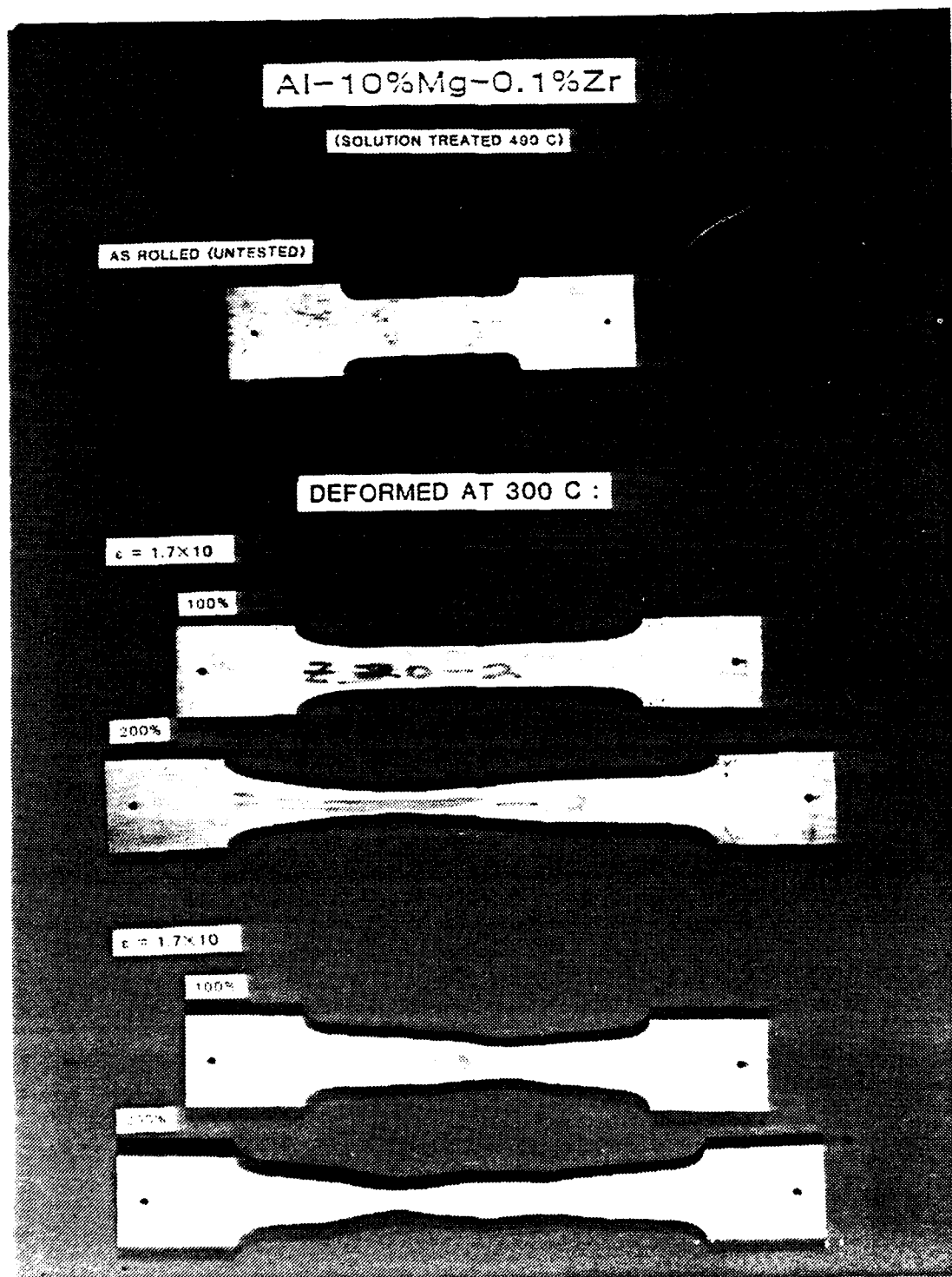


Figure 4.13 Specimens of Al-10Mg-0.1Zr Solution Treated at 490 C. Warm Deformed at 300 C..



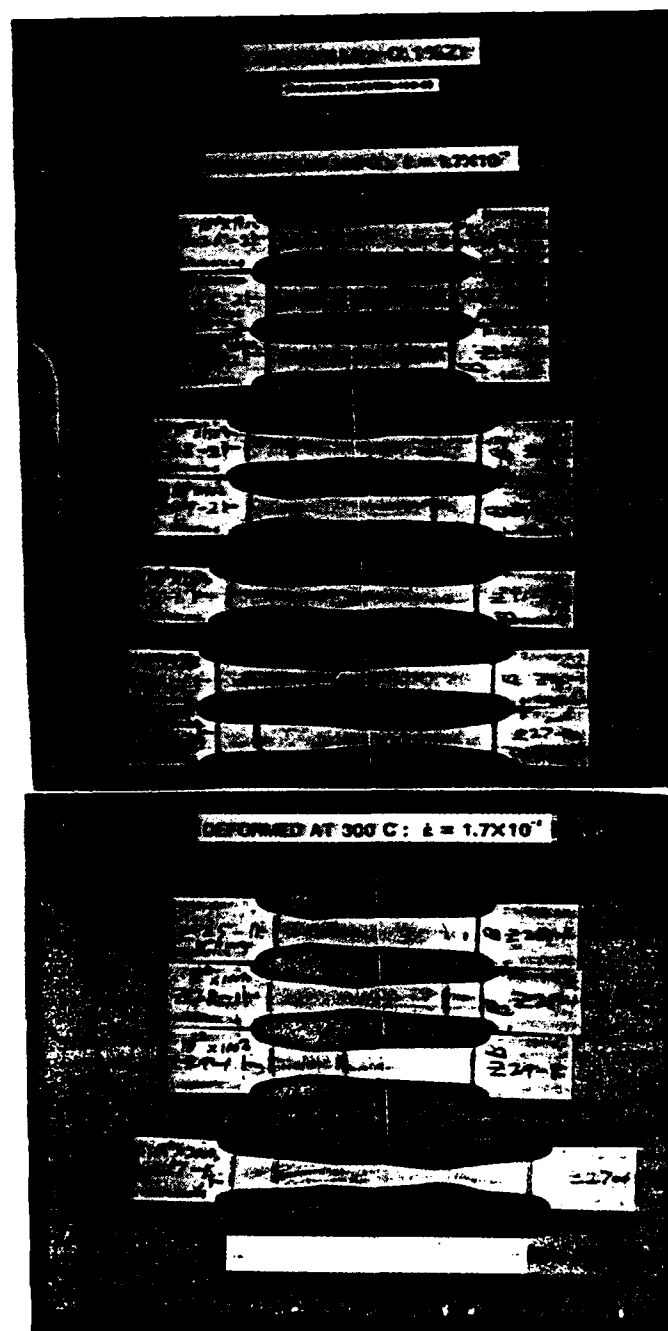


Figure 4.14 Al-10Mg-0.1Zr Solution Treated at 490 C All Samples Warm Deformed at 300 C.

**TABLE VIII**  
**DATA FOR AS-ROLLED AL-10MG-0.1ZR**  
**SOLUTION TREATED AT 490 C**

AL-10MG-0.1ZR  
(SOLUTION TREATED AT 490 C)

AS ROLLED:

BILLET NUMBER	$S_y$ (MPa)	$S_u$ (MPa)	$\sigma_y$ (MPa)	$\sigma_u$ (MPa)	%STRAIN MEASURED (%)
Zr21-1AR	317.6	484.3	318.2	522.0	4.9
Zr19-1AR	335.3	489.4	336.0	525.8	5.0
Zr19-2AR	308.5	458.9	309.1	496.7	5.1
Zr24-2AR	314.3	445.3	315.0	490.9	8.0
Zr24-1AR	295.6	441.6	296.2	489.3	9.0
Zr34-1AR	281.2	430.9	281.8	487.3	9.1
Zr20-1AR	316.6	496.2	317.2	553.3	9.2

AS ROLLED--ANNEALED 1 HR AT 300 C  
Zr34-2AR 310.3 646 252.9 476.4 12.2

AS ROLLED--ANNEALED 1 HR 15 MIN. AT 300 C  
Zr34-3AR 203.0 407.8 203.3 520.9 12.2

AL-10MG-0.1ZR  
(SOLUTION TREATED AT 490 C)

AS ROLLED:

BILLET NUMBER	$S_y$ (MPa)	$S_u$ (MPa)	$\sigma_y$ (MPa)	$\sigma_u$ (MPa)	%STRAIN MEASURED (%)
Zr26-1AR	331.0	507.3	331.6	552.4	4.6
Zr28-2AR	335.9	475.2	336.5	511.7	5.6
Zr28-1AR	320.7	474.5	321.3	522.6	7.0
Zr28-3AR	341.9	438.6	342.6	462.0	7.4
Zr25-1AR	312.0	448.5	312.6	492.4	9.4
Zr30-2AR	273.5	436.8	274.0	490.1	9.8
Zr30-1AR	286.3	433.3	286.9	488.5	10.5

AS ROLLED--ANNEALED 1 HR AT 300 C  
Zr25-2AR 261.4 416.3 261.9 481.1 12.2

AS ROLLED--ANNEALED 1 HR 15 MIN. AT 300 C  
Zr25-3AR 256.5 421.4 257.0 496.2 14.0

by Berthold [Ref. 22]. they are most likely formed above 660 C by reaction in the liquid.

### 3. Ambient Temperature Mechanical Properties

The results of the ambient temperature tensile testing on the specimens given simulated superplastic forming are presented in Table IX .

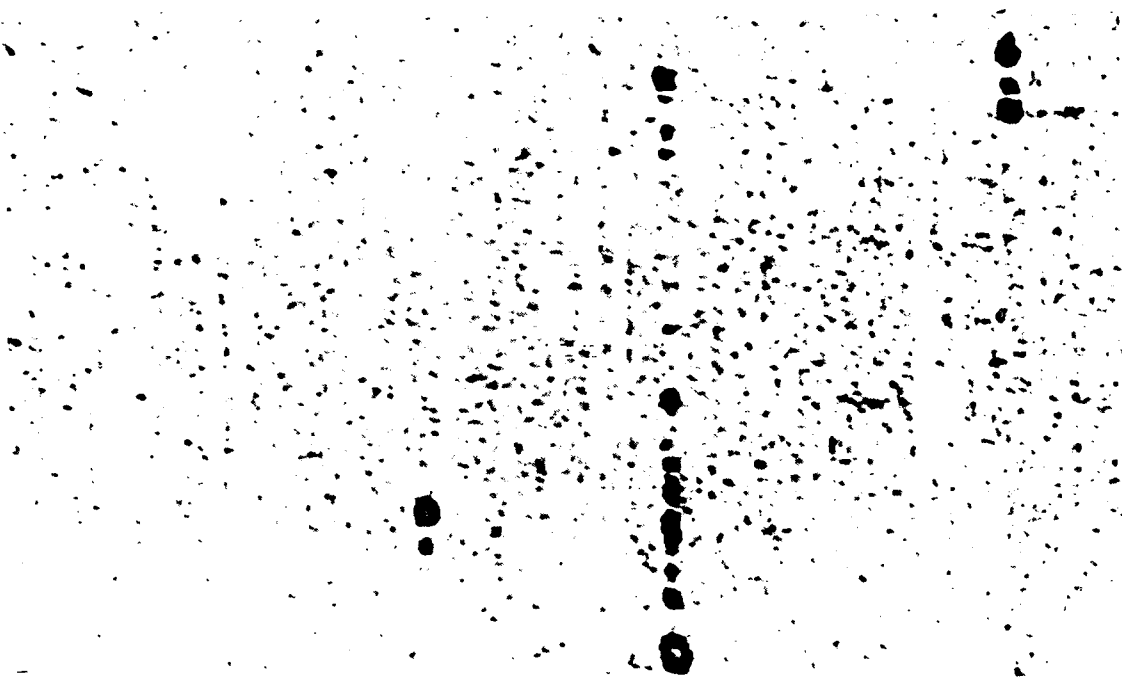
The data illustrates attractive properties for this alloy. First, it is superplastically deformable to 200 percent strain at  $1.67 \times 10^{-2}$  S<sup>-1</sup> strain rate ( 2%/second) The ambient temperature yield strength after simulated superplastic forming, about 260 MPa (38 KSI), is below that of the as-rolled condition but comparable to that of the annealed condition of this alloy and substantially higher than the strength of commercial Al-Mg alloys. This alloy/heat treatment combination has lower yield strengths (260 MPa vs 300 or 420 MPa) than Supral 100 or Supral 210 respectively as given by Barnes [Ref. 27: p. 7] but has equal ultimate strengths and nearly double (14.5 % vs 8 %) ambient temperature ductility after warm deformation. The higher ductilities in conjunction with the strength are very good. As with the Zirconium-containing alloy, solution treated at 440 C, there is no discernable pattern to the scatter in the ambient temperature ductility data. Again, optical microscopy does not reveal any cause for the variable ductility either.

#### E. AL-10MG-0.5MN SOLUTION TREATED AT 440 C

##### 1. Simulated Superplastic Forming at 300 C

Samples of the as-rolled material were warm deformed as specified in the test section. The inhomogeneities in deformation experienced with the Zirconium-containing alloy were not present in the Manganese -containing alloy. Figure 4.17 shows a representative set of warm deformation specimens, one for each strain/strain rate combination.

Figure 2Mn440all in appendix B shows all warm deformed specimens for this alloy/ heat treatment combination. Warm deformation flow stresses were consistent with those found by Self [Ref. 20: p. 66] as are shown in Figure 4.18.

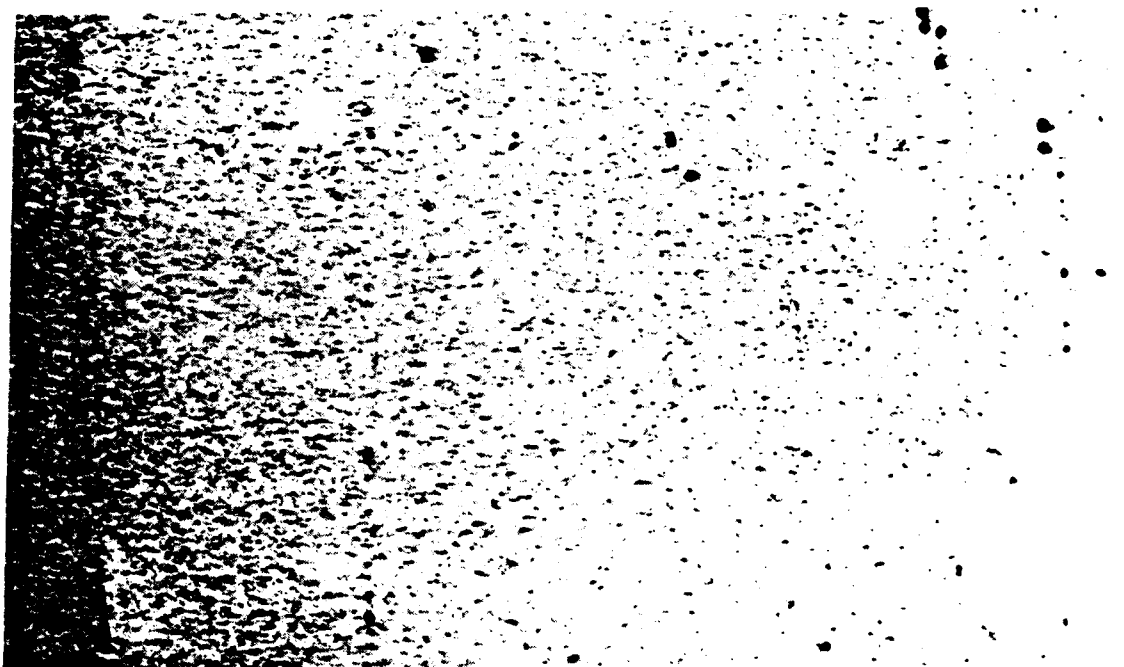


(a) Barkers etch, X100.



(b) Barkers etch, X800.

Figure 4.15 Large  $ZrAl_3$  Particles Present in the  
As-Rolled Al-10Mg-0.12Zr alloy solution treated at 440 C.



(a) Barkers etch, X100.



(b) Barkers etch, X800.

Figure 4.16 Large  $ZrAl_3$  Particles Present in the  
As-Rolled Al-10Mg-0.1Zr Alloy Solution Treated at 490 C.

**TABLE IX**  
**AMBIENT TEMPERATURE TENSILE TEST RESULTS**  
**FOR AL-10MG-0.1ZR SOLUTION TREATED AT 490 C**

WARM DEFORMED AT 300 C:

BILLET NUMBER	STRAIN RATE	STRAIN NOM	STRAIN LOCAL	$S_y$	$S_u$	$\sigma_y$	$\sigma_u$	% STRAIN MEASURED
	(S <sup>-1</sup> )	(%)	(%)	(MPa)	(MPa)	(MPa)	(MPa)	(%)
Zr28-2B	10 <sup>-3</sup>	155	100	261.0	281.0	261.5	283.4	1.4
Zr28-2A	10 <sup>-3</sup>	155	100	247.7	356.3	248.2	368.7	1.9
Zr29-2B	10 <sup>-3</sup>	150	100	268.5	428.6	241.3	459.5	4.0
Zr25-2	10 <sup>-3</sup>	100	100	276.9	390.1	277.4	409.2	5.2
Zr26-2	10 <sup>-3</sup>	100	100	232.0	404.0	232.5	440.9	7.0
Zr31-1B	10 <sup>-3</sup>	170	200	259.3	279.6	259.9	282.6	0.8
Zr26-1A	10 <sup>-3</sup>	200	200	273.5	428.8	273.9	492.3	9.8
Zr26-1B	10 <sup>-3</sup>	200	200	243.3	443.1	243.9	526.2	13.9
Zr29-2A	10 <sup>-3</sup>	150	225	254.3	454.7	254.8	511.5	14.5
Zr31-1A	10 <sup>-3</sup>	170	300	250.6	283.5	251.1	288.8	1.8
Zr25-1	10 <sup>-2</sup>	100	100	271.5	303.9	272.0	306.3	0.7
Zr29-1	10 <sup>-2</sup>	100	100	280.4	327.1	281.0	332.3	1.2

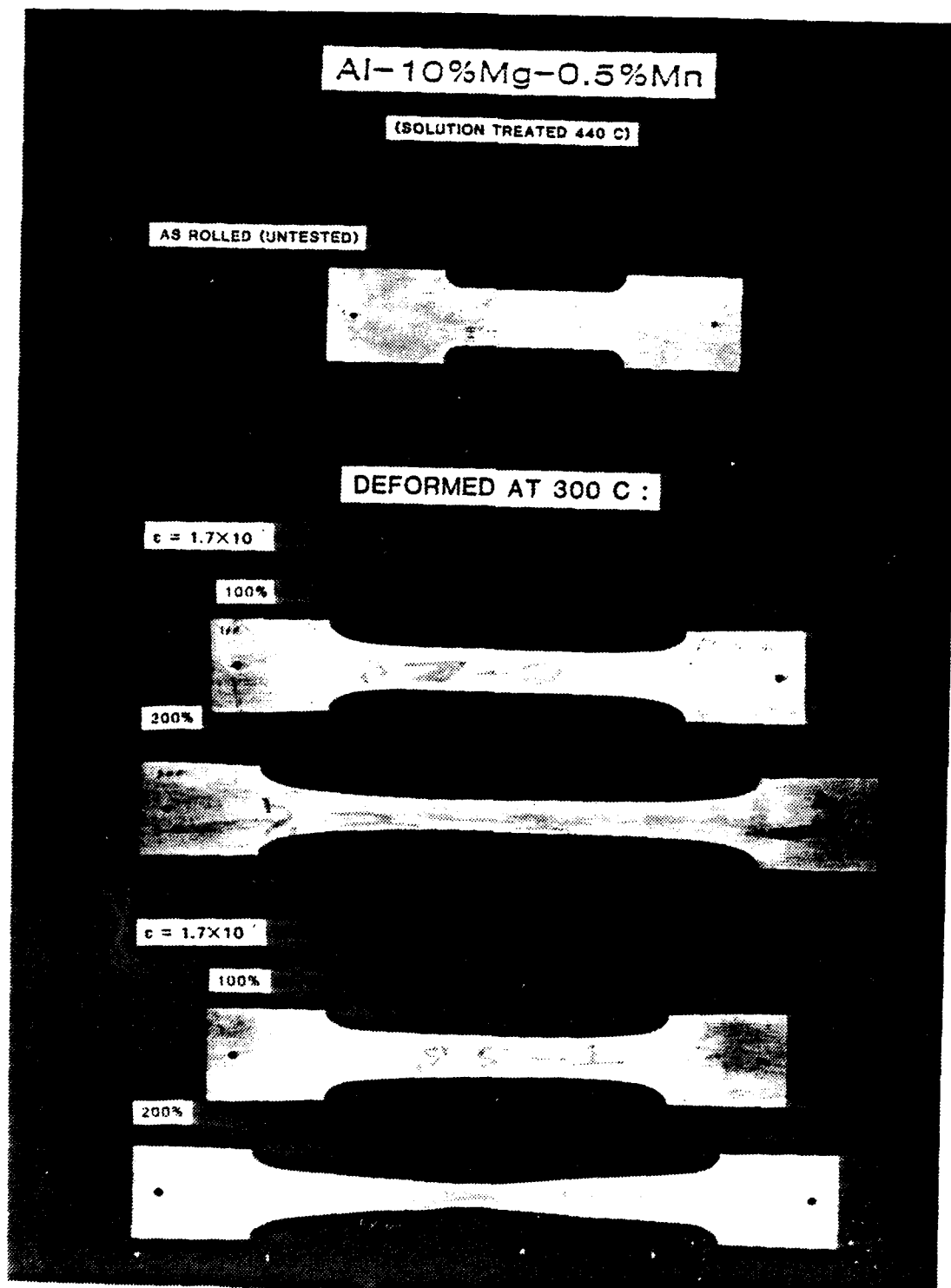


Figure 4.17 Al-10Mg-0.5Mn Solution Treated at 440 C  
Warm Rolled at 300 C.

# AL-10MG-0.5MN WARM FLOW STRESS

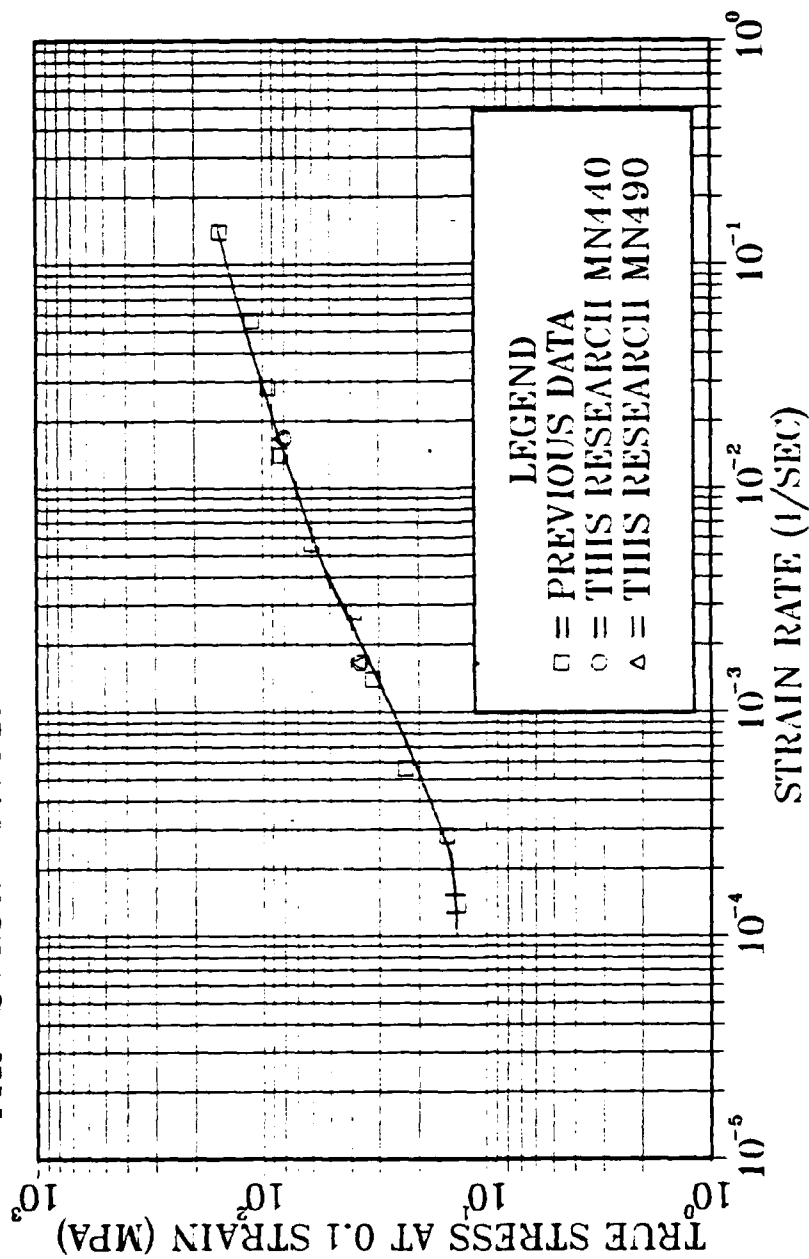


Figure 4.18 True Stress at 0.1 Strain vs Strain Rate  
During Simulated Superplastic Forming at 300 C.



The  $m$  value taken from the slope of the curve in Figure 4.18 is about 0.5. This is consistent with the  $m$  values found for this alloy by both Mills and Self [Refs. 14,20: pp. 45, 66]. It is also in the range of 0.3 to 0.7 Specified by Sherby and Wadsworth [Ref. 5: p.363] as being a normal  $m$  value for superplasticity.

## 2. As-rolled and As-rolled Plus Anneal

As-rolled samples were tested for comparison with previous work by Mills [Ref. 14]. Strain rate for this work was  $8.3 \times 10^{-4} \text{ S}^{-1}$ . Table X shows comparison of the ambient temperature mechanical test results between this work and previous work.

TABLE X  
DATA FOR AS-ROLLED AL-10MG-0.5MN  
TESTED AT AMBIENT TEMPERATURE

AL-10MG-0.5MN  
(SOLUTION TREATED AT 440 C)

### AS ROLLED:

BILLET NUMBER	$S_y$ (MPa)	$S_u$ (MPa)	$\sigma_y$ (MPa)	$\sigma_u$ (MPa)	% STRAIN MEASURED (%)
(1) (a)	**	**	**	414	3.0
(1) (b)	**	**	**	478	3.2
(1) (c)	**	**	**	503	3.2
MN7-2AR	299.3	470.4	300.0	496.7	2.8
MN6-3AR	258.8	481.7	259.3	495.9	3.4
MN2-3AR	309.4	410.7	310.1	514.4	4.0
MN2-2AR	246.7	482.2	297.3	515.5	4.2
MN2-1AR	340.6	504.4	341.3	538.2	5.1
MN7-1AR	375.8	522.0	376.6	552.8	5.8

AS ROLLED--ANNEALED 1 HR AT 300 C  
MN6-1AR 325.2 446.2 325.8 484.2 7.4

AS ROLLED--ANNEALED 1 HR 15 MIN. AT 300 C  
MN6-2AR 275.3 462.7 275.9 556.2 14.4

\*\* data not available

(1) Mills p. 47. Three strain rates ( $\text{S}^{-1}$ ):  $5.0 \times 10^{-4}$  (a),  $5.6 \times 10^{-3}$  (b) and  $5.6 \times 10^{-2}$  (c).

### 3. Ambient Temperature Mechanical Properties

The results of mechanical testing of the previously warm deformed material are presented in Table XI

TABLE XI  
DATA FOR AMBIENT TEMPERATURE MECHANICAL TESTS  
OF PREVIOUSLY WARM DEFORMED AL-10MG-0.5MN

(SOLUTION TREATED AT 440 C)

WARM DEFORMED AT 300 C

BILLET NUMBER	STRAIN RATE	STRAIN		$S_y$	$S_u$	$\sigma_y$	$\sigma_u$	% STRAIN MEASURED
	( $S^{-1}$ )	(%)	(%)	(MPa)	(MPa)	(MPa)	(MPa)	(%)
MN2-2	$10^{-3}$	100	100	296.8	317.5	297.4	320.3	0.4
MN2-2A	$10^{-3}$	100	100	293.3	422.7	293.9	450.3	4.1
MN2-2B	$10^{-3}$	100	100	289.2	412.2	289.8	436.9	4.5
MN5-2B	$10^{-3}$	200	200	304.1	428.9	304.7	454.7	3.1
MN6-2B	$10^{-3}$	200	200	317.7	445.8	318.3	498.2	6.2
MN1-1A	$10^{-3}$	200	200	257.3	446.7	257.7	497.2	7.6
MN1-1B	$10^{-3}$	200	200	244.7	434.5	245.4	478.0	8.2
MN6-2A	$10^{-3}$	200	200	319.6	468.3	320.3	518.7	9.0
MN5-2A	$10^{-3}$	200	200	317.4	459.8	318.1	524.0	9.5
MN7-1	$10^{-2}$	100	100	271.9	421.6	272.4	447.3	3.7
MN4-1	$10^{-2}$	100	100	306.0	442.0	306.6	472.9	4.6
MN3-1	$10^{-2}$	100	100	253.4	434.4	253.9	465.4	5.1

Yield and ultimate strengths do not show any appreciable decrease with the amount of prior simulated superplastic forming. The 290 MPa (42 KSI) in conjunction with the maximum ductilities obtained are a very good combination, in fact they are better than those for the zirconium-containing alloy. The problem of wide variability in room temperature ductility after simulated superplastic forming observed with the Zirconium-containing alloy were also observed in this alloy. A notable example are specimens Mn5-2B and Mn5-2A, the least and most ductile results in the 200% nominal strain section. These two specimens were remachined from the same warm deformation specimen. Photomicrographs, Figures 4.19 and 4.20, shown no obvious differences between these

two specimens. In fact the fracture surface of the less ductile sample has larger shear lips than the more ductile sample, Figure 4.19

Several of the more ductile, ambient-temperature specimens had load versus elongation curves more characteristic of mild steels than Aluminum. Figure 4.21 is a copy of a typical one of these curves, showing an appreciable Luders strain and finally a strain hardening region. The serrations throughout the curve were discussed in the background section and are likely due to the Magnesium in solid solution interacting with moving dislocations. The Luders straining would be indicative of an unlocking of dislocations from solute atmospheres.

#### 4. Optical Microscopy

Optical Microscopy was performed on this alloy to help determine the cause of the variability in the mechanical test results, particularly in the ambient temperature ductility of the previously warm deformed material. As shown earlier in Figures 4.19 and 4.20, optical microscopy provided no obvious cause for the variability in room temperature ductility.

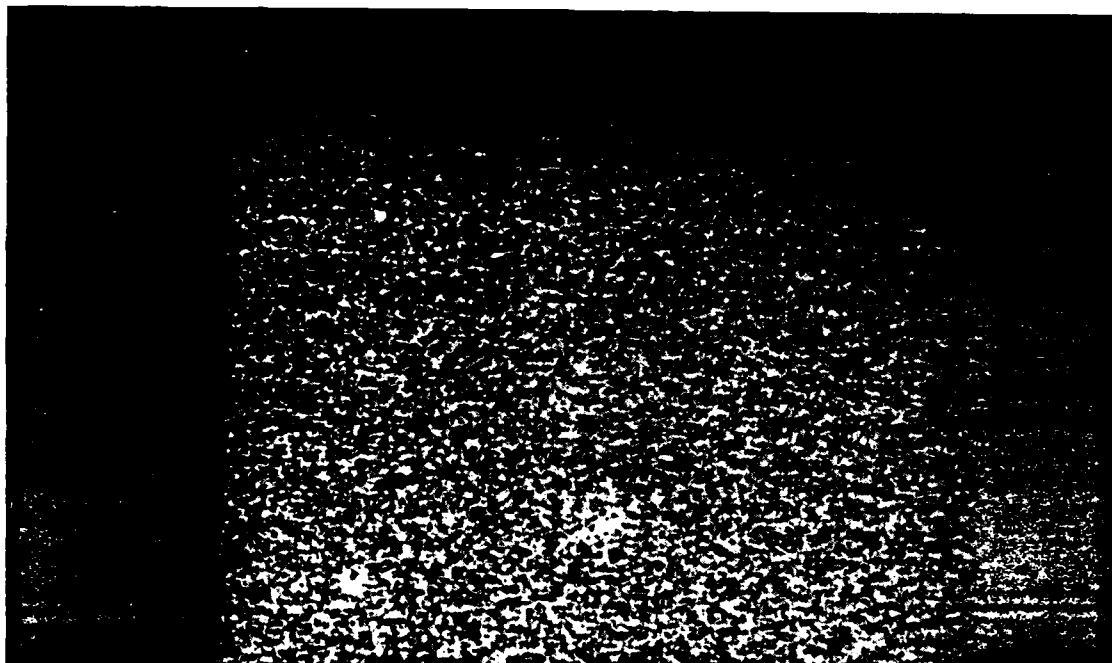
### F. AL-10MG-0.5MN SOLUTION TREATED AT 490 C

#### 1. Simulated Superplastic Forming at 300 C

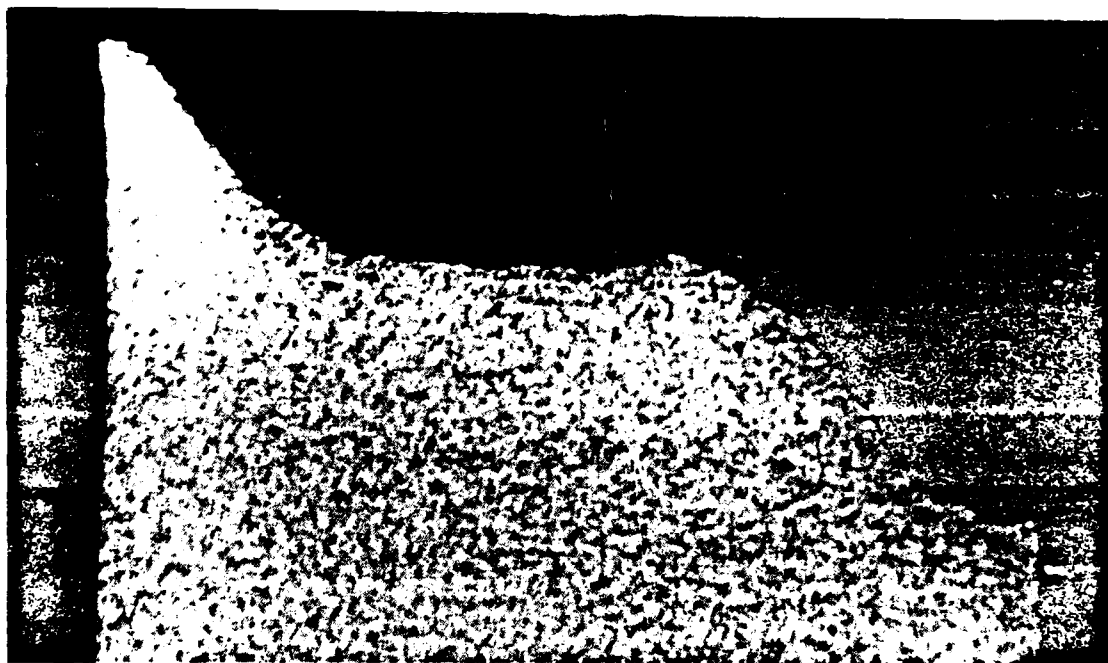
Figure 4.22 shows representative warm deformation specimens for each strain/strain rate combination applied to this alloy.

The notable feature of this alloy and solution treatment temperature combination was the uniformity of deformation of the gage section. Even at simulated superplastic forming strains of 200 % at  $1.67 \times 10^{-2} \text{ S}^{-1}$ , strain rate, gage section deformation was uniform, more so than any other alloy/TMP combination examined. Figure 4.23 shows all warm deformed specimens in this test group.

Figure 4.18 A comparison of the flow stresses at 300 C for this work, at both 490 C and 440 C solution treating

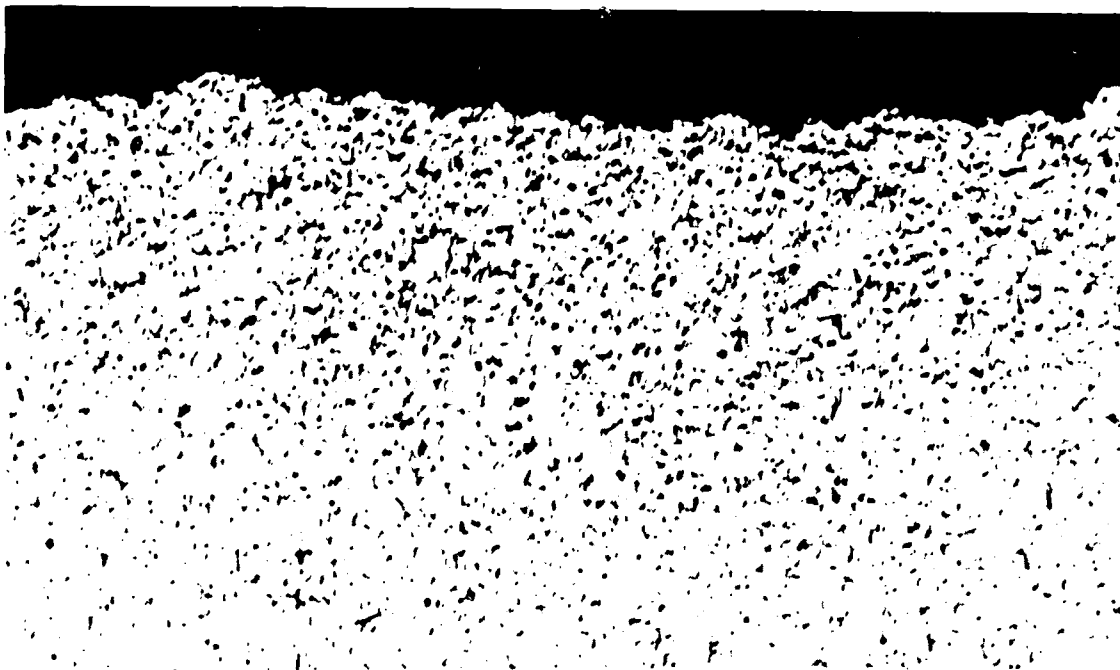


(a)

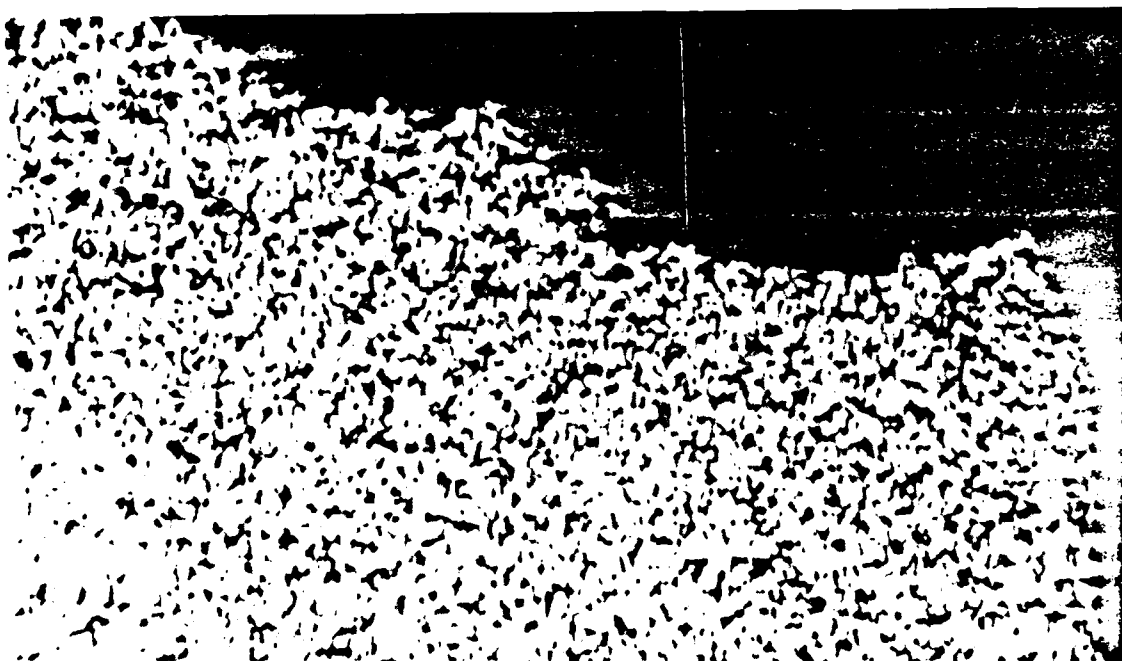


(b)

Figure 4.19 Al-10Mg-0.5Mn Warm Deformed to 200% Strain  
Room Temperature Ductility 9.5% (a) and 1.7% (b) Barkers etch  $\times 100$ .



(a)



(b)

Figure 4.20 Al-10Mg-0.5Mn Warm Deformed to 200% Strain  
Room Temperature Ductility 9.5% (a) and 3.1% (b) Barkers etch X800.

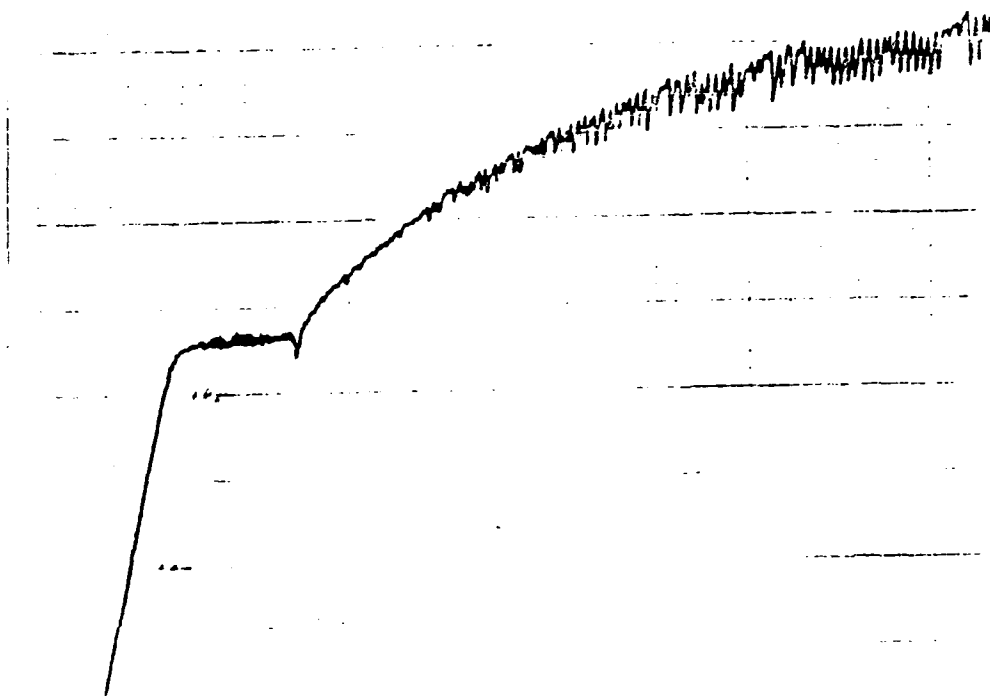


Figure 4.21 Instron Produced Load vs Elongation Chart for Al-10Mg-0.5Mn Specimen Showing Large Luders Section.

temperatures, and data from Mill's [Ref. 14: p. 39] previous work on this alloy, solution treated at 440 C. This comparison shows no apparent effect of solution treating temperature on flow stresses for this alloy in the strain rate range tested. The slope of the line segments from this work are about the same as Mills' work suggesting an "n" value of 0.4 to 0.5 for this alloy.

## 2. As-rolled and As-rolled Plus Anneal

As-rolled and as-rolled plus annealed samples were tested in tension at ambient temperature. Table XII gives the mechanical test results and provides a comparison with the results of the 440 C solution treated material. The

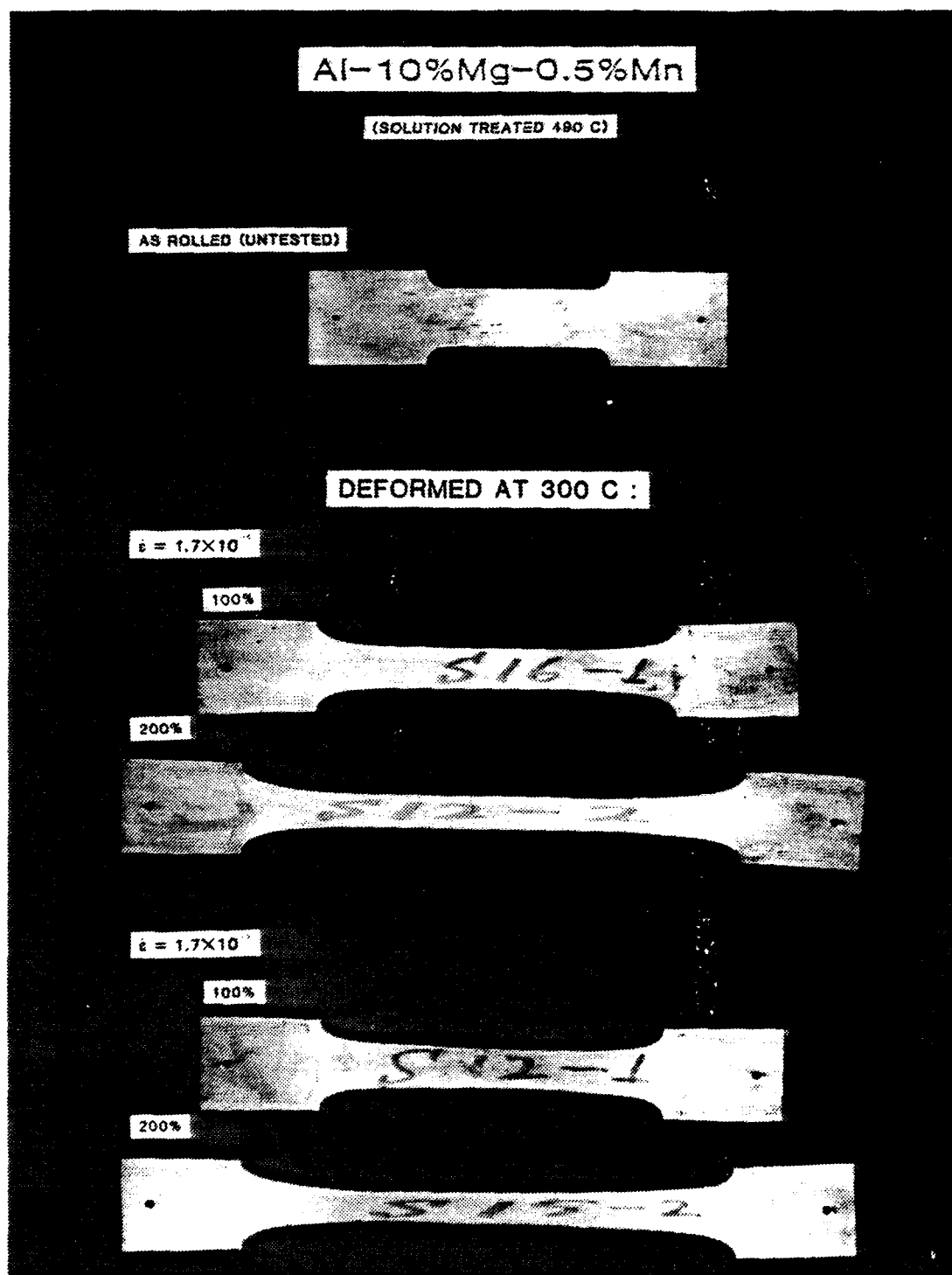


Figure 4.22 Al-10Mg-0.5Mn Solution Treated at 490 C  
Warm Deformed at 300 C.

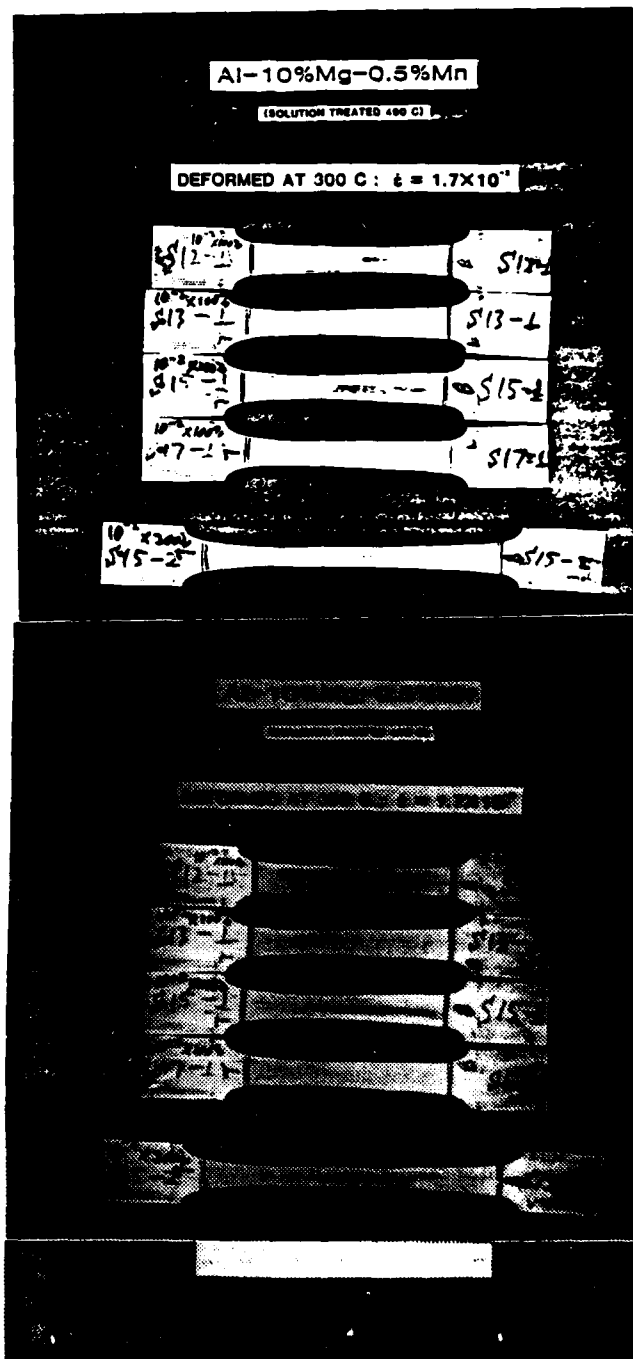


Figure 4.23 Al-10Mg-0.5Mn Solution Treated at 490 C  
All Specimens Warm Deformed at 300 C.



results are similar to the 440 C solution treatment, but have slightly better ambient temperature ductilities both as-rolled and after a 75 minute anneal at 300 C.

TABLE XII  
 AMBIENT TEMPERATURE TEST DATA FOR  
 AL-10MG-0.5MN SOLUTION TREATED AT 490 C

(SOLUTION TREATED AT 490 C)

AS ROLLED: BILLET#	S <sub>y</sub> (MPa)	S <sub>u</sub> (MPa)	σ <sub>y</sub> (MPa)	σ <sub>u</sub> (MPa)	% STRAIN MEASURED (%)
MN16-3AR	332.1	485.1	332.8	504.0	2.9
MN14-1AR	259.7	467.4	260.2	441.8	3.4
MN16-1AR	338.3	507.3	388.9	541.3	3.5
MN13-1AR	298.2	492.8	298.8	519.8	4.3
MN16-2AR	333.4	513.3	334.1	551.9	4.7
MN11-2AR	271.6	502.5	272.1	546.7	5.7
AS ROLLED--ANNEALED 1 HR 15 MIN. AT 300 C					
MN11-3AR	291.9	456.8	292.6	531.7	12.6

(SOLUTION TREATED AT 440 C)

AS ROLLED: BILLET NUMBER	S <sub>y</sub> (MPa)	S <sub>u</sub> (MPa)	σ <sub>y</sub> (MPa)	σ <sub>u</sub> (MPa)	% STRAIN MEASURED (%)
MN7-2AR	299.3	470.4	300.0	496.7	2.8
MN6-3AR	258.8	481.7	259.3	495.9	3.4
MN2-3AR	309.4	410.7	310.1	514.4	4.0
MN2-2AR	246.7	482.2	297.3	515.5	4.2
MN2-1AR	340.6	504.4	341.3	538.2	5.1
MN7-1AR	375.8	522.0	376.6	552.8	5.8
AS ROLLED--ANNEALED 1 HR AT 300 C					
MN6-1AR	325.2	446.2	325.8	484.2	7.4
AS ROLLED--ANNEALED 1 HR 15 MIN. AT 300 C					
MN6-2AR	275.3	462.7	275.9	556.2	14.4

### 3. Ambient Temperature Mechanical Properties

Results of ambient temperature mechanical testing on previously warm deformed samples are presented in Table XIII. The 315 MPa (45 KSI) yield strength and 515 MPa (75 KSI) ultimate strengths in conjunction with the higher ductilities are very attractive. Almost all results for material with 200% prior simulated superplastic forming were very

**TABLE XIII**  
**AMBIENT TEMPERATURE MECHANICAL TESTS FOR**  
**AL-10MG-0.5MN AFTER WARM DEFORMATION AT 300 C**

(SOLUTION TREATED AT 490 C)

WARM DEFORMED AT 300 C:

BILLET NUMBER	STRAIN RATE	STRAIN NOM	STRAIN LOCAL	S <sub>y</sub>	S <sub>u</sub>	σ <sub>y</sub>	σ <sub>u</sub>	% STRAIN MEASURED
	(S <sup>-1</sup> )	(%)	(%)	(MPa)	(MPa)	(MPa)	(MPa)	(%)
MN14-2	10 <sup>-3</sup>	100	100	296.0	339.0	296.6	344.4	1.2
MN13-2	10 <sup>-3</sup>	100	100	263.2	334.8	263.7	343.0	2.5
MN11-1	10 <sup>-3</sup>	100	200	299.6	426.7	300.2	455.2	3.82
MN14-1A	10 <sup>-3</sup>	200	200	318.0	460.4	318.2	516.4	8.00
MN14-1B	10 <sup>-3</sup>	200	200	315.7	457.1	316.3	516.2	8.75
MN16-2B	10 <sup>-3</sup>	200	200	317.6	455.5	318.3	512.2	8.84
MN11-2A	10 <sup>-3</sup>	200	200	323.1	454.7	323.3	512.6	9.14
MN16-2A	10 <sup>-3</sup>	200	200	324.3	457.1	324.5	513.1	9.63
MN11-2B	10 <sup>-3</sup>	200	200	299.1	453.4	303.2	522.8	10.64
MN13-1	10 <sup>-2</sup>	100	100	304.6	347.9	305.2	352.7	0.90
MN15-1	10 <sup>-2</sup>	100	100	286.7	434.9	287.2	468.6	4.41
MN17-1	10 <sup>-2</sup>	100	100	297.5	437.1	298.1	466.5	4.49

good. Barnes [Ref. 27: p. 7] lists the room temperature properties of a number of current commercial high strength superplastic Aluminum alloys. Only one, SP7475, is listed with a room temperature ductility after simulated superplastic forming greater than 8 %. As with the three previous alloy/solution treatment temperature combinations presented, there is variability in the room temperature ductilities of specimens with the same prior thermomechanical history. The yield and ultimate strengths show little degradation as result of prior simulated superplastic forming. As with the Manganese containing alloy solution treated at 440 C, a number of specimens had room temperature load versus elongation charts with appreciable Luders sections before strain hardening. Comparison of the data in Tables XI and XIII show equivalent strengths at all conditions for both solution treatments. The 490 C treatment has slightly better average room temperature ductilities after 200 % simulated superplastic forming but is not as ductile after 100 % warm deformation at either strain rate.

#### 4. Optical Microscopy

Optical microscopy performed on this alloy/solution treatment combination again did not provide any conclusive explanation for the variability in ambient temperature ductility observed. Figure 4.2, which compares both solution treating temperatures shows no apparent effect of the higher solution treating temperature.

#### G. AL-10MG-0.4CU SOLUTION TREATED AT 425 C

##### 1. Simulated Superplastic Forming at 300 C

Figure 4.24 shows a representative set of warm deformed specimens of this alloy, one at each strain/strain rate combination.

This alloy deforms very uniformly at  $1.67 \times 10^{-3} \text{ S}^{-1}$  even to 200 % strain but, begins to show nonuniform deformation at 200 % strain at  $1.67 \times 10^{-2} \text{ S}^{-1}$  strain rate.

TABLE XIII

AMBIENT TEMPERATURE MECHANICAL TESTS FOR  
AL-10MG-0.5MN AFTER WARM DEFORMATION AT 300 C

(SOLUTION TREATED AT 490 C)

warm Deformed At 300 C:

BILLET NUMBER	STRAIN RATE (S <sup>-1</sup> )	STRAIN NOM LOCAL (%)	S <sub>y</sub> (MPa)	S <sub>u</sub> (MPa)	$\sigma_y$ (MPa)	$\sigma_u$ (MPa)	% STRAIN MEASURED
MN14-2	10 <sup>-3</sup>	100	296.0	339.0	296.6	344.4	1.2
MN13-2	10 <sup>-3</sup>	100	263.2	334.8	263.7	343.0	2.5
MN11-1	10 <sup>-3</sup>	100	299.6	426.7	300.2	455.2	3.82
MN14-1A	10 <sup>-3</sup>	200	318.0	460.4	318.2	516.4	3.00
MN14-1B	10 <sup>-3</sup>	200	315.7	457.1	316.3	516.2	6.75
MN16-2B	10 <sup>-3</sup>	200	317.6	455.5	318.3	512.2	6.84
MN11-2A	10 <sup>-3</sup>	200	323.1	454.7	323.3	512.6	9.14
MN16-2A	10 <sup>-3</sup>	200	324.3	457.1	324.5	513.1	9.63
MN11-2B	10 <sup>-3</sup>	200	299.1	453.4	303.2	522.8	10.64
MN13-1	10 <sup>-2</sup>	100	304.6	347.9	305.2	352.7	0.90
MN15-1	10 <sup>-2</sup>	100	286.7	434.9	287.2	468.6	4.41
MN17-1	10 <sup>-2</sup>	100	297.5	437.1	298.1	466.5	4.49

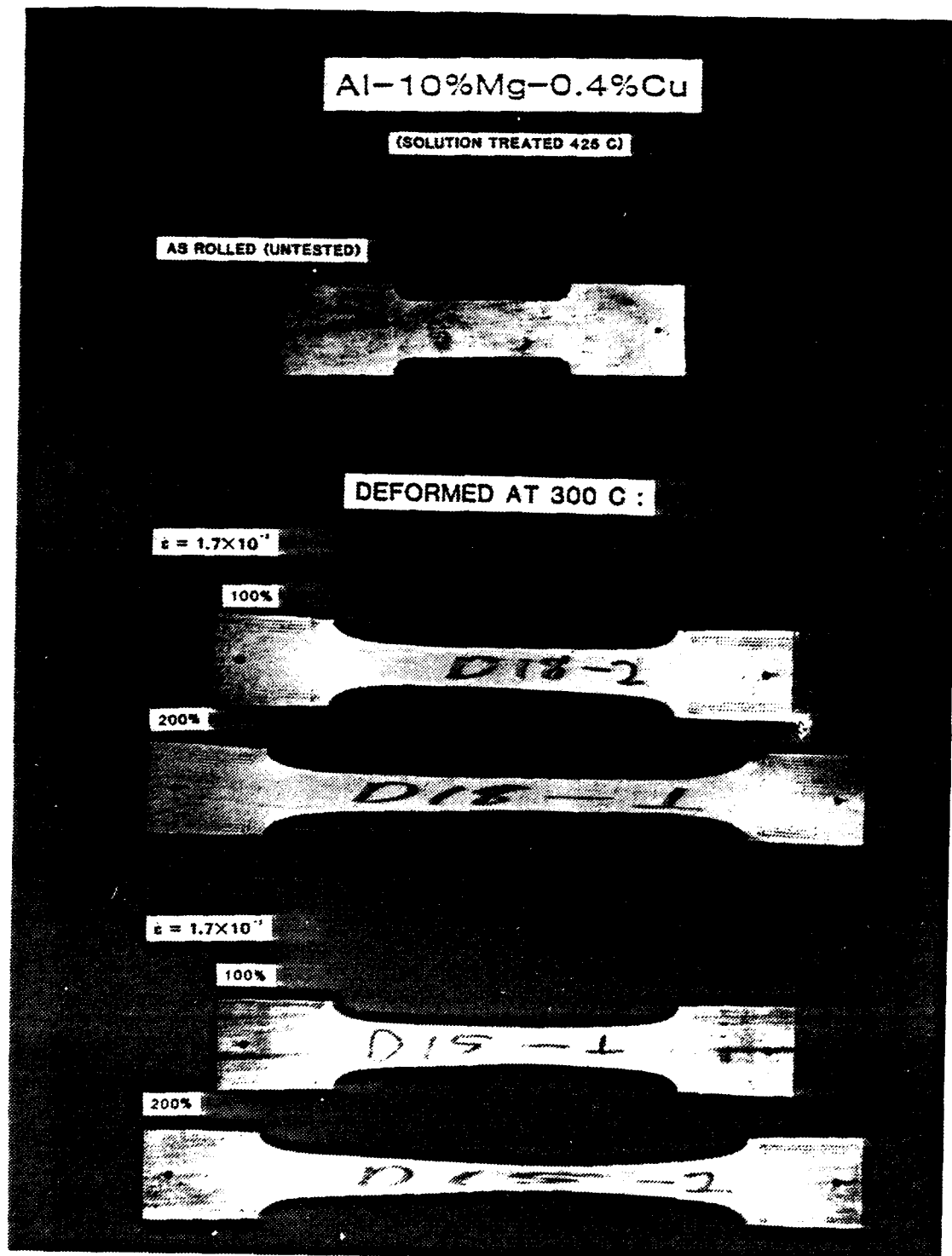


Figure 4.24 Al-10Mg-0.4Cu Solution Treated at 425 C  
Warm Deformed at 300 C.

# AL-10MG-0.4CU WARM FLOW STRESS

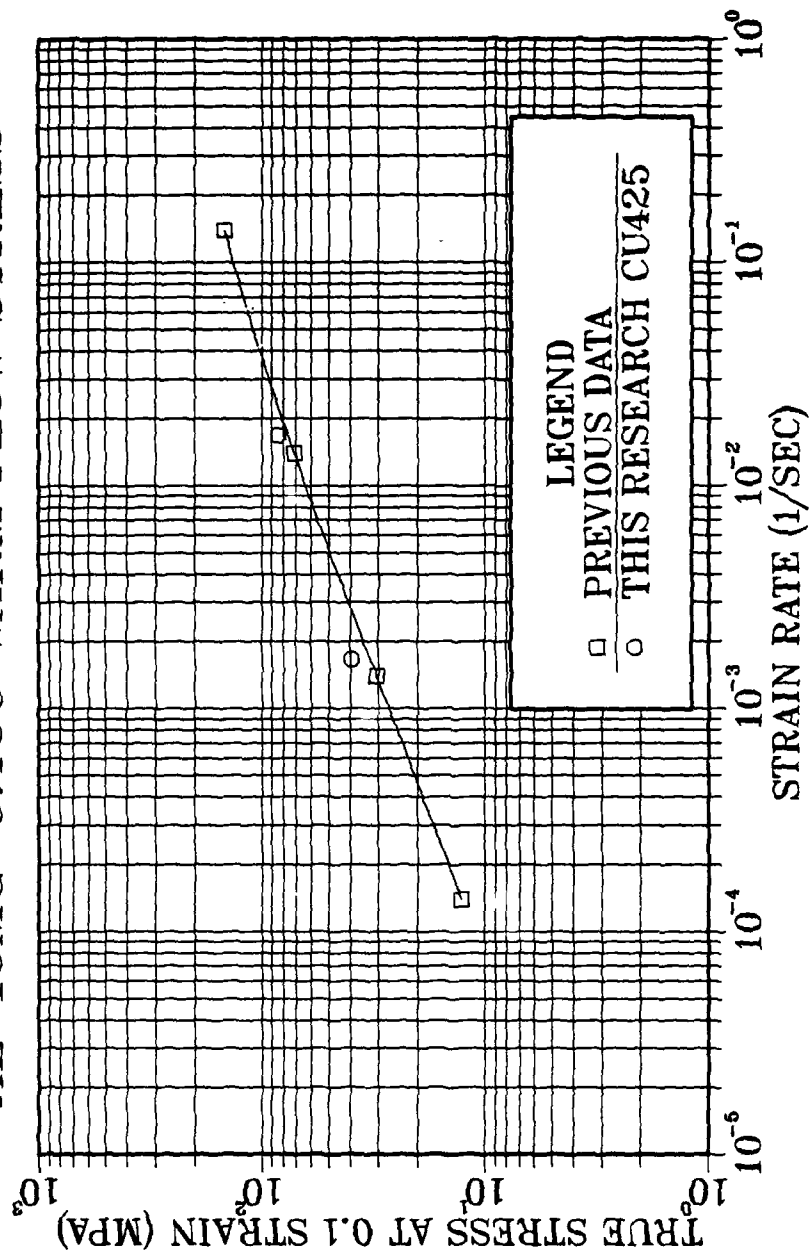
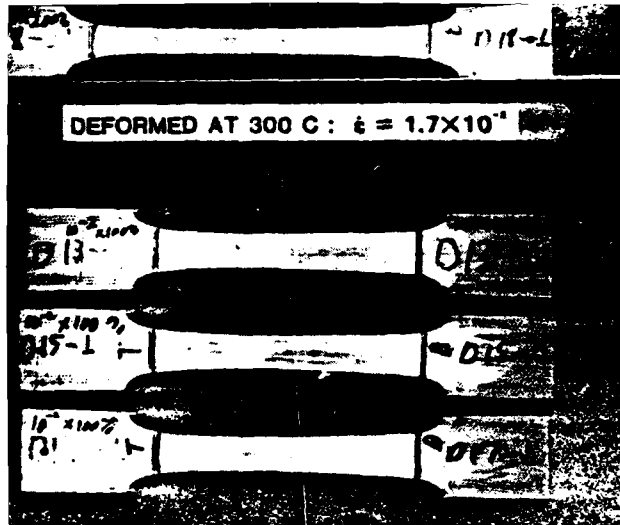


Figure 4.25 True Stress versus Strain Rate  
at 0.1 Plastic Strain for Warm Deformation at 300 C.

Figure 4.25 compares the flow stresses for this research with those obtained by Self [Ref. 20: p. 40] for this same alloy solution treated at 440 C. The flow stress values are consistent between both sets of data, with stress level increasing with strain rate as predicted by equation 2.4. The strain rate sensitivity coefficient,  $m$ , taken from the slope of these log-log plots is 0.3. This is consistent with previous work at NPS and is in the 0.3 to 0.7 range usually observed for superplasticity. In Self's work [Ref. 20: p. 50] a strain of 157 % at  $1.39 \times 10^{-2} \text{ S}^{-1}$  strain rate before fracture was obtained. In this work, two specimens, shown in Figure 4.26 (b), were each strained to 200 % at  $1.67 \times 10^{-2} \text{ S}^{-1}$  strain rate. At that point simulated superplastic forming was stopped to allow remachining of ambient temperature tensile test specimens from the warm deformed specimens. Although they were both beginning to deform nonuniformly, neither was near fracture. It has not been determined if this was due to the reduction in solution treating temperature or the larger cross section of the simulated superplastic forming specimens used in this work.

## 2. As-rolled and As-rolled Plus Anneal

As-rolled and rolled plus annealed specimens were tested in tension at room temperature at  $8.3 \times 10^{-4} \text{ S}^{-1}$  strain rate. Table XIV presents the results of the above mechanical testing along with comparative data from Self [Ref. 20]. The as-rolled data from this research has higher ultimate strengths with lower ductilities than Self's work. The as-rolled material, statically annealed for 75 minutes, gives the same results as Self's as-rolled data. There is no previous data available for statically annealed as-rolled strength and ductility for this alloy.



**TABLE XIV**  
**AMBIENT TEMPERATURE MECHANICAL TEST DATA**  
**FOR AS-ROLLED AL-10MG-0.4CU**

AL-10MG-0.4CU  
(SOLUTION TREATED AT 425 C)

AS ROLLED:

BILLET NUMBER	S <sub>y</sub>	S <sub>u</sub>	o <sub>y</sub>	o <sub>u</sub>	% STRAIN MEASURED
	(MPa)	(MPa)	(MPa)	(MPa)	(%)
{1} {a}	**	**	**	456.7	10.8
{1} {b}	**	**	**	450.5	10.9
Cu15-1AR	337.1	484.6	337.8	519.3	4.8
Cu18-1AR	328.8	458.7	329.4	483.4	5.1
Cu19-1AR	309.5	452.2	310.1	481.4	5.2
Cu16-1AR	352.7	503.7	353.4	540.2	6.0
Cu18-2AR	315.0	456.0	312.2	483.8	6.3
Cu18-3AR	310.8	461.5	311.4	496.8	6.4

AS ROLLED--ANNEALED 1 HR 15 MIN. AT 300 C  
Cu16-2AR 248.8 401.4 244.3 459.6 10.7

\*\* data not available

Self, p. 50. Two strain rates (S<sup>-1</sup>) 1.39X10<sup>-3</sup> (a)  
and 1.39X10<sup>-2</sup>.

### 3. Ambient Temperature Mechanical Properties

Results of the ambient temperature mechanical testing on previously warm deformed samples are presented in Table XV. The yield and ultimate strengths at ambient temperature after warm forming show about a 15 % decrease from the as-rolled values presented in Table XIV. This is similar to the results for the Zirconium-containing alloy but in contrast to the Manganese-containing alloy which showed no significant loss of yield or ultimate strength after with warm deformation.

The ductilities of the specimens at ambient temperature after simulated superplastic forming to 200 % strain at 1.67X10<sup>-3</sup> S<sup>-1</sup> strain rate are equivalent to several other current superplastic Aluminum alloys [Ref. 27]. The yield strengths and ductilities for the other three strains and strain rates are at or below other commercial superplastic alloys.



**TABLE XV**  
**AMBIENT TEMPERATURE MECHANICAL TEST DATA**  
**FOR AL-10MG-0.4CU AFTER SIMULATED SUPERPLASTIC FORMING**

AL-10MG-0.4CU  
(SOLUTION TREATED AT 425 C)

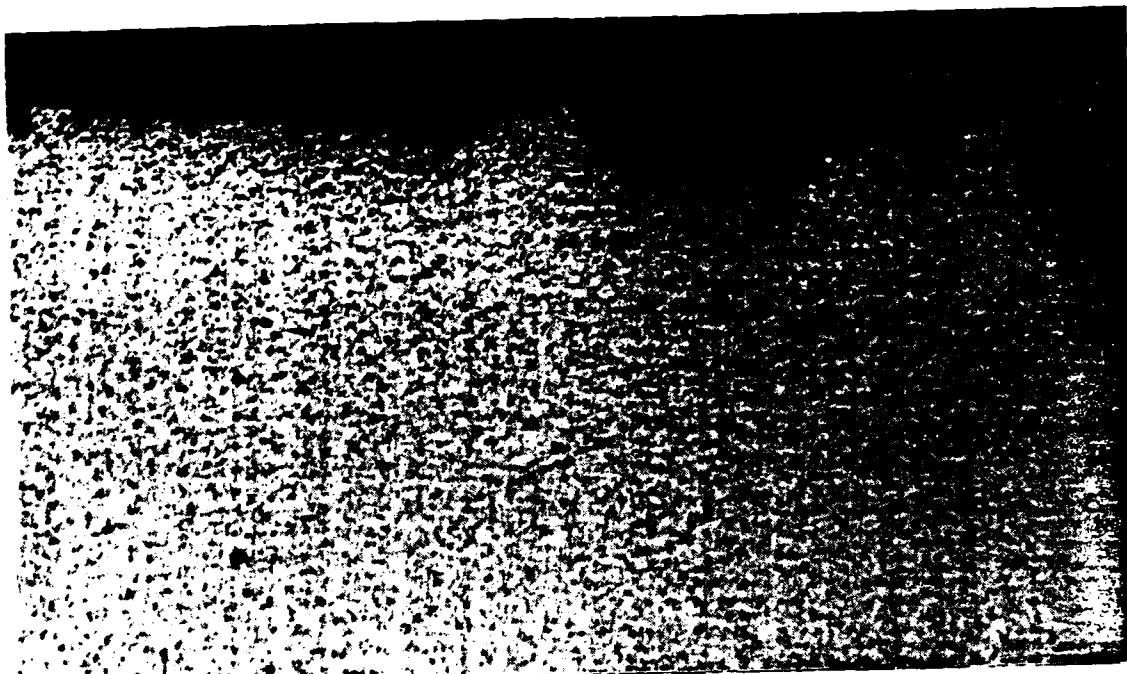
WARM DEFORMED AT 300 C:

BILLET NUMBER	STRAIN RATE	STRAIN		S <sub>y</sub>	S <sub>u</sub>	o <sub>y</sub>	o <sub>u</sub>	% STRAIN MEASURED
	(S <sup>-1</sup> )	(%)	LOCAL	(MPa)	(MPa)	(MPa)	(MPa)	(%)
Cu13-2	10 <sup>-3</sup>	100	100	225.1	313.9	225.5	322.6	1.9
Cu14-1	10 <sup>-3</sup>	100	100	275.2	398.0	275.7	431.9	6.1
Cu14-2A	10 <sup>-3</sup>	200	300	273.0	290.4	273.6	293.7	1.2
Cu19-1A	10 <sup>-3</sup>	200	200	267.2	298.4	262.8	303.0	1.9
Cu19-1B	10 <sup>-3</sup>	200	200		341.0			3.0
Cu14-2B	10 <sup>-3</sup>	200	150	269.5	393.5	270.0	420.0	4.7
Cu19-2B	10 <sup>-3</sup>	200	200	271.1	389.2	271.6	415.6	5.0
Cu19-2A	10 <sup>-3</sup>	200	250	252.8	394.3	253.3	425.1	5.7
Cu17-1	10 <sup>-2</sup>	100	100	274.0	404.7	274.6	431.7	4.2
Cu13-1	10 <sup>-2</sup>	100	100	233.1	411.8	233.5	443.2	4.8
Cu17-2B	10 <sup>-2</sup>	200	200	286.5	435.8	287.0	483.8	6.7
Cu17-2A	10 <sup>-2</sup>	200	200	295.9	450.2	296.5	507.6	8.7

#### 4. Optical Microscopy

As with the other four processing condition/alloy combinations examined in this work, optical microscopy did not provide any conclusive evidence of the cause for the variability in room temperature ductility observed. Figures 4.27 and 4.28 comparing specimens of this alloy warm deformed to 100 % at  $1.67 \times 10^{-3}$  S<sup>-1</sup> strain rate are good examples of this. One specimen had 6.7 % ambient temperature ductility, the other 1.9% ductility yet no apparent difference is evident at this level of magnification.

One of the specimens warm deformed to 100 % strain at  $1.67 \times 10^{-3}$  S<sup>-1</sup> strain rate then tensile tested at room temperature had a second crack about 12 mm away from the fracture surface. Figure 4.29 shows this crack, perpendicular to the tensile axis and covering about 50 % of the thickness of the specimen. Figures 4.30 are higher magnification photomicrographs of the tips of the crack. The dark



(a)



(b)

Figure 4.27 Al-10Mg-0.4Cu Warm Deformed to 100 % Strain  
Room Temp Ductility 6.1 % (A) and 1.9 % (b).



(a)



(b)

Figure 4.28 Al-10Mg-0.4Cu Warm Deformed to 100 % Strain  
Ductility 6.1 % (a) and 1.9 % (b) Kellers etch, X800.

etching artifacts that the crack seems to go through did not appear as voids in the sample before etching, but do etch preferentially. Spectrum analysis was not available to determine what elements were present at these sites. This was the only specimen examined in this work which had such a crack.

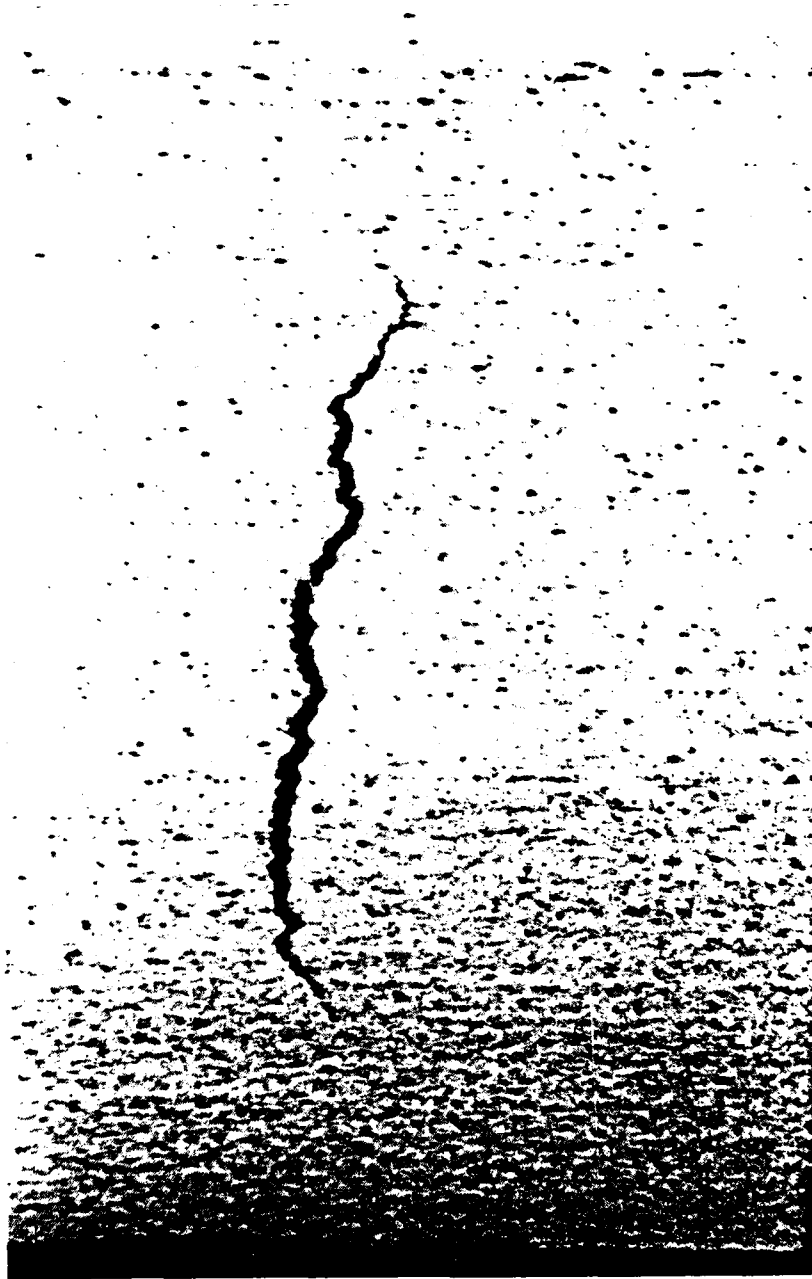
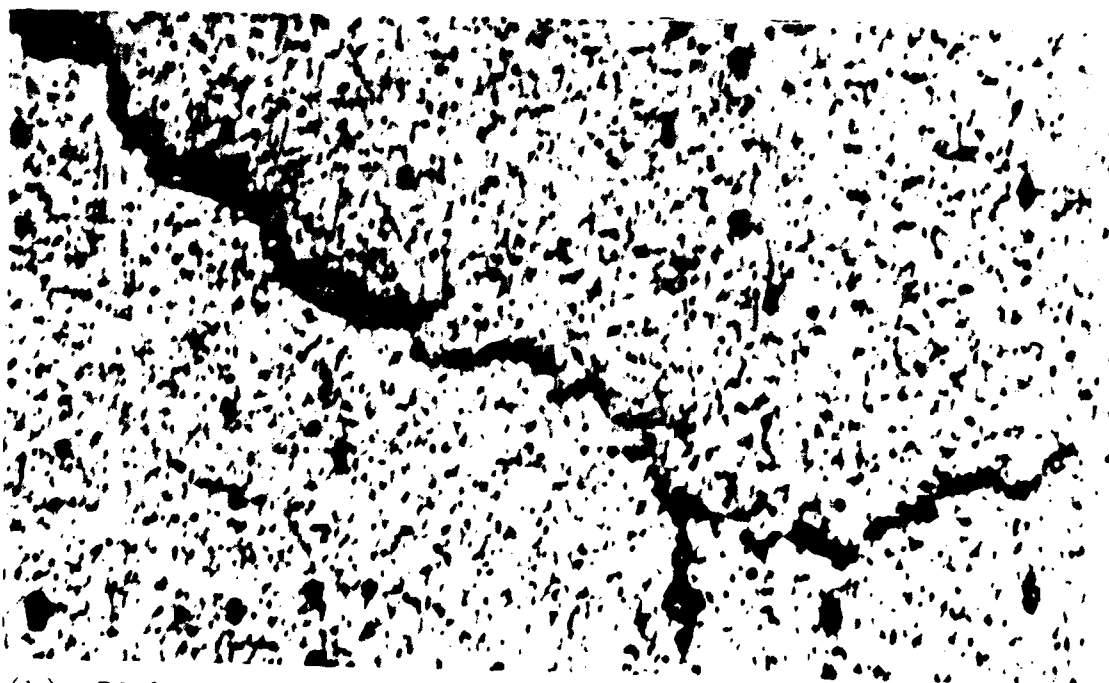


Figure 4.29 'Second Crack 12 mm Away From  
Actual Fracture Site. Al-10Mg-0.4Cu, Kellers etch X100.



(a) Left end



(b) Right end

Figure 4.30 Ends of Second Crack in  
Al-10Mg-0.4Cu Specimen. Kellers etch, X800.

## V. CONCLUSIONS AND RECOMMENDATIONS

### A. CONCLUSIONS

1. A successful modification of the test equipment was made to simulate superplastic forming , with sufficient sample size to permit subsequent evaluation of the ambient temperature mechanical properties after warm deformation.

2. Material was processed for all three alloys. This processing included material to evaluate the effect of solution treating temperature in the Al-10Mg-0.1Zr and Al-10Mg-0.5Mn alloys.

3. In simulation of superplastic forming, attained 200 % deformation at  $1.7 \times 10^{-2} \text{ s}^{-1}$  ( 2 % / second) for all alloys and processing conditions.

4. Following superplastic forming, the yield strenths were 300 MPa (40 KSI) to 325 MPa (45 KSI) for the Al-10Mg-0.5Mn alloy, 230 MPa (35 KSI) to 300 MPa (40 KSI) for the Al-10Mg-0.1Zr alloy and 250 MPa (35 KSI) to 300 MPa (40 KSI) for the Al-10Mg-0.4Cu alloy.

5. Ductilities varied widely with little apparent correlation to prior thermomechanical processing. Ambient temperature ductilities after simulated superplastic forming were 1.7 to 9.8 percent for the Al-10Mg-0.5Mn alloy, 1.0 to 14.2 percent for the Al-10Mg-0.1Zr alloy and 0.7 to 8.8 for the Al-10Mg-0.4Cu alloy.

6. The yield strength and ambient temperature ductility combinations for the more ductile samples in all three alloys are very good in comparison to other superplastic alloys.

7. Optical metallography does not reveal the cause for the variation in ductilities but does show that little cavitation occurs during warm deformation of these alloys. Metallography does show that the fracture path does not follow the constituent ZrAl , MnAl , or Cu particles.

## B. RECOMMENDATIONS

1. More detailed metallography (transmission electron microscopy) is needed to determine the cause of the variability in room temperature ductility.

2. Continue evaluation of microstructure evolution during superplastic flow.

3. Continue evaluation of the properties of structures produced during superplastic forming.



## LIST OF REFERENCES

1. Johnson, R. B. The Influence of Alloy Composition and Thermomechanical Processing Procedure on Microstructural and Mechanical Properties of High-Magnesium Aluminum Magnesium Alloys, M. S. Thesis, Naval Postgraduate School, Monterey, California June 1980
2. Becker, J., Superplasticity in Thermomechanically Processed High Magnesium, Aluminum-Magnesium Alloys, M.S. Thesis, Naval Postgraduate School, Monterey, California, March 1984
3. Moore, J. B., Tequesta, J., and Athey, R. L., U.S. Patent No. 3,951,967, 1976.
4. Hamilton, C.H. and Stacker, G. W., "Superplastic Forming of Titanium Alloys", Metal Progr., Vol. 109, p. 34, 1976.
5. Sherby, O. D. and Wadsworth, J., "Development and Characterization of Fine-Grain Superplastic Materials", Deformation, Processing, and Structure, pp.354-384, 1982.
6. Herring, C., "Diffusional Viscosity of A Polycrystalline Solid", Journal of Applied Physics, Volume 21, p. 437, 1950.
7. Coble, R. L., "A Model for Boundary Diffusion Controlled Creep in Polycrystalline Materials", Journal of Applied Physics, Volume 34, p. 1679, 1963.
8. Ashby, M. F. and Verrall, R. A., "Diffusion-Accommodated Flow and Superplasticity", Acta Metallurgica, Vol. 21, pp.149-163, 1973.
9. Langdon, T. G., "Experimental Observation in Superplasticity", Superplastic Forming of Structural Alloys, Conference Proceedings of TMS-AIME, pp. 27-40, June 1982.
10. Stowell, M. J., "Cavitation in Superplasticity", Superplastic Forming of Structure Alloys, Conference Proceeding of TMS-AIME, pp. 321-336, June 1982.
11. Hedworth, J. and Stowell, M. J., The Measurement of Strain Rate Sensitivity in Superplastic Alloys, Journal of Materials Science, pp. 1061-1069, 1971.

12. McNalley, T. R., Lee, E. W. and Mills, M. E. Superplasticity in a Thermomechanically Processed High-Mg, Al-Mg Alloy, Submitted to Metallurgical Transactions.
13. Lee, E. W., McNalley, T. R. and Stengel, A. F. The Influence of Thermomechanical Processing Variables on Superplasticity in a High-Mg, Al-Mg Alloy, submitted to Metallurgical Transactions.
14. Mills, M.E., Superplasticity in a Thermomechanically Processed Aluminum - 10.2% Mg, 0.5% Mn Alloy, M.S. Thesis, Naval Postgraduate School, Monterey, California, September 1984.
15. Stengel, A., Effects of Annealing Treatments on Superplasticity in a Thermo-Mechanically Processed Aluminum-10.2% Mg, 0.52% Mn alloy, M.S. Thesis, Naval Postgraduate School, Monterey, California, December, 1984.
16. Labusch, R., "Crystal Lattice Defects", Journal of Physics, v. 40 pp 89-94, 1961.
17. McNalley and Garg, "Development of Structure and Mechanical Properties in Al-10.2% Mg by Thermomechanical Processing", Scripta Metallurgica, v. 18, pp 917-920, 1984
18. Mondolfo, L. F., Aluminum Alloys: Structure and Properties Butterfield and Co. (publishers) 1975
19. Sniran, H. H., The Influence of Solution Time and Quench Rate on the Microstructure and Mechanical Properties of High-Magnesium Aluminum-Magnesium Alloys, M.S. Thesis, Naval Postgraduate School, Monterey, California, December 1981.
20. Self, R. J., The Effect of Alloy Additions on Superplasticity in Thermomechanically Processed High Magnesium Aluminum Magnesium Alloys, M.S. Thesis, Naval Postgraduate School, Monterey, California, December 1984.
21. Alcama, M. E., Effect of Strain and Strain Rate on the Microstructure of a Superplastically Deformed Al-10.2Mg-0.12Zn Alloy, Mechanical Engineer Thesis, Naval Postgraduate School, Monterey, California, June 85.
22. Berthold, D. B., Effect of Temperature and Strain Rate on the Microstructure of a Deformed, Superplastic Al-10.2Mg-0.12Zn alloy, M.S. Thesis, Naval Postgraduate School, Monterey, California, June 1985.
23. Hartmann, T. S., Mechanical Characteristics of a Superplastic Aluminum-10.2% Mg-0.12% Zn Alloy, M.S. Thesis, Naval Postgraduate School, Monterey, California, June 1985.

24. Alcoa Technical Center, ltr, August 1984.
25. Beberdick, L. E. A Preliminary Investigation of the Corrosion and Stress-Corrosion Susceptibility of Thermomechanically Processed High-Magnesium, Aluminum-Magnesium Alloy M.S. Thesis, Naval Postgraduate School, Monterey, California, September 1981.
26. Naval Air Development Center Report 1375, The Mechanical Properties of Thermomechanically Processed High-Magnesium, Aluminum-Magnesium Alloy by I. H. McNeelley p. 38, 10 June 1983.
27. Barnes, A. J., Advances in Superplastic Aluminum Alloys and Forming Technology, paper presented at Symposium on Superplasticity and Its Applications. Stanford University, Stanford, California, 14 May 1985.

# INITIAL DISTRIBUTION LIST

	No.	Copies
1. Defense Technical Information Center Cameron Station Alexandria, Virginia 22304-6145		2
2. Library, Code 0142 Naval Postgraduate School Monterey, California 93943-5100		2
3. Department Chairman, Code 69Mx Department of Mechanical Engineering Naval Postgraduate School Monterey, California 93943-5100		1
4. Professor T. R. McNelley, Code 69Mc Department of Mechanical Engineering Naval Postgraduate School Monterey, California 93943-5100		5
5. Naval Air Systems Command, Code Air 320 Naval Air Systems Command Headquarters Washington, DC 20361		1
6. Jeff Waldman Naval Air Development Center Materials Science Department Warminster, Pennsylvania 18974		1
7. Dr. Eui-Whee Lee Naval Air Development Center Materials Science Department Warminster, Pennsylvania 18974		1
8. LT Karl A. Klankowski Department Head School Command, Class 92 Newport, Rhode Island 02841		4

**END**

**FILMED**

**3-86**

**DTIC**